Ternary Alloys

Volume 21

MSI
Science Simplified

Ternary Alloys

A Comprehensive Compendium of Evaluated Constitutional Data and Phase Diagrams

critically evaluated by MSIT®

Volume 21

Selected Al-Fe-X Ternary Systems for Industrial Applications

Editors
Frank Stein, Martin Palm

Associate Editors
Liya Dreval, Oleksandr Dovbenko, Svitlana Iljenko

Authors
Materials Science International Team, MSIT®

MSI
Science Simplified

Editors: Frank Stein,
Martin Palm
Associate Editors: Liya Dreval
Oleksandr Dovbenko
Svitlana Iljenko

ISBN 978-3-932120-51-0

Vol. 21. Selected Al-Fe-X Ternary Systems for Industrial Applications. – 2022

This volume is part of the book series:
Ternary Alloys: A Comprehensive Compendium of Evaluated Constitutional Data and Phase Diagrams/
Materials Science International Services GmbH, Stuttgart, Germany

Group ISBN for the Ternary Alloys book series: 978-3-932120-41-1

Published by
MSI, Materials Science International Services GmbH, Stuttgart (Federal Republic of Germany)
Am Wallgraben 100, D-70565 Stuttgart, Germany
Postfach 800749, D-70507, Stuttgart, Germany
http://www.msiport.com
http://www.msi-eureka.com/

Printed on acid-free paper.

Printing and binding:
WIRmachenDRUCK GmbH, Mühlbachstraße 7, 71522 Backnang

Printed in the Federal Republic of Germany

Authors: Materials Science International Team, MSIT®

This volume results from collaborative evaluation programs performed by MSI and authored by MSIT®. In this program, data and knowledge are contributed by many individuals and have accumulated over almost thirty five years, up to the present day. The content of this volume is a subset of the ongoing MSIT® Evaluation Programs. Authors of this volume are:

Nataliya Bochvar, Moscow, Russia
Anatoliy Bondar, Kyiv, Ukraine
Gabriele Cacciamani, Genova, Italy
Lesley Cornish, Johannesburg, South Africa
Oleksandr Dovbenko, Stuttgart, Germany
Liya Dreval, Stuttgart, Germany
Yong Du, Changsha, China
Kiyaasha Dyal Ukabhai, Johannesburg, South Africa
Olga Fabrichnaya, Freiberg, Germany
Lorenzo Fenocchio, Genova, Italy
Sergio Gama, Campinas, Brasil
Gautam Ghosh, Evanston, USA
Bernd Grieb, Tübingen, Germany
Kiyohito Ishida, Sendai, Japan
Hermann A. Jehn, Stuttgart, Germany
Kostyantyn Korniyenko, Kyiv, Ukraine
Mario J. Kriegel, Freiberg, Germany
Ortrud Kubaschewski†, Aachen, Germany
K.C. Hari Kumar, Chennai, India
Bernard Legendre, Paris, France
Xiaojing Li, Changsha, China
Shuhong Liu, Changsha, China
Xing Jun Liu, Sendai, Japan
Annelies Malfliet, Heverlee, Belgium
Niraja Moharana, Chennai, India
Martin Palm, Düsseldorf, Germany
Jian Peng, Wuhan, China
Pierre Perrot, Lille, France
Alexander Pisch, Grenoble, France
Qingsheng Ran, Stuttgart, Germany
Maximilian Rank, Karlsruhe, Germany
Peter Rogl, Vienna, Austria
Lazar Rokhlin, Moscow, Russia
Rainer Schmid-Fetzer, Clausthal-Zellerfeld, Germany
Frank Stein, Düsseldorf, Germany
Vasyl Tomashyk, Kyiv, Ukraine
Lyudmila Tretyachenko†, Kyiv, Ukraine
Mikhail Turchanin, Kramatorsk, Ukraine
Oksana Tymoshenko, Kyiv, Ukraine
Thomas Vaubois, Chatillon, France
Alexander Walnsch, Freiberg, Germany
Chuanbin Wang, Wuhan, China
Cui Ping Wang, Sendai, Japan
Junjun Wang, Wuhan, China
Andrew Watson, Chesterfield, UK
Liming Zhang, München, Germany

Contents

Ternary Alloys
A Comprehensive Compendium of Evaluated Constitutional Data and Phase Diagrams

Volume 21
Selected Al-Fe-X Ternary Systems for Industrial Applications

Aluminium – Chromium – Iron

Kostyantyn Korniyenko, Liya Dreval

Introduction

There is a number of reasons for the scientific interest in the phase relations in the Al-Cr-Fe system, particularly as alloys of this system are employed as lightweight materials for structural applications and as accident-tolerant fuel-rod cladding materials due to very good oxidation and radiation resistance. The existence of quasicrystal approximants is also an interesting peculiarity of the Al-Cr-Fe system.

Reviews of the literature data concerning phase equilibria have been conducted by [1943Mon, 1953Cas, 1961Phi, 1969Wat, 1973Wil, 1976Mon, 1994Rag, 2003Rag, 2005Pal, 2012Rag, 2011Kho1, 2016Li1, 2019Eze, 2019Ran, 2020Ran], concerning crystal structures of the phases - by [2009Bau, 2013Bau]; critical assessments of the available data - by [1970Koz1, 1970Koz2, 1980Riv, 1987Sau, 1991Gho, 2004Gho, 2007Gho]. The most recent MSIT evaluation of [2007Gho] covers the literature data published before 2007. New works of [2011Kho2, 2019Eze, 2019Ran, 2020Ran] presented information about the liquidus surface. Recent data about the melting points of the alloys and the solidus surface projection constitution are given in the papers of [2008Pav3, 2009Pav, 2010Pav, 2011Kho1, 2019Eze, 2019Ran, 2020Ran]. The results of experimental investigations of phase relations at different temperatures along with isothermal sections have been recently presented by [2008Pav2, 2008Pav3, 2014Pav, 2015Zho, 2019Ran, 2020Ran]. No new experimental information besides the data of [1946Kor, 1969Bul1, 1991Tre] has been reported for the temperature-composition sections. There is a large number of papers concerning the data on the crystal structure of the ternary phases in the Al-Cr-Fe system, including the most recent findings of [2009Bau, 2010Bau, 2010Pav, 2011Bau, 2012Ume, 2014Gas]. [2008Jac, 2013Mar] reported new data on the thermodynamic properties of the (Cr, αδFe) phase. The most recent thermodynamic assessments of the system were performed by [2017Wan, 2019Cha, 2020Ran]. The experimental methods used by the investigators, as well as the temperature and composition ranges studied, are presented in Table 1. Despite the fact that the knowledge of the phase equilibria in the system has been significantly expanded, certain issues are still to be clarified.

Binary Systems

The Al-Cr system was evaluated within the MSIT Binary Evaluation Program in 2013 by [2013Khv] involving literature data available at that moment. Later, [2014Ste, 2014Wu, 2015Kur] further studied the phase equilibria in the system. Compared to [2013Khv], these experimental studies provided the following information. [2014Ste] performed the DTA measurements of the Cr-rich part of the diagram and adjusted the liquidus and solidus for the (Cr) phase, as well as phase boundaries involving the γ brasses and Cr_2Al. [2014Wu] confirmed that Cr_4Al_{11} is stable in the system and reported the temperature of its decomposition. [2015Kur] performed planar front solidification experiments and found (Al) to form *via* a peritectic reaction. The Al-Cr phase was thermodynamically assessed by [2013Hu, 2015Wit, 2017Cui]. All thermodynamic assessments result in certain discrepancies with respect to the data of [2014Ste] and melting temperatures of Cr_2Al_{11} and $CrAl_7$ as assessed by [2013Khv].

The phase diagram of [2013Khv] was modified here to take the recent data into account. For the Cr-rich part, the phase boundaries were adjusted according to [2014Ste]. The liquidus and homogeneity range of βCr_5Al_8 were modified according to [2015Wit], whose calculations show better agreement with the experimental data. For (Al), the peritectic reaction is accepted. The coordinates of the reaction are according to [2015Wit]. The temperature of Cr_4Al_{11} decomposition is according to [2014Wu]. Below 1100°C, a series of γ-brasses exists in the central part of the Al-Cr diagram. The corresponding phase equilibria were presented by [2013Khv]. Since no experimental information relevant to different γ-brasses modifications is available for the Al-Cr-Fe system, this part of the diagram was simplified by removing the phase boundaries between different modifications of γ-brasses below 1100°C. The resulting homogeneity range corresponds to a rhombohedrally distorted γ-brass structure denoted as αCr_5Al_8. The final phase diagram is presented in Fig. 1. The phase equilibria below 450°C are not included because of their uncertainty and lack of experimental data for the ternary phase diagram. [2013Khv] mentioned several possible crystal structures for Cr_2Al_{11}. According to the observations of [2008Gru, 2009Che, 2008Cao], this compound has a monoclinic *C*2/*c* structure. The *Cmcm* structure corresponds to the metastable ε-$CrAl_4$ compound.

The accepted Al-Fe binary phase diagram is according to [2022Ste] and presented in the *'Aluminium – Iron'* chapter. [2010Xio] thoroughly reviewed the phase equilibria in the Cr-Fe system. This system was subsequently assessed by [2011Xio, 2017Cui]. The phase diagram, as compiled by [2010Xio], is accepted in the present evaluation since it provides the best agreement with the available experimental data.

Solid Phases

Crystallographic data on the known unary and binary phases, as well as recently reported ternary ones, are listed in Table 2. Only binary phases that are relevant to the phase transformation in the ternary system have been included.

Solid solutions. According to [2011Kho1, 2019Eze], the addition of Cr slightly increases the solubility of iron in the (Al) phase, while Fe almost does not affect the Cr solubility in this solid solution. Similar to the Al-Cr and Al-Fe systems, the highest solubility of Cr and Fe is observed at solidus temperatures.

Experimental observations of [1946Kor] are the only source of data concerning the (γFe) homogeneity range in the ternary system. The extended (γFe) solubility range, which reaches up to 7.7 at.% Al and 8.2 at.% Cr at 900 and 1000°C, is most probably due to the low purity of the samples. The as-prepared alloys contained in average 0.04 mass% C and 0.15 mass% Si.

Disordered (Cr, αδFe) solution and its ordered polymorphs. There is a variety of studies on the phase equilibria involving (Cr, αδFe) and its ordered polymorphs – $B2$ (FeAl), $D0_3$ (Fe_3Al) and its ternary $L2_1$ equivalent – Heusler phase $CrFe_2Al$. These phases have the same cubic lattice with a similar lattice parameter but differ in the ordering of the Fe and Al atoms. Therefore, the ordered polymorphs can easily precipitate coherently in the Al-Fe matrix even during severe quenching of the samples and have a very fine scale. Consequently, the XRD measurements of the quenched structures at room temperature may show the existence of an ordered phase, though a sample had a disordered structure at the annealing temperature. In general, the ordering type can be observed using *in-situ* TEM technique. But the analysis of anti-phase domain (APD) structures in TEM foils at room temperature also allows to retrieve the structure which has been stable at a particular annealing temperature before quenching. The chemical driving forces for ordering in the Al-Cr-Fe are very low, so the formation of an ordered phase in the ternary system may become apparent after long annealing at high Cr concentration. This also affects the establishment of the order-disorder transformation temperatures resulting in a high scatter of the reported data and difficulties in interpretation of the transformations occurring at a particular temperature. Thus, systematic and comprehensive studies of the order-disorder transformations require the production of a series of samples at different annealing temperatures and times, as well a combination of various techniques, such as high-resolution SEM, *in-situ* TEM and TEM APD examination at room temperature, DSC and DTA. For the Al-Cr-Fe system, there are no such experimental investigations that meet all these requirements. But several studies reveal the complex nature of the phase equilibria involving (Cr, αδFe) and its ordered polymorphs.

[1945Kor, 1946Kor, 1958Chu, 1976Vla, 1991Tre, 1997Pal, 2014Pav, 2012Ume, 2019Ran, 2020Ran] reported the compositions of the disordered (Cr, αδFe) solution at different temperatures. For the Cr-rich side of the triangle, [2019Ran, 2020Ran] found that the addition of iron slightly increases Al solubility in the phase at 900°C. Only [2012Ume] used a TEM technique to study the concentration region in which the formation of ordered polymorphs was expected. They analyzed the APD structure of the $Cr_{25}Fe_{50}Al_{25}$ (at.%) sample annealed at 1150°C and subsequently quenched. [2012Ume] found that the sample had a disordered (Cr, αδFe) structure at this temperature. During quenching from 1150°C, FeAl precipitated so that the structure at room temperature was two-phase.

Below 500°C, the (Cr, αδFe) miscibility gap exists in the Cr-Fe system. [1976Vla] studied the decomposition behavior of a Cr-68.3Fe-10.4Al (at.%) alloy after quenching from 750°C and subsequent annealing at 490°C for up to 200 h. The authors observed phase separation into two isomorphous solid solutions, which were depleted or enriched in Cr, respectively.

There is a variety of studies on the phase equilibria involving the ordered $B2$ (FeAl), and $D0_3$ (Fe_3Al)/$L2_1$ ($CrFe_2Al$) phases. Note that in some papers, [2004Zha, 2012Sah] for example, usage of the term “Heusler phase” is misleading since no $L2_1$ ordering was observed by the authors. The majority of the studies [1968Bul, 1969Bul1, 1969Bul2, 1969Sel, 1994Hyd, 1995Ant, 1995Yos, 1997Nis1, 1997Nis2, 2012Yil, 2019Ran, 2020Ran] is focused on the establishment of the order-disorder transition temperatures though. [1972Kaj, 1974Niz, 1975Lit, 1977Tys, 1995Yos, 1997Nis1, 1997Nis2, 1997Sat, 1998Kim, 1999Wit, 2001Alo, 2007Pad] studied the crystal structure of the samples after slow cooling using different methods (see Table 1). [1981Bus, 1985Okp, 1991Tre, 1997Pal, 1998Sun, 2001Alo, 2008Shr, 2012Lam] produced annealed samples but detailed TEM examinations were not available to the authors.

The studies of annealed samples performed using *in-situ* TEM or TEM APD examination are limited to the works of [1989McK, 1994Mor, 2012Ume]. [2006Gol1, 2006Gol2, 2008Gol, 2009Gol] also examined the APD structures using TEM. Their samples contained from 0.005 to 0.004 at.% C though, and the authors suspected the formation of carbides in their films but did not perform further investigation of this issue. [2012Ume] observed the $B2$ (FeAl) phase at $Cr_{25}Fe_{50}Al_{25}$ (at.%) and 600°C. The $D0_3$ (Fe_3Al) single-phase structure was reported to exist up to 6 at.% Cr at 28 at.% Al and 500°C by [1989McK, 1994Mor], at $Cr_5Fe_{69}Al_{26}$, $Cr_8Fe_{67}Al_{25}$ (at.%) and 477°C by [2006Gol1,

2006Gol2, 2008Gol, 2009Gol]. [1994Mor] performed further *in-situ* TEM observations between 500 and 600°C but did not discuss their finding for the Al-Cr-Fe system in detail.

TEM APD studies performed by [2006Gol1, 2006Gol2, 2008Gol, 2009Gol] and [2012Ume] revealed formation of very fine $D0_3$ (Fe_3Al)/$L2_1$ ($CrFe_2Al$) domains in the $Cr_{25}Fe_{50}Al_{25}$ (at.%) thin films annealed at 477°C and 400°C. Even 20 days of annealing by [2012Ume] did not produce coarsened well-developed $L2_1$ ($CrFe_2Al$) structure. This shows that the stoichiometric $L2_1$ Heusler phase is not stable at either 477 or 400°C. The energy of formation of the stoichiometric $CrFe_2Al$ compound was calculated by [2003Kel, 2016Dah] using full potential linearized augmented plane waves method and by [2021Liu] using the Perdew–Burke–Ernzerhof functional in the generalized gradient approximation. The calculated energies of formation are negative suggesting that the stoichiometric $L2_1$ ($CrFe_2Al$) Heusler phase is not thermodynamically unstable in the Al-Cr-Fe system. But whether it is metastable or forms at a lower temperature after extremely long annealing is open to debate.

There are several studies on the occupation of Cr on the lattice sites of ordered phases. Using the mean-field approximation, [2002Ban] has found that Cr has a stronger preference for occupying the Fe sublattice in the *B*2 (FeAl) phase. Based on their neutron studies, [1997Sat, 1998Sun] also reported that preferential occupancy of the Fe_I sites by Cr.

σ phase. [1955Tag] and [1958Chu] studied the phase equilibria involving the σ phase, which originates from the Cr-Fe system. The alloy used by [1955Tag] contained up to 0.09 mass% C and therefore had lower purity than samples used by [1958Chu]. Furthermore, [1958Chu] employed a thorough heat-treatment regime and a larger number of samples. Nevertheless, the σ + (Cr, αδFe) two-phase boundaries established for the Cr-Fe edge in both studies conflict with the binary Cr-Fe phase diagram accepted in the present evaluation. On the other hand, the σ homogeneity region constructed by [1958Chu] is in satisfactory agreement with the binary data. According to [1958Chu], the σ phase dissolves between 1 at.% Al at 750°C and 3 at.% Al at 600°C. To the best of our knowledge, no experimental data on the Al influence on the σ formation temperatures were published in the literature.

Al-Cr-based compounds. [2019Eze] found that the monoclinic $CrAl_7$ compound dissolves up to 2.5 at.% Fe at solidus temperatures. [2011Kho1, 2011Kho2] reported approximately the same value in their study of the solidus surface. [2019Eze] also measured the lattice parameters of the phase in a three-phase sample annealed at 650°C for 500 h and subsequently quenched.

[1997Pal] performed the very first detailed study of the phase equilibria involving $CrAl_4$. It has been reported that this compound dissolves up to 12 at.% Fe. Unfortunately, a TEM technique was not available for [1997Pal] at that time. By using an XRD technique only, the authors could not distinguish between different ternary quasicrystal approximants, which exist in this part of the diagram as confirmed by later TEM, neutron or electron diffraction measurements, see for example [2008Pav2, 2009Pav, 2010Pav, 2010Bau, 2011Bau]. According to [2010Bau, 2011Bau, 2011Kho1, 2014Pav], the Fe solubility in $CrAl_4$ does not exceed 2 at.%.

The experimental data about Cr_2Al_{11} are contradictory. Based on the powder XRD and TEM examinations, [2010Pav, 2014Pav] suggested that the homogeneity range of Cr_2Al_{11} extends up to 4 at.% Fe at around 78 at.% Al. Based on neutron diffraction and TEM measurements, [1995Sui, 1997Sui, 2010Bau, 2011Bau, 2013Bau] found that Czochralski-grown single crystals containing 2-6 at.% Fe and around 78 at.% Al present a ternary orthorhombic phase (o-(Cr,Fe)Al_4) which has a highly modulated structure as was later reported by [2013Bau, 2014Gas]. The argumentation of [2010Pav, 2014Pav] is essentially based on a comparison of the XRD patterns calculated using [1991Ben]'s structural model for monoclinic Cr_2Al_{11} and [2004Den]'s structural model for orthorhombic o-(Cr,Fe)Al_4 with their own experimental powder patterns for Fe-rich compositions. [2010Pav, 2014Pav] stated that the powder XRD calculated using both structural models showed remarkable similarity and were in good agreement with the experimental powder patterns. However, powder diffraction data used by [2010Pav, 2014Pav] are not enough to determine any modulation in the structure and are less reliable in comparison to the single crystal XRD as performed by [1995Sui, 1997Sui, 2004Den, 2010Bau, 2011Bau, 2013Bau]. Finally, the o-(Cr,Fe)Al_4 structural model reported by [2004Den], as well as by [2013Bau, 2014Gas], present "average" models of the real modulated structure with the model of [2013Bau] giving the best fitting of the experimental data so far. Thus, a comparison of the powder XRD patterns made by [2010Pav, 2014Pav] is questionable.

The majority of the data on the phase equilibria involving Cr_2Al_{11}, including liquidus and solidus temperatures, were reported by [2010Pav, 2014Pav] and by [2011Kho1, 2011Kho2], who used the results of the former for the interpretation of the experimental results. Liquidus and solidus temperatures of Cr_2Al_{11} reported by [2010Pav] and [2019Eze] are questionable as the temperatures for the L+$CrAl_4$ ⇌ Cr_2Al_{11} and L+Cr_2Al_{11} ⇌ $CrAl_7$ reactions in the Al-Cr measured in these studies suggest. [2013Khv] discussed various factors affecting this transformation in the binary system earlier. Hence, phase equilibria with Cr_2Al_{11} are still open to debate. In the present evaluation, it has

been assumed that the ternary o-(Cr,Fe)Al_4 exists at 3-6 at.% Fe and ~78 at.% Al, and Cr_2Al_{11} extends up to 3 at.% Fe at *ca.* 80 at.% Al.

No experimental data regarding the phase equilibria involving Cr_4Al_{11} can be found in the literature.

[1940Kor1, 1946Kor] suggested that isostructural Fe_5Al_8 and βCr_5Al_8 compounds of the cubic γ-brass-type form continuous solid solution $(Cr,Fe)_5Al_8$. This was later confirmed by [2011Kho1, 2014Pav, 2019Ran, 2020Ran] by considering the SEM and EPMA data. By cooling, $(Cr,Fe)_5Al_8$ either transforms to room temperature αCr_5Al_8 in Cr-rich samples or decomposes to the mixture of the neighboring phases in Fe-rich samples. [2011Kho1] also measured the lattice parameters of this compound in several multicomponent alloys. The heat treatment of these samples is not described in detail. Therefore, these data are not included in the present evaluation.

The low-temperature αCr_5Al_8 phase has an extended homogeneity range [1997Pal, 2014Pav]. According to [2014Pav], αCr_5Al_8 can dissolve up to 35 at.% Fe. Lattice parameters of the phase in dependence of Fe content were measured by [1997Pal] (Fig. 2). According to [2011Kho1, 2011Kho2, 2014Pav], the addition of Fe also increases the αCr_5Al_8 melting temperatures. It forms *via* a three-phase peritectic reaction at 1185°C according to [2011Kho1].

Based on their XRD and metallographic observations, [1958Chu] suggested that Cr_2Al ($MoSi_2$-type) might dissolve a significant amount of Fe. This was experimentally confirmed later by [1969Kal, 2015Sus, 2019Ran, 2020Ran]. According to the EPMA/WDX results of [2019Ran, 2020Ran], the Fe solubility in this compound extends to up to 22 at.% at 700°C. [1969Kal, 2015Sus] measured the lattice parameters for a series of the $Cr_{2-x}Fe_xAl$ alloys. The authors did not describe the heat treatment procedure of the samples in detail. Therefore, it is not clear to which temperature the measured values can be attributed. The results of [1969Kal, 2015Sus] are in good agreement though and show that the *a* parameter diminishes, and the *c* parameter slightly increases with increasing Fe content: *a* = 300.4-295.4 pm and *c* = 864-874 pm for 0-13.3 at.% Fe. The effect of iron on the formation temperature of Cr_2Al is not studied. The Cr_2Al compound exhibits antiferromagnetic behavior. As shown by [1969Kal, 2015Sus], the doping with Fe results in rapid suppression of the antiferromagnetic order and a decrease of the Néel temperature. Reported temperatures differ significantly, especially for higher Fe concentrations.

Al-Fe-based compounds. $FeAl_2$, Fe_2Al_5, and Fe_4Al_{13} dissolve up to 4.5, 6.2, and 7 at.% Cr according to [1997Pal, 2014Pav, 2019Ran, 2020Ran]. Cr has no effect on the formation temperatures of these compounds.

Ternary phases. Four quasicrystal approximants and a decagonal phase are usually denoted using either Greek or Latin letters, for which no ideal stoichiometries were reported. This type of denomination with certain amendments was accepted in this evaluation.

The icosahedral ε-(Cr,Fe)Al_4 approximant has an orthorhombic structure. [2011Kho1] found that it belongs the *Pbnm* space group, while [2014Pav] proposed the *Immm* space group. Detailed XRD study of the Czochralski-grown single crystal by [2010Bau, 2011Bau] showed that this phase has a *Cmcm* structure. It originates from the Al-Cr system being however metastable in the binary system. Small additions of the third component stabilize this compound, so it becomes a real ternary phase. ε-(Cr,Fe)Al_4 forms *via* a three-phase peritectic reaction at 1055°C according to [2011Kho1]. It is stable in a narrow composition range at around 2-3 at.% Fe and 78-77 at.% Al [2010Bau, 2011Bau, 2011Kho1].

The decagonal approximant o-(Cr,Fe)Al_4 was for the first observed by [1995Sui] and by [1997Sui] (reported as O-AlFeCr), [1998Lia] and later confirmed by [2004Den, 2009Bau, 2010Bau, 2011Bau, 2013Bau, 2014Gas] As it was already discussed above, o-(Cr,Fe)Al_4 has a highly modulated structure according to [2013Bau, 2014Gas] and is structurally very similar to the binary Cr_2Al_{11} compound. The o-(Cr,Fe)Al_4 crystal structure is still not fully solved. The structural models reported by [2004Den, 2010Bau, 2011Bau, 2013Bau, 2014Gas] present an “average” model. The model of [2013Bau] was accepted in the present evaluation since it yields the best fitting of the experimental data. The available experimental data on the phase equilibria with o-(Cr,Fe)Al_4 are scarce. As suggesting the data of [2010Bau, 2011Bau, 2014Pav], this compound most probably forms between 1000°C and 1042°C and has small homogeneity range (see Table 2).

The decagonal approximant O_1 was observed in a slowly cooled multiphase sample by [2000Dem] (denoted as $C_{3,I}$) and later confirmed by [2008Pav2, 2010Pav, 2014Pav] in their studies of equilibrated samples. Its structure is still not solved, and the lattice parameters were reported without specifying the composition of the phase. While [2000Dem] reported orthorhombic primitive cell with *a* = 3270 pm, *b* = 1250 pm, *c* = 2380 pm, [2008Pav2] suggested a *B*-centered orthorhombic cell with *a* ≈ 3270 pm, *b* ≈ 1240 pm, *c* ≈ 2340 pm. Neither [2010Pav] nor [2014Pav] made attempts to further clarify the O_1 crystal structure. The results of [2010Pav, 2011Kho1, 2011Kho2, 2014Pav] suggest that the homogeneity range extends between approximately $Cr_{15.0}Fe_{11.0}Al_{74.0}$ to $Cr_{19.7}Fe_{4.3}Al_{76.0}$ and $Cr_{15.0}Fe_{6.9}Al_{78.1}$ to $Cr_{18.3}Fe_{8.9}Al_{72.8}$ (at.%). According to [2011Kho1], O_1 forms *via* a three-phase peritectic reaction at 1087°C.

[1999Sui, 2000Mo, 2003Zou, 2008Pav3, 2010Bau, 2011Bau] reported on the formation of a ternary hexagonal icosahedral approximant – H phase. Based on their high-resolution electron microscopy measurements, [1999Sui, 2000Mo] concluded that this compound with a $Cr_{11}Fe_8Al_{81}$ (at.%) composition belongs to the $P6_3/m$ space group. [2008Pav3] and later [2010Pav] claimed that this type of structure was not found in their samples containing the H phase. Detailed study of the $Cr_{12.26}Fe_{7.45}Al_{80.29}$ and $Cr_{13.35}Fe_{6.63}Al_{80.02}$ (at.%) single crystals grown by the Czochralski-method using the XRD method by [2010Bau, 2011Bau] revealed that the H compound has a rhombohedral $R\bar{3}$ structure with a large elementary cell containing 1512 atoms. This structure was accepted in the present evaluation. The H homogeneity range extends between approximately $Cr_{12.0}Fe_{8.0}Al_{80.0}$ to $Cr_{19.7}Fe_{4.3}Al_{76.0}$ and $Cr_{11.0}Fe_{6.3}Al_{82.7}$ to $Cr_{13.5}Fe_{7.0}Al_{79.4}$ (at.%) [2019Eze, 2011Kho1]. According to [2011Kho1], this phase forms *via* a four-phase peritectic reaction at 998°C.

A decagonal phase, D, was for the first time reported by [2008Pav2] as a result of their TEM examination. [2009Pav] and later [2020Ma] reported that this phase has periodicity along the 10-fold symmetry axis, and its structure is similar to the D_3 decagonal phase in the Al-Mn-Pd system [1994Ste, 1999Gru]. According to [2009Pav, 2014Pav], D is structurally related to the O_1 compound so that these phases can be reliably resolved using the TEM technique only. The D homogeneity range extends from 70 to 72 at.% Al and from 14 to 18 at.% Cr. It forms *via* a three-phase peritectic reaction at 1096°C according to [2011Kho1].

Metastable phases. In the Cr-Fe system, the metastable miscibility gap of (Cr, αδFe) is observed between 500 and 600°C - in the temperature range of the σ phase existence, if the formation of the latter is suppressed. In spite of numerous investigations, the determined location of the metastable miscibility gap seems still ambiguous even in the binary system, especially for the critical temperature of the miscibility gap. In the ternary system, [1971Yam] studied the influence of Al on the metastable miscibility gap of (Cr, αδFe). The authors studied several Cr-rich samples that were annealed for 5 hours at around 1200°C and subsequently aged at 480°C. According to [1971Yam], the critical temperatures of the miscibility gap slightly increase due to the addition of aluminium. The region itself extends up to 5 at.% Al inside the ternary system.

[1993Sta, 1995Sta, 1995Zia, 2006Kar] observed an icosahedral six-dimensional structure (denoted as *i* in the present evaluation) in the $Cr_8Fe_6Al_{86}$, $Cr_{3.4}Fe_8Al_{88.6}$, $Cr_3Fe_3Al_{94}$, $Cr_2Fe_4Al_{94}$, $Cr_3Fe_1Al_{94}$ (at.%) alloys. Earlier a metastable icosahedral ternary phase was also reported by [1987Wou, 1988Man, 1989Man, 1988Sch, 1989Law1, 1989Law2, 1989Man]. According to [1993Sta, 1995Sta], the value of the six-dimensional hypercubic lattice constant is a_{6D} = 654 pm. [1995Zia] performed the EDX measurements using a scanning transmission electron microscopy and suggested the composition of the phase to be $Cr_{12\pm1}Fe_{12\pm1}Al_{75\pm0.5}$ (at.%). The *i* phase is metastable and emerges during the rapid solidification of the samples. The as-prepared structure usually consists of the icosahedral phase distributed in the (Al) matrix. Upon heating, the *i* phase decomposes into a mixture of stable and metastable phases depending on the heat treatment conditions [1993Sta, 1995Sta, 1995Zia, 2006Kar]. Equilibrium Fe_3Al_{14}, $CrAl_7$, and metastable $FeAl_6$ phase are often reported among the products of the icosahedral phase decomposition. [1995Zia] also detected an unknown metastable phase with an orthorhombic structure. The authors argued that this structure could be an allotrope of Fe_3Al_{14}. The crystal structure however remained unsolved.

[1999Sui, 2000Dem, 2001Dem, 2006Dem] reported several other structures to exist in multiphase samples: hexagonal κ-(Al-Cr-Fe) [1999Sui], orthorhombic decagonal O_1-AlCrFe approximant [2000Dem, 2001Dem], and two decagonal approximants denoted as O_A-(Al-Cr-Fe) and O_B-(Al-Cr-Fe) by [2006Dem]. The orthorhombic O_1-AlCrFe approximant was also observed in thin films produced by a flash evaporation technique by [2004Dem]. [2004Dem] also reported cubic β-AlCrFe phase, orthorhombic decagonal O_F-AlCrFe and O_E-AlCrFe approximants, and monoclinic X-AlCrFe phase. None of these structures were observed in the subsequent studies on the phase equilibria published since 2008. [2000Dem, 2001Dem, 2006Dem] provided neither compositions nor stoichiometries of the observed phases. The compositions measured by the EDS technique [2004Dem] are doubtful, as suggested by the values measured for the Fe_4Al_{13} compound. Hence, the structures reported by [2000Dem, 2001Dem, 2004Dem, 2006Dem] were not included in Table 2.

Invariant Equilibria

The data on the invariant equilibria were reported by [1932Tai1, 1932Tai2, 1943Mon, 1960Zol2, 1973Wil, 1976Mon, 1987Sau, 1995Zia, 1995Sta] (discussed in the previous evaluation by [2007Gho]) and recently by [2011Kho2, 2019Eze]. The reaction scheme shown in Fig. 3 is based on that drawn by [2011Kho2], which is the most detailed one. But further modifications were introduced to preserve consistency with the Al-Fe and Al-Cr phase diagrams accepted in the present evaluation and to take the recent results of [2010Bau, 2011Bau, 2013Bau, 2014Gas] on o-$(Cr,Fe)Al_4$ and [2019Eze] for liquidus and solidus projections into account. In particular, reactions with

o-(Cr,Fe)Al_4 were introduced in the reaction scheme. They are shown with dashed lines because of the contradictions in the data reported for this compound and closely related Cr_2Al_{11} (see the discussion in the *'Solid Phases'* section).

[2010Bau, 2011Bau] observed o-(Cr,Fe)Al_4 instead of Cr_2Al_{11} being in equilibrium with the liquid phase at around 1000°C. Based on the experimental data of [2010Bau, 2010Pav, 2011Bau, 2011Kho1, 2011Kho2, 2014Pav], it has been therefore assumed in the present evaluation that o-(Cr,Fe)Al_4 forms at around 1026°C. The peritectic L + ε-(Cr,Fe)Al_4 + O_1 ⇌ Cr_2Al_{11} reaction as reported by [2011Kho2] was replaced by L + ε-(Cr,Fe)Al_4 + O_1 ⇌ o-(Cr,Fe)Al_4 (denoted as P_1 in Fig. 3). In the subsequent U_5 and U_6 reactions, the participation of o-(Cr,Fe)Al_4 instead of Cr_2Al_{11} was assumed.

Despite the scatter in the reported liquidus and solidus temperatures measured by [2010Pav, 2011Kho1, 2011Kho2, 2014Pav], the reported values reveal that Fe increases the Cr_2Al_{11} melting temperature. Therefore, it has been suggested in the present evaluation that Cr_2Al_{11} forms between 913 and 985°C in the ternary system *via* the P_3 peritectic reaction. The additional U_7 reaction at 900 < *T* < 980°C was introduced in the reaction scheme to preserve agreement with the data reported by [2011Kho1, 2011Kho2, 2014Pav, 2019Eze] for lower temperature.

The L + H ⇌ $CrAl_7$ + (Al) and L + H ⇌ Fe_4Al_{13} +(Al) reactions reported by [2011Kho1, 2011Kho2] for 660 and 657°C were replaced by L + H ⇌ $CrAl_7$ + Fe_4Al_{13} (U_9) and L + $CrAl_7$ ⇌ Fe_4Al_{13} + (Al) (U_{10}) found by [2019Eze]. [2019Eze] used longer annealing at sub-solidus temperatures for their samples than [2011Kho1, 2011Kho2], which allowed achieving a greater equilibrium state in the samples at low temperatures. The temperatures of U_9 and U_{10}, as well as of the U_8 reaction, are accepted after [2011Kho2]. The values determined by [2019Eze] for U_8 and U_9 are most probably too high due to the overheating effect as the temperature measured for the L+Cr_2Al_{11}⇌$CrAl_7$ reaction in the Al-Cr system suggests. The compositions of solid phases participating in the P_2 and U_8 reactions are also accepted according to [2011Kho1], as these values are in better agreement with the data reported by [2010Bau, 2011Bau, 1997Pal, 2014Pav] than those measured by [2019Eze].

The resulting reaction scheme is shown in Fig. 3, and the coordinates of the invariant reactions are given in Table 3.

Liquidus and Solidus Surfaces

[2007Gho] evaluated the experimental data [1932Tai1, 1932Tai2, 1935Gru, 1945Kor, 1951Pra, 1954Chi, 1960Zol1, 1960Zol2, 1970Koz1, 1970Koz2, 1987Sau, 1991Tre] and calculation results [1970Koz1, 1970Koz2, 1974Vya, 1987Sau] published for the Al-Cr-Fe liquidus and solidus surfaces until 2007. At that time, the corresponding information was limited to the partial liquidus surface in the Al corner and tentative isotherms of liquid phase drawn in the composition range between 0-60 at.% Al. The studies of [2011Kho1, 2011Kho2, 2019Eze] significantly contributed to the establishment of liquidus and solidus surface projections at 50-100 at.% Al. For lower Al content, new experimental data are limited to the works of [2019Ran, 2020Ran], who measured liquidus and solidus temperatures for four alloys containing 5-35 at.% Fe at 52.5 at.% Al and three alloys containing 13-28 at.% Fe at 66 at.% Al. [2020Ran] thermodynamically assessed the Al-Cr-Fe system and calculated a liquidus surface projection in the whole composition range. Not all invariant reactions reported by [2011Kho1, 2011Kho2, 2019Eze] could be reproduced in the calculations by [2020Ran], which is probably due to the fact that homogeneity ranges of ternary compounds were not modeled, and O_1 reported by [2004Den, 2008Pav2] and o-(Cr,Fe)Al_4 found by [2010Bau, 2011Bau, 2013Bau, 2014Gas] were considered as the same ternary phase. This assessment is still of high importance as it presents a good attempt to model quite complex phase equilibria in the whole composition range.

The liquidus surface projection in the whole composition range is shown in Fig. 4a. It is a combination of the liquidus surface projection reported by [2011Kho2] for 55-100 at.% with amendments described in the *'Invariant Equilibria'* section and liquidus surface projection calculated by [2020Ran] for 0-50 at.% Al with modifications described below.

No invariant reactions were reported in the composition range between 0 and 50 at.% Al. The isotherms of the liquid phase calculated by [2020Ran] were adjusted to preserve consistency with the Al-Cr and Cr-Fe phase diagrams. In the Cr-rich part, the deviation between the liquidus lines of the Al-Cr and Cr-Fe phase diagrams accepted in the present evaluation and those used by [2020Ran] is significant. Therefore, the isotherms at 1550-1800°C were drawn based on the data for the binary phase diagrams and ternary system reported by [1945Kor, 1991Tre]. The relevant experimental information is scarce and uncertain. Hence, the isotherms are shown with dashed lines. The isotherms at 1350-1500°C calculated by [2020Ran] were slightly adjusted.

The type and coordinates of the invariant reaction between liquid, (Cr, αδFe), ordered FeAl, and $(Cr,Fe)_5Al_8$ were neither established experimentally nor calculated by [2020Ran]. The extension of the corresponding monovariant lines into the ternary system is schematical. The reactions and monovariant lines involving o-(Cr,Fe)Al_4 and Cr_2Al_{11} are also tentative since the relevant experimental data are contradictory (Fig. 4b).

Figure 5 shows solidus surface projection in the range of compositions 60-100 at.% Al. It is based on the solidus presented by [2011Kho1] with further amendments required to preserve the consistency with the binary Al-Cr and Al-Fe diagram, as well with the reaction scheme and liquidus surface constructed in the present evaluation. The tie-lines corresponding to the maxima in the monovariant lines were added to the solidus surface projection in the present evaluation. The position of the tie-lines is tentative and drawn with dashed lines based on the experimental data [1997Pal, 2011Kho1, 2011Kho2, 2014Pav]. The solubility of iron in Fe_4Al_{13} below 998°C (the P_2 reaction) was adjusted, taking the data reported for the isothermal sections by [1997Pal, 2014Pav] into account.

Isothermal Sections

Partial isothermal sections were constructed by [1945Kor, 1946Kor] at 1150°C, by [1958Chu] at 600-900°C, by [1997Pal] and [2008Pav2] at 1000°C, by [2009Pav] at 1075°C, by [2014Pav] at 700-1160°C, by [2015Zho] at 700°C, and by [2019Ran] at 700, 900°C. [2017Wan] calculated phase equilibria at 50-100 at.% Al and 700-1160°C. Full isothermal sections were calculated by [2019Cha] at 320-925°C and [2020Ran] 700-1160°C. The calculated sections present a simplification of the phase equilibria in the ternary system, since the homogeneity ranges of ternary phases and $CrAl_2$ were not modeled. None of the assessments includes o-(Cr,Fe)Al_4 found by [2010Bau, 2011Bau, 2013Bau, 2014Gas]. The sections by [2020Ran] were however used in the present evaluation to construct the phase equilibria in the Cr- and Fe-rich part of the system in view of the lack of reliable experimental data for this composition region. The order-disorder transition as modeled by [2020Ran] is not included in the sections because of the controversial nature of the data used for the modeling (see *'Solid Phases'* section). The extension of the corresponding phase boundary into the ternary system is tentative in all the sections.

Figure 6 shows an isothermal section at 1160°C. [2014Pav] reported only six tie-lines for this section. The corresponding segments of the (Cr, Fe)$_5Al_8$ homogeneity range and the (Cr, Fe)$_5Al_8$ + FeAl phase boundary are shown with solid lines. The rest of the phase boundaries are tentative. The αCr_5Al_8 homogeneity range, L+αCr_5Al_8+(Cr, αδFe) tie-triangles, and phase boundary involving the liquid phase are constructed based on the liquidus and solidus data by [2011Kho1, 2011Kho2]. The (γFe) homogeneity range is according to [2020Ran]. This section shows a continuous solid solution existing between $\beta CrAl_8$ and Fe_5Al_8. Figure 7 shows the isothermal section at 1100°C. The phase equilibria, which were experimentally confirmed by [2014Pav], are shown with solid lines. The phase equilibria involving the liquid phase were slightly amended in accordance with the liquidus and solidus data by [2011Kho1, 2011Kho2]. The phase boundaries involving (Cr, αδFe) and (γFe) are reproduced according to the modeling of [2020Ran]. All phase boundaries were adjusted to preserve compatibility with the Al-Cr and Al-Fe diagrams.

The isothermal section at 1075°C in Fig. 8 is based on the data reported by [2014Pav] with the (Cr, αδFe) and (γFe) phase boundaries accepted after [2020Ran]. Small adjustments to preserve compatibility with the Al-Cr and Al-Fe diagrams were introduced. The main change introduced in this section concerns the O_1 phase. Contrary to [2011Kho1, 2011Kho2], [2009Pav, 2014Pav] stated that O_1 does not exist at 1075°C but forms at 1048°C according to the DTA measurements performed by [2014Pav]. First and foremost, the proposed temperature of the O_1 formation is only 6°C higher than the isothermal section at 1042°C (Fig. 9) also constructed by [2014Pav]. In this section, O_1 already has a large homogeneity range suggesting that the ternary phase forms at temperatures higher than 1048°C. Since [2011Kho1, 2011Kho2] and [2014Pav] used comparable annealing times at approximately the same temperatures, the data of [2011Kho1, 2011Kho2] were preferred to those of [2009Pav, 2014Pav]. The O_1 homogeneity range and the corresponding phase equilibria were added in the section. Figure 8 also shows the U_2 plane as reported by [2011Kho1, 2011Kho2]. Figure 9 shows phase equilibria at 1042°C. The partial isothermal section reported by [2014Pav] was complemented by the (Cr, αδFe) and (γFe) phase boundaries reported by [2020Ran]. At this temperature, ε-(Cr,Fe)Al_4 is already stable in the ternary system.

The isothermal section at 1000°C (Figs. 10a and 10b) is based on the data of [1997Pal, 2011Kho1, 2011Kho2, 2014Pav, 2020Ran]. The phase equilibria confirmed experimentally are shown with solid lines. The o-(Cr,Fe)Al_4 homogeneity range and relevant phase equilibria are constructed taking the data of [2010Bau, 2011Bau, 2013Bau, 2014Gas] into account. The phase transformations involving o-(Cr,Fe)Al_4, ε-(Cr,Fe)Al_4, and $CrAl_4$ (Fig. 10b) are tentative and require further experimental confirmation.

The isothermal sections at 900°C (Figs. 11a and 11b) and 700°C (Figs. 12a and 12b) constructed by [2019Ran] were adopted in the present evaluation. They were further modified to take the homogeneity ranges of D, O_1, o-(Cr,Fe)Al_4, ε-(Cr,Fe)Al_4 and H into account. This was done using the data of [2011Kho1, 2011Kho2, 2014Pav, 2019Eze]. The tie-line and tie-triangles measured by [2015Zho] in the Al-corner at 700°C were ignored in the present evaluation. They contradict other experimental datasets in the ternary system and the Al-Fe and Al-Cr phase diagrams. The phase boundary involving Cr_2Al at 900°C was added in the present evaluation to preserve agreement with the accepted

binary phase diagram. The (γFe) and σ phase boundaries are according to [2020Ran]. The σ homogeneity range at 700°C is in good agreement with the experimental data of [1958Chu], while the (Cr, αδFe)+σ region is much wider than that constructed by [1958Chu].

650°C is the lowest temperature at which the isothermal section was constructed in the present work. The experimental data at this temperature are limited to the data of [2019Eze] in the Al-rich corner and [1958Chu] for the σ phase. The isothermal section at 650°C shown in Fig. 13 is very similar to that at 700°C. The main difference is the $CrAl_7$+(Al)+Fe_4Al_{13} and $CrAl_7$+H+Fe_4Al_{13} tie-triangles that replace L+H+Fe_4Al_{13} and L+H+$CrAl_7$ as a result of the U_{10} reaction according to [2019Eze]. The σ homogeneity range is reproduced according to [1958Chu]. The (Cr, αδFe)+σ boundary is drawn in the present evaluation and is tentative.

The partial isothermal sections at 1150°C by [1945Kor, 1946Kor], at 600, 750°C by [1958Chu], and at 800°C by [2014Pav] do not provide any new information on the phase equilibria. The available experimental data are too scarce to construct full sections, and no calculations were performed at these temperatures. Hence, these sections are not reproduced in the present evaluation.

Temperature – Composition Sections

Attempts to construct the vertical sections were made by [1969Bul1, 1946Kor, 1991Tre, 2019Ran, 2020Ran]. [1946Kor] gave four isopleths at constant mass ratios of Cr/Fe. These diagrams contradict the isothermal sections shown in Figs. 6 to 13. Partial isopleths at 25 at.% Al and 75 at.% Fe constructed by [1969Bul1] include the order-disorder transformations only. As discussed in the *'Solid Phases'* section, the relevant experimental data are contradictory, and the formation of the stoichiometric Heusler phase reported by [1969Bul1] is doubtful. [2019Ran, 2020Ran] constructed a partial isopleth at 52.5 at.% Al. This isopleth contradicts both the Al-Cr and Al-Fe phase diagrams. The available information is not enough to correct it. Therefore, the vertical sections reported by [1969Bul1, 1946Kor, 1991Tre, 2019Ran, 2020Ran] are not reproduced here.

Figure 14 shows the temperature-composition section Cr-FeAl of the phase diagram according to [1991Tre] with slight corrections according to the accepted boundary binary Al-Fe system constitution. The order-disorder transformation reported by [1991Tre] was not included in the diagram.

Thermodynamics

The experimental studies on the thermodynamic properties of the Al-Cr-Fe phases were performed by [1961Gul, 1977Ost, 1992Hil, 1997Rud, 2008Jac, 2013Mar]. [1977Ost] studied the heats of dissolution of aluminium in a melt of $Cr_{30}Fe_{70}$ (at.%) at temperatures between 1550 and 1600°C. The experimental results, which have been available in the literature at that time, are in good agreement with calculations based on the application of the subregular model. The heat capacities of the Fe_3Al-based alloy with a Cr content of 5 at.% have been measured in the temperature range from 20 to 700°C by [1997Rud] (also cited in the review of [2004Sim]).

[1961Gul, 1992Hil, 2008Jac, 2013Mar] measured activities of Al, Cr, Fe in the (Cr, αδFe) phase using different methods. [2008Jac] analyzed the experimental data reported by other research groups and came to the conclusion that the results of [1961Gul] are not consistent with those of [1992Hil, 2008Jac]. [1992Hil] studied the vaporization of the $Cr_{19.8}Fe_{75.4}Al_{4.8}$ (mass%) ($Cr_{19.96}Fe_{70.72}Al_{9.32}$ in at.%) alloy using Knudsen effusion mass spectrometry (KEMS) in the temperature range 1040-1283°C. This composition virtually agrees with those of the commercial Aluchrom and MA956 alloys. [2008Jac] studied two samples – $Cr_{15.1}Fe_{45.1}Al_{39.8}$ and $Cr_{30.2}Fe_{49.9}Al_{19.9}$ (at.%) – in the temperature range between 877 and 1277°C using KEMS. [2013Mar] investigated the vaporization of seven ternary alloys in the temperature range 961-1335°C by KEMS. This later study reveals the deviation from Raoult's law is slightly positive for a_{Cr}, negative for a_{Cr}, and sign-changing for a_{Al}. The obtained thermodynamic data are summarized in Table 4.

Thermodynamic properties of ordered phases were calculated by [1988Hoc, 2003Kel, 2016Dah, 2019Wan, 2021Liu]. Applying a defect model, [1988Hoc] calculated the activity of Cr in FeAl, assuming that FeAl is either a compound or a solid solution. The calculated results do not show a significant discrepancy, and both cases suggest complete solid solubility between Cr and FeAl. The energy of formation of the ordered $CrFe_2Al$ ($L2_1$) compound was calculated by [2003Kel, 2016Dah, 2021Liu]. The calculated energies of formation are negative suggesting that the stoichiometric $L2_1$ Heusler phase can form in the Al-Cr-Fe system. By combining first-principle and cluster variation method calculations, [2019Wan] calculated energies of formation of the phases with different ordering types and isothermal sections between 327 and 2727°C. The authors predicted the formation of a $B32$ ternary ordered phase in the system. The modeling of [2003Kel, 2016Dah, 2019Wan, 2021Liu] does not include other phases which are stable in the ternary system. Hence, they did not give an answer whether the $L2_1$ and $B32$ phases are equilibrium or metastable in

the Al-Cr-Fe system. For the same reason, the isothermal sections of [2019Wan], which include only (Cr, αδFe), and its ordered polymorphs do not reflect the real phase equilibria in the system.

[1975Kau, 1970Koz2, 1987Sau] performed the very first thermodynamic modeling of the phase equilibria in the system. [2000Sub, 2017Wan, 2019Cha, 2020Ran] performed thermodynamic assessments of the Al-Cr-Fe system in the frameworks of the standard CALPHAD method. [2020Ran] presented the most comrehensive assessment of the system by calculating the isothermal sections between 700 and 1160°C, as well as the liquidus surface. However, these works present a simplification of the phase equilibria in the ternary system, since the homogeneity ranges of many phases, in particular ternary ones, were not modeled.

Notes on Materials Properties and Applications

Al-Cr-Fe alloys are of interest as lightweight alloys for structural applications, in particular, for the production of protective coatings formed by alumina scales from alloys of compositions that lie in the Al-rich corner of the system. Al-Cr-Fe quasicrystal approximants are also potential candidates for new applications because of their specific properties. Alternatively, the addition of chromium to Fe_3Al- and FeAl-based alloys produces excellent candidates for moderate and high-temperature applications. The Al-Cr-Fe alloys serve as a basis of high-chromium-containing single-phase ferritic alloys surfaces that are commonly used in high-temperature radiant heating applications. Data on some investigations regarding materials properties are listed in Table 4.

[2005Pal] showed that strengthening of Al-Fe-based alloys at high temperatures could be achieved through solid-solution hardening, precipitation of incoherent or coherent particles and by ordering. However, in the Al-Cr-Fe ternary system, within a large composition region (up to 50 at.% Al) strengthening of the alloys can be achieved only through solid solution hardening. At higher Al contents, the possibility of precipitating a second phase, *e.g.* $(Cr,Fe)_5Al_8$ phase, exists.

Mechanical properties of Fe_3Al-based alloys were investigated by [1991Sik1, 1993Kni, 1998Sun, 2004Hua]. According to [1991Sik1], room-temperature tensile ductility of the samples with 2 to 5 mass% Cr (1.3 and 3.3 at.%, respectively), prepared using the melting process described in [1991Sik2], approach 20%, which should be acceptable for many practical applications, and [1993Kni] established that increasing the Cr content from 2 to 5 mass% has a small effect on the ductility of the alloys based on Fe_3Al. [1998Sun] established that chromium significantly affected the room temperature tensile properties in a vacuum. In comparison with binary Fe_3Al, in the $Cr_{5.38}Fe_{70.42}Al_{24.20}$ (at.%) alloy (arc melted, then forged at 1000°C, rolled into plates with thickness of 1.0-1.2 mm within the temperature range between 950 and 600°C; the plates were then annealed at 750°C for 1 h, followed by ordering treatment at 500°C for 13 d) a decrease in yield strength from 841 to 695 MPa, increase in elongation from 5.18 to 9.1% and ultimate tensile strength from 990 to 1084 MPa take place. Two large ingots weighing 269 or 104 kg, with the approximate composition of 5.5Cr-78.6Fe-15.9Al (at.%) and the presence (according to the conventional chemical analysis) of small amounts of C, Si, Mn, P and S, were prepared by [2004Hua] using vacuum induction melting and top cast. They had a satisfying surface appearance, and no crack was detected. Conventional thermomechanical processes were used to produce bars, sheets and seamless tubes. By controlling the thermomechanical treatment, a room temperature ductility with a value of more than 10% was achieved. The creep lifetime at 600°C and 200 MPa was more than 2000 h after annealing.

A high-temperature alloy $Cr_5Fe_{82.5}Al_{12.5}$ (mass% or $Cr_{4.7}Fe_{72.55}Al_{22.75}$ in at.%) has been developed for applications in the range from room temperature to 300°C. The billets of the alloy were obtained by [2013Nei] in two ways: using gas-atomized and water-atomized powders. Structural analysis shows that particles of the second phase in the water-atomized powders are finer and their number in the aluminum matrix is greater than that in the gas-atomized powders. The rods extruded from the water-atomized powders have much higher hardness, ultimate strength, and yield stress than those from the gas-atomized powders, plasticity being acceptable at all temperatures (20, 190, and 300°C). An additional powder metallurgy operation – pulsed hot pressing – does not increase the strength of billets from either the water-atomized or gas-atomized powders. The alloy based on the water-atomized 0-63 μm powder shows the maximum strength: 483, 332, and 261 MPa at 20, 190, and 300°C, respectively.

Electrical resistance anomaly in Fe_3Al-based alloys, in particular with chromium, is analyzed in the review of [1998Nis]. It was noted that the electrical resistivity shows an anomalous temperature dependence: an appearance of a resistance maximum near the Curie point and a negative resistivity slope at higher temperatures.

It was noted by [2011Kim] that the alloy $Cr_{22}Fe_{72.2}Al_{5.8}$ (mass%) or $Cr_{21.9}Fe_{66.95}Al_{11.15}$ (at.%) has been drawing industrial attention for its outstanding high-thermal and oxidation resistance as well as for its applicability as a filter and support material.

The main modes of isothermal oxidation of Al-Cr-Fe, Al-Cr-Ni, and Al-Cr-Co alloys in oxygen at 1000 and 1200°C are summarized in [1971Sto]. It was noted that where protective αAl_2O_3 scales always predominate, their ease of formation was in the order Al-Cr-Fe > Al-Cr-Ni > Al-Cr-Co, however, where catastrophic breakaway is possible, Al-Cr-Fe produces the most locally catastrophic breakaway. [2002Dem] concluded that resistance to oxidation in water as well as at high temperatures is signicantly enhanced thanks to the addition of Cr. Electron energy loss spectroscopy measurements of the very thin Al-Cr-Fe films (10-30 nm) obtained by the flash evaporation technique show that all of them are not oxidized except for the presence of a native oxide layer that forms in an ambient atmosphere with a thickness that cannot exceed 0.3 nm [2004Dem]. It was concluded by [2005Zha] that the addition of chromium is obviously beneficial for the oxidation resistance of $Fe_{90}Al_{10}$ (at.%) by inhibiting the formation of fast-growing Fe-containing oxides and promoting the development of an exclusive alumina layer, however, the effect of chromium is different from the classical third-element effect.

The catalytic activity of the Al-Cr-Fe alloys was studied by [2008For]. As a whole, catalytic devices play a very important role in drastic reduction of the noxious contaminants released by combustion engines. Common devices consist of functionalized ceramic monoliths; an interesting alternative can be realized with a support material made of a high-temperature compatible metal alloy, like Al-Cr-Fe. In [2008For], the $Cr_{25}Fe_{70}Al_5$ (at.%) fibers used to make a device similar to the ceramic monolith were thermally treated to obtain alumina whiskers, which were homogenously covered with alumina or ceria-zirconia-alumina washcoats. Pt or Pt and Pd have been loaded over the functionalized fibers obtaining an innovative oxidation catalyst. The good catalytic activity after severe aging treatments conrms the possibility of use of these innovative functionalized metallic stacks in air pollution control applications [2008For]. The Al-Cr-Fe alloys are proposed for use as a support for monolithic catalysts Cu_xCo_{1x}/Al_2O_3/CrFeAl for toluene catalytic combustion [2010Zha].

A review of the mechanical properties and application of the Al-Fe-based, particularly Al-Cr-Fe, alloys is presented by [2005Pal].

Miscellaneous

[1970Koz3] reported the solubility of C in liquid Al-Cr-Fe alloys at different temperatures. The formation and growth characteristics of iron-based aluminide diffusion layers at the Al-Fe interface have been analyzed by [1998Akd] in terms of interfacial interaction potentials based on the statistico-thermodynamical theory of multicomponent alloys combined with electronic theory in the pseudopotential approximation. The pairwise interatomic interaction potentials and partial ordering energies have been calculated to predict the effect of various alloying additions, in particular, of chromium, on the activity coefficient of Al atoms and considered up to 1 at.%. The calculation results show that chromium decreases the activity coefficient of Al atoms in (αFe). So as to reduce the thickness of the Al-Fe intermetallic diffusion layer. The influence of aluminium on the kinetics of the σ phase formation in alloys at the equiatomic Cr/Fe ratio with fine- and coarse-grained structures was studied by [2000Bla] using ^{57}Fe Mössbauer spectroscopy. It was found that the addition of 0.2 at.% Al slightly accelerated the kinetics in the coarse-grained samples, and practically did not affect the fine-grained samples. On the other hand, doping with 1 at.% Al resulted in significant retardation of the σ phase formation both in the fine-grained samples as well as in the coarse-grained samples.

[1989Aku] measured interdiffusion coefficients at 31 points in the (αδFe) phase at 900°C. The results indicate that $\overline{D}^{Fe}_{CrCr}$ falls quickly with increasing chromium concentration, with aluminium concentration more than 20 at.%, but is not a strong function of aluminium content. Conversely, $\overline{D}^{Fe}_{AlAl}$ is not a strong function of aluminium concentration but decreases with increasing chromium content.

According to [2010Air], *ab initio* calculations combined with experiments on the $Cr_{10}Fe_{80}Al_{10}$ (at.%) alloy show that the beneficial effect of Cr on the oxidation resistance is signicantly related to bulk effects. The comparison of experimental and calculated results indicated a clear correlation between the Cr-Fe chemical potential difference and the formation of the protective oxide scales.

[2015Sus] have performed an experimental and theoretical study comparing the effects of Fe-doping of Cr_2Al, an antiferromagnet with a Neel temperature of 670 K, with known results on Fe-doping of antiferromagnetic *bcc* Cr. $(Cr_{1-x}Fe_x)_2Al$ materials are found to exhibit a rapid suppression of antiferromagnetic order with the presence of Fe, decreasing T_N to ≈ 170 K for $x = 0.10$. Antiferromagnetic behavior disappears entirely at $x = 0.125$, after which point increasing paramagnetic behavior is exhibited. This is unlike the effects of Fe doping of *bcc* antiferromagnetic Cr, in which T_N gradually decreases, followed by the appearance of a ferromagnetic state. Theoretical calculations explain that the Cr_2Al-Fe suppression of magnetic order originates from two causes: the first is band narrowing caused by doping of additional electrons from Fe substitution that weakens itinerant magnetism; the second is magnetic frustration of the Cr itinerant moments in Fe-substituted Cr_2Al. In pure-phase Cr_2Al, the Cr moments have an

antiparallel alignment; however, these are destroyed through Fe substitution and the preference of Fe for parallel alignment with Cr. This is unlike bulk Fe-doped Cr alloys in which the Fe anti-aligns with the Cr atoms, and speaks to the importance of the Al atoms in the magnetic structure of Cr_2Al and Fe-doped Cr_2Al.

Acknowledgments

The authors express their gratitude to Dr. Martin Palm (Department of Structure and Nano/Micromechanics of Materials, Max-Planck-Institut für Eisenforschung GmbH, Düsseldorf, Germany), Prof. Peter Franz Rogl (Department of Materials Chemistry, Department of Physical Chemistry, University of Vienna, Austria), Prof. Andreas Leineweber (Institute of Materials Science, TU Bergakademie Freiberg, Germany), and Prof. Vitaliy Romaka (Chair of Inorganic Chemistry, TU Dresden, Germany) for their comments and help with the critical evaluation of the Al-Cr-Fe system.

References

[1932Tai1] Taillandier, M.Ch., "Contribution on the Study of Aluminium-Iron-Chromium Alloys, Part I" (in French), *Rev. Metal.*, **29**, 315-325 (1932) (Phase Diagram, Phase Relations, Experimental, 8)

[1932Tai2] Taillandier, M.Ch., "Contribution on the Study of Aluminium-Iron-Chromium Alloys, Part II" (in French), *Rev. Metal.*, **29,** 348-356 (1932) (Phase Diagram, Phase Relations, Experimental, 19)

[1935Gru] Grunert, A., Hesselbruch, W., Schistal, K., "On the High Heat-Resistant Cr-Al-Fe Alloys with and without Cobalt" (in German), *Electrowaerme*, **5**, 131-132 (1935) (Phase Relations, Experimental, 2)

[1940Kor1] Kornilov, I.I., Mikheev, V.S., Konenko-Gracheva, O.K., "Equilibrium Diagram of the Ternary Fe-Cr-Al System (Preliminary Communication)" (in Russian), *Stal'*, (5/6), 57-59 (1940) (Phase Diagram, Experimental, *, 3)

[1940Kor2] Kornilov, I.I., "New Heat-Resistant Fe-Cr-Al Alloys with High Electrical Resistance" (in Russian), *Izv. Akad. Nauk SSSR, Ser. Khim*., (5), 751-757 (1940) (Morphology, Experimental, Electrical Properties, 15)

[1943Mon] Mondolfo, L.F., "Al-Cr-Fe", in "*Metallography of Aluminium Alloys*", John Wiley & Sons Inc., New York, 70-71 (1943) (Phase Diagram, Review, *, 1)

[1945Kor] Kornilov, I.I., "Alloys of Fe-Cr-Al" in "*Iron Alloys*" (in Russian), **1**, Akad. Nauk SSSR, Leningrad, Moscow (1945) (Phase Diagram, Experimental, *)

[1946Kor] Kornilov, I.I., Mikheeva, V.S., Konenko-Gracheva, O.K., Mints, R.S., "Equilibrium Diagram of the Ternary System Fe-Cr-Al" (in Russian), *Izv. Sekt. Fiz.-Khim. Anal*., **16**, 100-115 (1946) (Phase Diagram, Experimental, Electrical Properties, Mechanical Properties, Physical Properties, *, 48)

[1951Pra] Pratt, J.N., Raynor, G.V., "The Aluminium-Rich Alloys of the System Aluminium-Chromium-Iron", *J. Inst. Met.*, **80**, 449-458 (1951) (Phase Diagram, Experimental, *, 15)

[1953Cas] Case, S.L., van Horn, K.R., "The Constitution of Binary and Complex Iron-Aluminium Alloys", in "*Aluminium in Iron and Steel*", John Wiley & Sons Inc., New York, 265-278 (1953) (Phase Diagram, Review, *, 19)

[1954Ber] Bergman G., Shoemaker D.P., "The Determination of the Crystal Structure of the sigma Phase in the Iron-Chromium and Iron-Molybdenum Systems", *Acta Crystallogr.*, **7**, 857-865 (1954), doi:10.1107/S0365110X54002605 (Crystal Structure, Experimental, 49)

[1954Chi] Chinetti, J., "Research on the Formation of Coarse Precipitates in Light Alloys Containing Cr" (in French), *Metaux*, **29**, 151-161 (1954) (Crystal Structure, Morphology, Experimental, 8)

[1955Tag] Tagaya, M., Nenno, S., "The Effect of Aluminium on the Sigma Formation in Fe-Cr System", *Technol. Repts., Osaka Univ.,* (5), 149-152 (1955) (Crystal Structure, Morphology, Experimental, Mechanical Properties, 4)

[1958Chu] Chubb, W., Alfant, S., Bauer, A.A., Jablonowski, E.J., Schober, F.R., Dickenson, R.F., "Constitution, Metallurgy and Oxidation Resistance of Fe-Cr-Al Alloys", *Batelle Memorial Institute*, Columbus (1958) (Crystal Structure, Morphology, Phase Diagram, Experimental, Review, Kinetics, Mechanical Properties, Physical Properties, *, 66)

[1958Tag] Tagaya, M., Nenno, S., Kawamoto, M., "Effect of Al on Sigma Formation in the Fe-Cr System" (in Japanese), *Nippon Kinzoku Gakkai Shi*, **22**, 387-389 (1958) (Crystal Structure, Morphology, Experimental, Mechanical Properties, 4)

[1958Tay] Taylor, A., Jones, R.M., "Constitution and Magnetic Properties of Iron-Rich Iron-Aluminium Alloys", *J. Phys. Chem. Solids*, **6**, 16-37 (1958), doi:10.1016/0022-3697(58)90213-0 (Crystal Structure, Experimental, Magnetic Properties, 49)

[1960Zol1] Zoller, H., "The Influence of Zn, Mg, Si, Cu, Fe, Mn, Ti on the Primary Crystallisation of Al_7Cr. Part 1-5" (in German), *Schweiz. Arch. Angew. Wiss. Techn.*, **26**, 437-448 (1960) (Crystal Structure, Morphology, Phase Relations, Experimental, 20)

[1960Zol2] Zoller, H., "The Influence of Zn, Mg, Si, Cu, Fe, Mn, Ti on the Primary Crystallisation of Al_7Cr. Part 6-12" (in German), *Schweiz. Arch. Angew. Wiss. Techn.*, **26**, 478-491 (1960) (Crystal Structure, Morphology, Phase Relations, Experimental, 33)

[1961Fel] Felten, E.J., "High-Temperature Oxidation of Fe-Cr Base Alloys with Particular Reference to Fe-Cr-Y Alloys", *J. Electrochem. Soc.*, **108**(6), 490-495 (1961), doi:10.1149/1.2428122 (Crystal Structure, Morphology, Experimental, Kinetics, Physical Properties, 14)

[1961Gul] Gulbransen, E.A., Andrew, K.F., "Vapor Pressure Studies on Iron and Chromium and Several Alloys of Iron, Chromium, and Aluminum", *Trans. Metall. Soc. AIME*, **221**(6), 1247-1252 (1961) (Experimental, Thermodynamic, 33)

[1961Phi] Phillips, H.W.L., "Al-Cr-Fe", in "*Equilibrium Diagrams of Aluminium Alloy Systems. Information Bull. 25*", Aluminium Development Association, London, 1-78 (1961) (Phase Diagram, Review, 1)

[1965Wal] Walford, L.K., "The Structure of the Intermetallic Phase $FeAl_6$", *Acta Cryst.,* **18**(2), 287-291 (1965), https://doi.org/10.1107/S0365110X65000610 (Crystal Structure, Experimental, 13)

[1968Bul] Bulycheva, Z.N., Tolochko, M.N., Svezhova, S.I., Kondrat'ev, V.K., "Influence of Cr on the Ordering of Fe-Al Alloys" (in Russian), *Akad. Nauk Ukr. SSR, Metallofiz.*, **20**, 120-124 (1968) (Crystal Structure, Experimental, Electrical Properties, Mechanical Properties, 9)

[1969Bul1] Bulycheva, Z.N., Tolochko, M.N., Svezhova, S.I., Kondrat'ev, V.K., "Change in the Ordering Temperature of Fe_3Al on Adding a Third Element" (in Russian), *Ukrain. Fiz. Zh.*, **14**(10), 1706-1708 (1969) (Crystal Structure, Phase Diagram, Experimental, *, 5)

[1969Bul2] Bulycheva, Z.N., Kondrat'ev, V.K., Pogosov, V.Z., Svezhova, S.I., Tolochko, M.N., "The Effect of Cr and Co on the Structure and Properties of Ordered Fe-Al Alloys" (in Russian), *Sb. Tr. T. N.- Inst. Chern. Met. (Moscow)*, **71**, 55-62 (1969) (Crystal Structure, Phase Diagram, Experimental, *, 7)

[1969Kal] Kallel, A., "Antiferromagnetic Order in the Alloys $AlCr_{2-x}Fe_x$" (in French), *Compt. Rend. Acad. Sci., Paris*, **268B**, 455-458 (1969) (Crystal Structure, Experimental, Magnetic Properties, 8)

[1969Sel] Selissky, Ya.P., Tolochko, M.N., "High-Temperature X-Ray Diffraction Study of Fe-Al-Cr, Fe-Al-Mo and Fe-Al-W Alloys" (in Russian), *Ukr. Fiz. Zhurn.*, **14**(10), 1692-1694 (1969) (Crystal Structure, Phase Diagram, Experimental, *, 7)

[1969Wat] Watanabe, H., Sato E., "Phase Diagrams of Aluminum-Base Systems" (in Japanese), *Keikinzoku*, **19**(11), 499-535 (1969) (Phase Diagram, Phase Relations, Review, 232)

[1970Koz1] Kozheurov, V.A., Ryss, M.A., Pigasov, S.E., Antonenko, V.I., Kuznetsov, Yu.S., Mikhailov, G.G., Pashkeev, I.Yu., "The Fe-Cr-Al Phase Diagram" (in Russian), *Sb. Nauchn. Tr. Chel. Polit. Inst.*, **78**, 3-15 (1970) (Phase Diagram, Experimental, Review, *, 2)

[1970Koz2] Kozheurov, V.A., Ryss, M.A., Pigasov, S.E., Antonenko, V.I., Kuznetsov, Yu.S., Mikhailov, G.G., Pashkeev, I.Yu., "The Phase Diagram of Fe-Cr-Al in the Region of Crystallisation of the Solid Solution from the Melt" (in Russian), *Sb. Trud. Chelyab. Elektromet. Kombinata*, **2**, 69-79 (1970) (Phase Diagram, Experimental, Review, *)

[1970Koz3] Kozheurov, V.A., Ryss, M.A., Pigasov, S.E., Antonenko, V.I., "Solubility of Carbon in Melts of Fe-Cr-Al System" (in Russian), *Sb. Trud. Chelyab. Elektromet. Kombinata*, **2**, 62-68 (1970) (Crystal Structure, Phase Relations, Experimental, 9)

[1971Sto] Stott, F.H., Wood, G.C., Hobby, M.G., "A Comparison of the Oxidation Behavior of Fe-Cr-Al, Ni-Cr-Al, and Co-Cr-Al Alloys", *Oxid. Met.*, **3**(2), 103-113 (1971), doi:10.1007/BF00603481 (Crystal Structure, Experimental, Interface Phenomena, Kinetics, 3)

[1971Yam] Yamaguchi, M., Umakoshi, Y., Mima, G., "On the Miscibility Gap in the Fe-Cr-X (X=Cu, Mn, Mo, Ni, V, Si and Al) System", *Proc. Int. Conf. Sci. Technol. Iron Steel Tokyo*, **11**, 1015-1019 (1971) (Crystal Structure, Morphology, Phase Relations, Experimental, Electronic Structure, 35)

[1972Kaj] Kajzar, F., Lesniewska, B., Niziol, S., Oles, A., Pacyna, A., Tucharz, Z., "Neutron Diffraction Study of Ordered Arrangement of Fe-Cr-Al Alloys", *Inst. Tech. Jad.*, *AGH Rep., No. 22/PS*, Institute of Nuclear Physics, Cracow (1972) (Crystal Structure, Experimental)

[1973Wil] Willey, L.A., "Al-Cr-Fe Aluminum-Chromium-Iron)" in "*Metal Handbook*", 8th Edition, ASM, Metals Park, OH, 382 (1973) (Phase Diagram, Review, *, 3)

[1974Niz] Niziol, S., Oles, A., Tucharz, Z., Tyszko, Z., "Crystallographic Ordering and Magnetic Properties of Alloys" (in Russian), *Trans. Internat. Conf. on Magnetism*, 1973, **2**, Nauka, Moscow, 227-231 (1974) (Crystal Structure, Experimental, Magnetic Properties, 10)

[1974Vya] Vyatkin, G.P., Mishchenko, V.Ya., Povolotskii, D.Ya., "Using the Simplex-Lattice Method for Calculating the Equilibrium Diagram of the Fe-Cr-Al System" (in Russian), *Izv. Vyssh. Ucheb. Zaved. Chern. Metall.,* (8), 9-12 (1974) (Phase Diagram, Calculation, 4)

[1975Kau] Kaufman, L., Nesor, H., "Calculation of Superalloy Phase Diagrams: Part IV", *Met. Trans.*, **6A**(11), 2123-2131 (1975), doi:10.1007/BF03161839 (Phase Diagram, Calculation, Thermodynamics, Theory, 38)

[1975Lit] Litinska, L., Niziol, S., "Crystallographic Structure and Magnetic Properties of $(FeCr)_3Al$ Type Phases in Iron-Chromium-Aluminium ($Fe_{0.67}Cr_{0.08}Al_{0.23}$) Alloys", *Inst. Tech. Jad.*, *AGH Rep., No. 70/PS*, Institute of Nuclear Physics, Cracow (1975) (Crystal Structure, Experimental, Magnetic Properties)

[1976Mon] Mondolfo, L.F., "*Aluminium Alloys: Structure and Properties*", Butterworths, London, 480-481 (1976) (Phase Diagram, Review, *, 38)

[1976Vla] Vlasova, E.N., Prokoshin, A.F., "Formation of $L2_1$ Superstructure and Stratification in Solid Fe-Cr Solutions Doped with Al and V" (in Russian), *Dokl. Akad. Nauk SSSR*, **231**, 599-602 (1976) (Crystal Structure, Morphology, Experimental, 2)

[1977Ost] Ostrovskii, O.I., Stomakhin, A.Ya., Ditrikh, E., Grigoryan, V.A., "Heats of Dissolution of Aluminium, Silicon and Titanium in the Melts Iron-Chromium and Nickel-Chromium" (in Russian), *Seventh International Conference on Calorimetry,* (Broadened Abstracts), I-HOP, Chernogolovka (Russia), 59-63 (1977) (Thermodynamics, Experimental, 11)

[1977Tys] Tyszko, Z., Oles, A., Niziol, Z., "Structure and Physical Properties of Fe-Cr-Al Alloys" (in French), *Cercle d'Etudes de Metaux*, **13**, 473-492 (1977) (Crystal Structure, Experimental, Physical Properties, 20)

[1980Riv] Rivlin, V.G., Raynor, G.V., "Critical Evaluation of Constitution of Al-Cr-Fe System", *Int. Met. Rev.*, **25**, 139-157 (1980), doi:10.1179/imtr.1980.25.1.139 (Phase Diagram, Assessment, Review, #, *, 45)

[1981Bus] Buschow, K.H.J., van Engen, P.G., "Magnetic and Magneto–Optical Properties of Heusler Alloys Based on Aluminium and Gallium", *J. Magn. Magn. Mater.*, **25**(1), 90-96 (1981), doi:10.1016/0304-8853(81)90151-7 (Crystal Structure, Thermodynamics, Calculation, Experimental, Review, Magnetic Properties, Optical Properties, 24)

[1982Nao] Naohara, T., Inoue, A., Minemure, T., Masumoto, T., Kumada, K., "Microstructure, Mechanical Properties and Electrical Resistivity of Rapidly Quenched Fe-Cr-Al Alloys", *Metall. Trans. A*, **13A**(3), 337-343 (1982), doi:10.1007/BF02643342 (Crystal Structure, Morphology, Experimental, Electrical Properties, Mechanical Properties, 10)

[1983Bus] Buschow, K.H.J., van Engen, P.G., Jongebreur, R., "Magneto-Optical Properties of Metallic Ferromagnetic Materials", *J. Magn. Magn. Mater.*, **38**, 1-22 (1983), doi:10.1016/0304-8853(83)90097-5 (Crystal Structure, Experimental, Magnetic Properties, Optical Properties, 23)

[1985Okp] Okpalugo, D.E., Booth J.G., Faunce, C.A., "Onset of Ferromagnetism in 3*d*-Substituted FeAl Alloys. I: Ti, V and Cr Substituents", *J. Phys. F, Met. Phys.*, **15**, 681-692 (1985), doi:10.1088/0305-4608/15/3/020 (Experimental, Morphology, Magnetic Properties, 19)

[1986Sme] Smeggil, J.G., Shuskus, A.J., "The Oxidation Behavior of Some FeCrAlY, FeAlCr and Yttrium Ion-Implanted FeCrAl Alloys Compared and Contrasted", *J. Vac. Sci. Technol.*, **4**(6), 2577-2582 (1986), doi:10.1116/1.573730 (Crystal Structure, Morphology, Experimental, Interface Phenomena, Kinetics, 19)

[1987Sau] Saunders, N., Rivlin, V.G., "A Critical Review and Thermodynamic Calculations for the Al-Rich Portion of the Al-Cr-Fe Phase Diagram", *Z. Metallkd.,* **78**, 795-801 (1987) (Phase Diagram, Phase Relations, Thermodynamics, Assessment, Calculation, *, 36)

[1987Wou] van der Woude, F., Schurer, P.J., "A Study of Quasi-Crystalline Al-Fe Alloys by Mössbauer Spectroscopy and Diffraction Techniques", *Canad. J. Phys.*, **65**(10), 1301-1308 (1987), doi:10.1139/p87-205 (Crystal Structure, Morphology, Experimental, 39)

[1988Hoc] Hoch, M., "Thermodynamic Behavior of Very Stable Binary Compounds with a Wide Homogeneity Range: Their Influence in the Liquid Phase and in the Ternary and Higher Component Systems in the Solid State", *Z. Metallkd.*, **79**, 426-434 (1988) (Phase Relations, Theory, Thermodynamics, Calculation, 34)

[1988Man] Manaila, R., Florescu, V., Jianu, A., Badescu, A., "Icosahedral Phases in the Al-Fe-Cr Alloys System", *Phys. Status Solidi A*, **109**(1), 61-66 (1988), doi:10.1002/pssa.2211090105 (Crystal Structure, Experimental, 15)

[1988Sch] Schurer, P.J., Koopmans, B., van der Woude, F., "Structure of Icosahedral Al-($M_{1-x}Fe_x$) Alloys (M = Cr, Mn, or Fe)", *Phys. Rev. B.*, **37**(1), 507-510 (1988), doi:10.1103/PhysRevB.37.507 (Crystal Structure, Experimental, 25)

[1989Ell] Ellner, M., Braun, J., Predel, B., "X-Ray Study on Cr-Al Phases of the W-Family", *Z. Metallkd.*, **80**(5), 374-383 (1989) (Crystal Structure, Phase Diagram, Experimental, 38)

[1989Aku1] Akuezue, H.C., Stringer, J., "Interdiffusion in Ternary Fe-Cr-Al Alloys", *Metall. Trans. A*, **20**(12), 2767-2781 (1989), doi:10.1007/BF02670169 (Experimental, Kinetics, 39)

[1989Law1] Lawther, D.W., Dunlap, R.A., Lloyd, D.J., McHenry, M.E., "Structure and Stability of Rapidly Quenched $Al_{86}Cr_{14-x}Fe_x$ Alloys", *J. Mater. Sci.*, **24**(9), 3076-3080 (1989), doi:10.1007/BF01139021 (Crystal Structure, Morphology, Phase Relations, Experimental, 18)

[1989Law2] Lawther, D.W., Dunlap, R.A., Srivinas, V., "On the Question of Stability and Disorder in Icosahedral Aluminium - Transition Metal Alloys", *Canad. J. Phys.*, **67**(5), 463-467 (1989), doi:10.1139/p89-082 (Crystal Structure, Phase Relations, Experimental, 17)

[1989Man] Manaila, R., Florescu, V., Jianu, A., Radulescu, O., "On the Transition Metal Quasisublattice in Icosahedral Al-Cr-Fe Phases", *Phil. Mag.*, **B60**(5), 589-599 (1989), doi:10.1080/13642818908206041 (Crystal Structure, Experimental, 33)

[1989McK] McKamey, C.G., Horton, J.A., Liu, C.T., "Effect of Chromium on Properties of Fe_3Al", *J. Mater. Res.*, **4**(5), 1156-1163 (1989), doi:10.1557/JMR1989.1156 (Crystal Structure, Morphology, Experimental, Mechanical Properties, 24)

[1990Ioa] Ioannidis, E.K, Sheppard, T., "Powder Metallurgy Aluminium Alloys: Characteristics of an Al-Cr-Fe Rapidly Solidified Alloys", *J. Mater. Sci.*, **25**(9), 3965-3975 (1990), doi:10.1007/BF00582468 (Crystal Structure, Morphology, Experimental, Mechanical Properties, 15)

[1991Ben] Bendersky, L.A., Roth, R.S., Ramon, J.T., Shechtman, S., "Crystallographic Characterization of Some Intermetallic Compounds in the Al-Cr System", *Metall. Trans. A*, **22**(1), 5-10 (1991), doi:10.1007/BF03350943 (Crystal Structure, Morphology, Experimental, 11)

[1991Gho] Ghosh, G., "Al-Cr-Fe Ternary Phase Diagram Evaluation", in *MSI Eureka*, Effenberg, G. (Ed.), MSI, Materials Science International Services GmbH, Stuttgart (1991), Document ID: 10.14873.1.1 (Crystal Structure, Phase Diagram, Phase Relations, Assessment, 48)

[1991Pra] Prakash, U., Buckley, R.A., Jones, H., "Mechanical Properties of Ordered Fe-Al-X Alloys", *Mater. Res. Soc. Symp. Proc.: High-Temp. Ordered Intermetallic Alloys IV*, **213**, 691-696 (1991) (Crystal Structure, Morphology, Experimental, Mechanical Properties, 19)

[1991Sik1] Sikka, V.K., Baldwin, R.H., Reinshagen, J.H, Knibloe, J.R., Wright, R.N., "Powder Processing of Fe_3Al-Based Iron-Aluminide Alloys", *Mater. Res. Soc. Symp. Proc.: High-Temp. Ordered Intermetallic Alloys IV*, **213**, 901-906 (1991) (Crystal Structure, Morphology, Experimental, Physical Properties, 4)

[1991Sik2] Sikka, V.K., "Production of Fe_3Al-Based Intermetallic Alloys", *Mater. Res. Soc. Symp. Proc.: High-Temp. Ordered Intermetallic Alloys IV*, **213**, 907-912 (1991) (Morphology, Experimental, 2)

[1991Tre] Tret'yachenko, L.A., Prima, S.B., Petyukh, V.M., "The Polythermal Cr-FeAl Section of the Phase Diagram of the Ternary System Cr-Fe-Al" (in Russian), *Diagr. Sostoyaniya v Materialoved.*, Akad. Nauk Ukr. SSR. Nauch. Sov. Akad. Nauk Ukr. SSR Probl. Khim. Termodin. i Term. Anal., Kiev, 143-146 (1991) (Crystal Structure, Morphology, Phase Diagram, Experimental, #, *, 4)

[1992Bra] Braun, J., Ellner, M., Predel, B., "Structure of the High-Temperature Phase Cr_5Al_8(h)" (in German), *J. Alloys Compd.*, **183**, 444-448 (1992), doi:10.1016/0925-8388(92)90766-3 (Crystal Structure, 17)

[1992Hil] Hilpert, K., Miller, M., "Study of the Vaporization of Ni-Cr-Al and Fe-Cr-Al Base Alloys by Knudsen Effusion Mass Spectrometry", *Z. Metallkd.*, **83**(10), 739-743 (1992) (Thermodynamics, Experimental, 15)

[1993Kat] Kattner, U.R., Burton, B.P., "Al-Fe (Aluminum-Iron)" in "*Phase Diagrams of Binary Iron Alloys*", Okamoto, H. (Eds.), Mater. Park OH: ASM Int., 12-28 (1993) (Crystal Structure, Electrical Properties, Magnetic Properties, Mössbauer, Phase Diagram, Review, Thermodynamics, *, 99)

[1993Kni] Knibloe, J.R., Wright, R.N., Trybus, C.L., Sikka, V.K., "Microstructure and Mechanical Properties of Fe_3Al Alloys with Chromium", *J. Mater. Sci.*, **28**(8), 2040-2048 (1993), doi:10.1007/BF00367560 (Crystal Structure, Morphology, Experimental, Mechanical Properties, 8)

[1993Sta] Stadnik, Z.M., Mueller, F., Goldberg, F., Rosenberg, M., Stroink, G., "Physical Properties of Icosahedral $Al_{86}Cr_8Fe_6$", *J. Non-Cryst. Solids*, **156**, 909-913 (1993), doi:10.1016/0022-3093(93)90094-E (Crystal Structure, Experimental, Phase Relations, 30)

[1994Bur] Burkhardt, U., Grin, J., Ellner, M., Peters, K., "Structure Refinement of the Iron-Aluminium Phase with the Approximate Composition Fe_2Al_5", *Acta Cryst. B: Struct. Crystallogr. Crys. Chem.*, **B50**, 313-316 (1994), doi:10.1107/S0108768193013989 (Crystal Structure, Experimental, 9)

[1994Hyd] Hyde, T.A., Sellers, C.H., Wright, J.K., Wright, R.N., "Electrical Resistance Analysis of the $D0_3 \rightleftharpoons B2$ Transition in Alloys of Fe_3Al", *Scr. Metall. Mater.*, **30**(1), 113-118 (1994), doi:10.1016/0956-716X(94)90368-9 (Morphology, Experimental, Electrical Properties, 29)

[1994Mor] Morris, D.G., Leboeuf, M., Gunther, S., Nazmy, M., "Disordering Behaviour of Alloys Based on Fe_3Al", *Philos. Mag. A*, **70**(6), 1067-1090 (1994), doi:10.1080/01418619408242950 (Experimental, Morphology, Phase Relations, 31)

[1994Rag] Raghavan, V., "Al-Cr-Fe (Aluminum-Chromium-Iron)", *J. Phase Equilibria*, **15**(4), 409 (1994), doi:10.1007/BF02647563 (Phase Diagram, Phase Relations, Review, 6)

[1994Ste] Steurer, W., Haibach, T., Zhang, B., Beeli, C., Nissen, H.U., "The Structure of Decagonal $Al_{70.5}Mn_{16.5}Pd_{13}$", *J. Phys.: Condens. Matter*, **6**(3), 613-632 (1994), doi:10.1088/0953-8984/6/3/004 (Crystal Structure, Experimental, 24)

[1995Ant] Anthony, L., Fultz, B., "Effects of Early Transition Metal Solutes on the $D0_3$-$B2$ Critical Temperature of Fe_3Al", *Acta Metall. Mat.*, **43**(10), 3885-3891 (1995), doi:10.1016/0956-7151(95)90171-X (Crystal Structure, Phase Relations, Experimental, Theory, Kinetics, 35)

[1995Sta] Stadnik, Z.M., Mueller, F., "Thermal, Structural and Magnetic Properties of Icosahedral $Al_{86}Cr_8Fe_6$ Alloy", *Philos. Mag. B*, **71**(2), 221-238 (1995), doi:10.1080/01418639508240307 (Crystal Structure, Experimental, Magnetic Properties, 67)

[1995Sui] Sui, H.X., Liao, X.Z., Kuo, K.H., "A Non-Fibonacci Type of Orthorhombic Decagonal Approximant", *Philos. Mag. Lett*., **71**(2), 139-145 (1995), doi:10.1080/09500839508241006 (Crystal Structure, Experimental, 18)

[1995Yos] Yoshimi, K., Terashima, H., Hanada, S., "Effect of APB Type on Tensile Properties of Cr Added Fe_3Al with $D0_3$ Structure", *Mater. Sci. Eng. A*, **194**(1), 53-61 (1995), doi:10.1016/0921-5093(94)09659-7 (Experimental, Mechanical Properties, Morphology, 17)

[1995Zia] Ziani, A., Michot, G., Pianelli, A., Redjaimia, A., Zahra, C.Y., Zahra, A.M., "Transformation of the Quasicrystalline Phase Al-Cr-Fe Induced by Rapid Solidification", *J. Mater. Sci.*, **30**(11), 2921-2929 (1995), doi:10.1007/BF00349664 (Crystal Structure, Morphology, Experimental, 27)

[1996Jim] Jimenez, J.A., Frommeyer, G., "Creep Behavior of Intermetallic Fe-Al and Fe-Al-Cr Alloys", *Mater. Sci. Eng. A*, **A220**(1-2), 93-99 (1996), doi:10.1016/S0921-5093(96)10480-9 (Morphology, Experimental, Mechanical Properties, 18)

[1997Li] Li, X.Z., Sugiyama, K., Hiraga, K., Sato, A., Yamamoto, A., "Crystal Structure of Orthorhombic ε-Al_4Cr", *Z. Krist.,* **212**(9), 628-633 (1997), doi:10.1524/zkri.1997.212.9.628 (Crystal Structure, Experimental, 17)

[1997Nis1] Nishino, Y., Asano, S., Ogawa, T., "Phase Stability and Mechanical Properties of Fe_3Al with Addition of Transition Elements", *Mater. Sci. Eng. A*, **A234-236**, 271-274 (1997), doi:10.1016/S0921-5093(97)00191-3 (Crystal Structure, Experimental, Mechanical Properties, Phase Relations)

[1997Nis2] Nishino, Y., Kumada, C., Asano, S., "Phase Stability of Fe_3Al with Addition of 3*d* Transition Elements", *Scr. Mater.*, **36**(4), 461-466 (1997), doi:10.1016/S1359-6462(96)00395-8 (Crystal Structure, Electrical Properties, Experimental, Phase Diagram, Phase Relations, 26)

[1997Pal] Palm, M., "The Al-Cr-Fe System – Phases and Phase Equilibria in the Al-Rich Corner", *J. Alloys Compd*., **252**(1-2), 192-200 (1997), doi:10.1016/S0925-8388(96)02719-3 (Crystal Structure, Phase Diagram, Phase Relations, Experimental, 41)

[1997Rud] Rudajevova, A., Shima, V., "Thermal Properties of the Fe_3Al_5-5 at.% Cr Intermetallic Compound and Thermal Diffusivity Anomaly in $D0_3$ Phase", *Mater. Res. Bull.,* **32**(4), 441-449 (1997), doi:10.1016/S0025-5408(96)00201-2 (Thermodynamics, Experimental, 15)

[1997Sat] Satula, D., Dobrzynski, L., Waliszewski, J., Szymanski, K., Recko, K., Malinowski, A., Brueckel, Th., Schaerpf, O., Blinowski, K., "Structural and Magnetic Properties of Fe-Cr-Al Alloys with $D0_3$-Type Structure", *J. Magn. Magn. Mater.*, **169**(3), 240-252 (1997), doi:10.1016/S0304-8853(96)00758-5 (Crystal Structure, Experimental, Magnetic Properties, 29)

[1997Sui] Sui, H.X., Liao, X.Z., Kuo, K.H., Zou, X., Hovmoeller, S., "Structural Model of the Orthorhombic Non-Fibonacci Approximant in the $Al_{12}Fe_2Cr$ Alloy", *Acta Crystallogr., Sect. B: Struct. Crystallogr. Crys. Chem.*, **B53**, 587-595 (1997), doi:10.1107/S0108768197000220 (Crystal Structure, Experimental, 41)

[1998Akd] Akdeniz, M.V., Mekhrabov, A.O., "The Effect of Substitutional Impurities on the Evolution of Fe-Al Diffusion Layer", *Acta Mater.,* **46**(4), 1185-1192 (1998), doi:10.1016/S1359-6454(97)00318-2 (Morphology, Calculation, Experimental, Interface Phenomena, 55)

[1998Kim] Kim, S.M., Morris, D.G., "Long Range Order and Vacancy Properties in Al-rich Fe_3Al and $Fe_3Al(Cr)$ Alloys", *Acta Mater.*, **46**(8), 2587-2602 (1998), doi:10.1016/S1359-6454(97)00464-3 (Crystal Structure, Morphology, Phase Relations, Experimental, Kinetics, 18)

[1998Lia] Liao, X.Z., Sui, H.X., Kuo, K.H., "A New Monoclinic Approximant of the Decagonal Quasicrystal in Al-Co-Cu-W and Al-Fe-Cr Alloys", *Philos. Mag. A,* **78**(1), 143-156 (1998), doi:10.1080/014186198253723 (Crystal Structure, Experimental, 19)

[1998Nis] Nishino, Y., "Electrical Resistance Anomaly in Fe_3Al-Based Alloys", *Mater. Sci. Eng. A*, **A258**(1-2), 50-58 (1998), doi:10.1016/S0921-5093(98)00916-2 (Crystal Structure, Review, Electronic Structure, Electrical Properties, 47)

[1998Su] Su, J.-Q., Gao, S.-J., Hu, Zh.-Q., "The Influence of Chromium and Boron on Mechanical Properties of Fe-30Al Alloy", *J. Mater. Sci. Lett.*, **17**(23), 2021-2023 (1998), doi:10.1023/A:1006629210538 (Morphology, Experimental, Mechanical Properties, 12)

[1998Sun] Sun, Z.Q., Yang, W.Y., Shen, L.Z., Huang, Y.D., Zhang, B.S., Yang, J.L., "Neutron Diffraction Study on Site Occupation of Substitutional Elements at Sub Lattices in Fe-Al Intermetallics", *Mater. Sci. Eng. A*, **258**(1-2), 69-74 (1998), doi:10.1016/S0921-5093(98)00919-8 (Crystal Structure, Morphology, Experimental, Magnetic Properties, Mechanical Properties, 19)

[1999Gru] Grushko, B., Yurechko, M., Tamura, N., "A Contribution to the Al-Pd-Mn Phase Diagram", *J. Alloys Compd.*, **290**(1-2), 164-171 (1999), doi:10.1016/S0925-8388(99)00192-9 (Experimental, Phase Diagram, Phase Relations)

[1999Sui] Sui, H.X., Li, X.Z., Kuo, K.H., "Hexagonal $Al_{81}Fe_8Cr_{11}$ with a = 4.00 nm and c = 1.24 nm", *Philos. Mag. Lett.*, **79**, 181-185 (1999), doi:10.1080/095008399177417 (Crystal Structure, Experimental, 10)

[1999Wit] Wittmann, R., Spindler, S., Fischer, B., Wagner, H. Gerthsen, D., Lange, J., Brede, M., Kloewer, J., Schunk, P., Schimmel, T., "Transmission Electron Microscopic Investigation of the Microstructure of Fe-Cr-Al Alloys", *J. Mater. Sci.*, **34**(8), 1791-1798 (1999), doi:10.1023/A:1004559108952 (Crystal Structure, Morphology, Phase Relations, Experimental, 26)

[2000Bla] Blachowski, A., Dubiel, S.M., Zukrowski, J., Cieslak, J., Sepiol, B., "On the Kinetics of the α-σ Phase Transformation in an Al-Doped Fe-Cr Alloy", *J. Alloys Compd.*, **313**(1-2), 182-187 (2000), doi:10.1016/S0925-8388(00)01139-7 (Phase Relations, Experimental, Kinetics, 15)

[2000Dem] Demange, V., Wu, J.S., Brien, V., Machizaud, F., Dubois, J.M., "New Approximant Phases in Al-Cr-Fe", *Mater. Sci. Eng. A,* **294-296**, 79-81 (2000), doi:10.1016/S0921-5093(00)01083-2 (Crystal Structure, Experimental, 13)

[2000Mo] Mo, Z.M., Zhou, H.Y., Kuo, K.H., "Structure of ν-$Al_{80.61}Cr_{10.71}Fe_{8.68}$, a Giant Hexagonal Approximant of a Quasicrystal Determined by a Combination of Electron Microscopy and X-Ray Diffraction", *Acta Cryst. B: Struct. Crystallogr. Crys. Chem.*, **56**, 392-401 (2000), doi:10.1107/S0108768199015761 (Crystal Structure, Experimental, 16)

[2000Spi] Spindler, S., Wittmann, R., Gerthsen, D., Lange, J., Brede, M., Kloewer, J., "Dislocation Properties of Polycrystalline Fe-Cr-Al Alloys and their Correlation with Mechanical Properties", *Mater. Sci. Eng. A*, **289**, 151-161 (2000), doi:10.1016/S0921-5093(00)00910-2 (Crystal Structure, Morphology, Experimental, Mechanical Properties, 27)

[2000Sub] Subasic, N., Sundman, B., "Thermodynamic Assessment of the Al-Cr-Fe System and Reassessment of the Al-Cr System", *Proc. Disc. Meet. Thermodyn. Alloys*, 42 (2000) (Thermodynamics, Abstract, Assessment, Calculation, 0)

[2001Alo] Al-Omari, I.A., "Structural and Mössbauer Spectroscopic Studies of $Fe_{0.7-x}Cr_xAl_{0.3}$ Alloys", *J. Magn. Magn. Mater.*, **225**(3), 346-350 (2001), doi:10.1016/S0304-8853(01)00065-8 (Crystal Structure, Experimental, 21)

[2001Dem] Demange, V., Anderegg, J.W., Ghanbaja, J., Machizaud, F., Sordelet, D.J., Besser, M., Thiel, P.A., Dubois, J.M., "Surface Oxidation of Al-Cr-Fe Alloys Characterized by X-Ray Photoelectron Spectroscopy", *Appl. Surf. Sci.*, **173**(3-4), 327-338 (2001), doi:10.1016/S0169-4332(01)00011-3 (Crystal Structure, Experimental, 30)

[2002Ban] Banerjee, R., Amancherla S., Banerjee, S., Fraser, H. L., "Modeling of Site Occupancies in *B*2 FeAl and NiAl Alloys with Ternary Additions", *Acta Mater.*, **50**(3), 633-641 (2002), doi:10.1016/S1359-6454(01)00371-8 (Crystal Structure, Theory, 21)

[2002Dem] Demange, V., Machizaud, F., Dubois, J.M., Anderegg, J.W., Thiel P.A., Sordelet, D.J., "New Approximants in the Al-Cr-Fe System and their Oxidation Resistance", *J. Alloys Compd.*, **342**(1-2),

24-29 (2002), doi:10.1016/S0925-8388(02)00118-4 (Crystal Structure, Experimental, Interface Phenomena, Kinetics, 20)

[2002Zho] Zhou, Z.C., Wei, J.N., Han, F.S., "Influences of Heat Treatment and Grain Size on the Damping Capacity of an Fe-Cr-Al Alloy", *Phys. Status Solidi A*, **191**(1), 89-96 (2002) (Experimental, Mechanical Properties, Physical Properties, 14)

[2003Kel] Kellou, A., Fenineche, N.E., Grosdidier, T., Aourag, H., Coddet, C., "Structural Stability and Magnetic Properties in X_2AlX' (X = Fe, Co, Ni; X′= Ti, Cr) Heusler Alloys from Quantum Mechanical Calculations", *J. Appl. Phys.*, **94**(5), 3292-3298 (2003), doi:10.1063/1.1592297 (Calculation, Crystal Structure, Magnetic Properties, Mechanical Properties, 27)

[2003Rag] Raghavan, V., "Al-Cr-Fe (Aluminum-Chromium-Iron)", *J. Phase Equilib.*, **24**(3), 257-258 (2003), doi:10.1361/105497103770330587 (Crystal Structure, Phase Diagram, Phase Relations, Review, 19)

[2003Zou] Zou, X.D., Mo, Z.M., Hovmoeller, S., Li, X.Z., Kuo, K.H., "Three-Dimensional Reconstruction of the ν-AlCrFe Phase by Electron Crystallography", *Acta Cryst., Sect. A: Found. Crystallogr.*, **59**(6), 526-539 (2003), doi:10.1107/S0108767303018051 (Crystal Structure, Electronic Structure, Experimental, 24)

[2004Dem] Demange, V., Ghanbaja, J., Beeli, C., Machizaud, F., Dubois, J.M., "Study of Decagonal Approximant and γ-Brass-Type Compounds in Al-Cr-Fe Thin Films", *J. Mater. Res.*, **19**(8), 2285-2297 (2004), doi:10.1557/JMR.2004.0311 (Crystal Structure, Morphology, Experimental, Interface Phenomena, Kinetics, Optical Properties, Amorphous, 32)

[2004Den] Deng, D.W., Mo, Z.M., Kuo, K.H., "Crystal Structure of the Orthorhombic $Al_4(Cr, Fe)$ Approximant of the Al-Cr-Fe Decagonal Quasicrystal", *J. Phys.: Condens. Matter*, **16**(13), 2283-2296 (2004), doi:10.1088/0953-8984/16/13/009 (Crystal Structure, Experimental, 33)

[2004Gho] Ghosh, G., Velikanova, T., Korniyenko, K., Sidorko, V., "Al-Cr-Fe Ternary Phase Diagram Evaluation", in *MSI Eureka*, Effenberg, G. (Ed.), MSI, Materials Science International Services GmbH, Stuttgart (2004), Document ID: 10.14873.2.0 (Crystal Structure, Phase Diagram, Thermodynamics, Assessment, Electronic Structure, Mechanical Properties, Physical Properties, 121)

[2004Hua] Huang, Y.D., Yang, W.Y., Sun, Z.Q., Froyen, L., "Preparation and Mechanical Properties of Large-Ingot Fe_3Al-Based Alloys", *J. Mat. Proc. Tech.*, **146**(2), 175-180 (2004), doi:10.1016/j.jmatprotec.2003.10.014 (Morphology, Experimental, Mechanical Properties, 23)

[2004Sim] Sima, V., "Order-disorder Transformations in Materials", *J. Alloys Compd.*, **378**(1-2), 44-51 (2004), doi:10.1016/j.jallcom.2003.11.166 (Crystal Structure, Thermodynamics, Review, Magnetic Properties, 20)

[2004Wu] Wu, D., Baker, I., Munroe, P.R., "The Effect of Substitutional Elements on the Strain-Induced Ferromagnetism in *B*2-Structured Fe-Al Single Crystals", *Intermetallics*, **12**(7-9), 851-858 (2004), doi:10.1016/j.intermet.2004.02.036 (Crystal Structure, Morphology, Calculation, Experimental, Magnetic Properties, 19)

[2004Zha] Zhang, M., Brueck, E., de Boer, F.R., Wu, G., "Electronic Structure, Magnetism, and Transport Properties of the Heusler Alloy Fe_2CrAl", *J. Magn. Magn. Mater.*, **283**(2-3), 409-416 (2004), doi:10.1016/j.jmmm.2004.06.013 (Crystal Structure, Calculation, Experimental, Electronic Structure, Electrical Properties, Magnetic Properties, Transport Phenomena, 22)

[2005Bel] Belin-Ferre, E., Klanjsek, M., Jaglicic, Z., Dolinsek, J., Dubois, J.M., "Experimental Study of the Electronic Density of States in Aluminium-Based Intermetallics", *J. Phys.: Condens. Matter*, **17**(43), 6911-6924 (2005), doi:10.1088/0953-8984/17/43/010 (Crystal Structure, Experimental, Electronic Structure, Electrical Properties, Magnetic Properties, 26)

[2005Pal] Palm, M., "Concepts Derived from Phase Diagram Studies for the Strengthening of Fe-Al-Based Alloys", *Intermetallics*, **13**(12), 1286-1295 (2005), doi:10.1016/j.intermet.2004.10.015 (Morphology, Phase Diagram, Review, Mechanical Properties, 81)

[2005Reg1] Regina, J.R., DuPont, J.N., Marder, A.R., "Gaseous Corrosion Resistance of Fe-Al-Based Alloys Containing Cr Additions: Part I: Kinetic Results", *Mater. Sci. Eng. A*, **404**(1-2), 71-78 (2005), doi:10.1016/j.msea.2005.05.053 (Morphology, Experimental, Interface Phenomena, Kinetics, 20)

[2005Reg2] Regina, J.R., DuPont, J.N., Marder, A.R., "Gaseous Corrosion Resistance of Fe-Al Based Alloys Containing Cr Additions: Part II. Scale Morphology", *Mater. Sci. Eng. A*, **405**(1-2), 102-110 (2005), doi:10.1016/j.msea.2005.05.085 (Morphology, Experimental, Interface Phenomena, Kinetics, 24)

[2005Zha] Zhang, Z.G., Niu, Y., "Effect of Chromium on the Oxidation of a Fe-10 Al Alloy at 1000°C", *Mater. Sci. Forum*, **475-479**, 685-688 (2005), doi:10.4028/www.scientific.net/MSF.475-479.685 (Morphology, Experimental, Interface Phenomena, Kinetics, 18)

[2006Bih] Bihar, Z., Bilusic, A., Lukatela, J., Smontara, A., Jeglic, P., McGuiness, P.J., Dolinsek, J., Jaglicic, Z., Janovec, J., Demange, V., Dubois, J.M., "Magnetic, Electrical and Thermal Transport Properties of Al-Cr-Fe Approximant Phases", *J. Alloys Compd.*, **407**(1-2), 65-73 (2006), doi:10.1016/j.jallcom.2005.06.055 (Crystal Structure, Experimental, Electrical Properties, Magnetic Properties, Transport Phenomena, 30)

[2006Dem] Demange, V., Ghanbaja, J., Dubois, J.M., "Electron Microscopy Study of Approximant Phases in the Al-Cr-Fe System", *Philos. Mag.,* **86**(3-5), 469-474 (2006), doi:10.1080/14786430500269501 (Crystal Structure, Experimental, Theory, 19)

[2006Gol1] Golovin, I.S., "Anelastic Relaxation in Ternary Fe-Al-Me Alloys: Me = Co, Cr, Ge, Mn, Nb, Si, Ta, Ti, Zr", *Mater. Sci. Eng. A*, **442**(1-2), 92-98 (2006), doi:10.1016/j.msea.2006.03.118 (Crystal Structure, Morphology, Phase Relations, Experimental, Mechanical Properties, 38)

[2006Gol2] Golovin, I.S., Strahl, A., Neuhäuser, H., "Anelastic Relaxation and Structure of Ternary Fe-Al-Me Alloys with Me = Co, Cr, Ge, Mn, Nb, Si, Ta, Ti, Zr", *Int. J. Mater. Res. (Z. Metallkd.)*, **97**(8), 1078-1092 (2006), doi:10.3139/ijmr-2006-0170 (Crystal Structure, Experimental, Mechanical Properties, Morphology, Phase Relations, Thermodynamics, 79)

[2006Gru] Grushko, B., Przepiorzynski, B., Kowalska-Strzeciwilk, E., Surowiec, M., "New Phase in the High-Al Region of Al-Cr", *J. Alloys Compd.*, **420**, L1-L4 (2006), doi:10.1016/j.jallcom.2005.10.0465 (Crystal Structure, Morphology, Phase Relations, Experimental, 7)

[2006Kar] Karpets, M.V., Firstov, S.O., Kulak, L.D., Gorna, I.D., Kuzmenko, N.N., Sarzhan, G.F., "Peculiarity Phase Formation in Rapidly Solidified Al-Fe-Cr Alloys at present Quasicrystalls" (in Ukrainian), *Phys. Chem. Solid State*, **7**(1), 147-151 (2006) (Crystal Structure, Phase Relations, Experimental, 8)

[2006Sha] Sharma, G., Kishore, R., Sundararaman, M., Ramanujan, R.V., "Superplastic Deformation Studies in Fe-28Al-3Cr Intermetallic Alloy", *Mater. Sci. Eng. A*, **419**(1-2), 144-147 (2006), doi:10.1016/j.msea.2005.12.015 (Morphology, Experimental, Mechanical Properties, 14)

[2007Chi] Chiang, Ch.-Ch., Wang, Sh.-H., Chen, J.-Sh., Chu, J.P., Hsu, Y.-F., "Bending Embrittlement of As-Welded FeAl Alloys", *Intermetallics*, **15**(4), 564-570 (2007), doi:10.1016/j.intermet.2006.09.008 (Morphology, Experimental, Mechanical Properties, 13)

[2007Cho] Choe, H.C., Park, S.J., Eun, S.W., Ko, Y.M., "Intergranular and Pitting Corrosion Behavior of Fe-25Al-6Cr Intermetallic Compounds Containing Mo, Nb and B", *Mater. Sci. Forum*, **539-543**, 1583-1588 (2007), doi:10.4028/www.scientific.net/MSF.539-543.1 (Morphology, Phase Relations, Experimental, Interface Phenomena, Kinetics, 11)

[2007Gho] Ghosh, G., Velikanova, T., Korniyenko, K., Sidorko, V., "Al-Cr-Fe Ternary Phase Diagram Evaluation", in *MSI Eureka*, Effenberg, G. (Ed.), MSI, Materials Science International Services GmbH, Stuttgart (2007), Document ID: 10.14873.3.4 (Crystal Structure, Morphology, Phase Diagram, Thermodynamics, Assessment, Mechanical Properties, 135)

[2007Pad] Paduani, C., Poettker, W.E., Ardisson, J.D., Schaf, J., Takeuchi, A.Y., Yoshida, M.I., Soriano, S., Kalisz, M., "Mössbauer Effect and Magnetization Studies of the $Fe_{2+x}Cr_{1-x}Al$ System in the $L2_1$ (X_2YZ) Structure", *J. Phys.: Condens. Matter*, **19**(15), 156204 (2007), doi:10.1088/0953-8984/19/15/156204 (Crystal Structure, Experimental, Magnetic Properties, 8)

[2007Pan] Panjan, P., Cekada, M., Dolinsek, J., Vrtic, B., Zalar, A., Kek-Merl, D., "Diffusion Processes during Heat Treatment of Al-Cr-Fe Thin Films", *Vacuum*, **82**(2), 286-289 (2007), doi:10.1016/j.vacuum.2007.07.002 (Crystal Structure, Experimental, Electrical Properties, Mechanical Properties, Transport Phenomena, Nano, 8)

[2007Ste] Stein, F., Palm, M., "Re-Determination of Transition Temperatures in the Fe-Al System by Differential Thermal Analysis" *Int. J. Mat. Res*., **98**, 580-588 (2007), doi:10.3139/146.101512 (Crystal Structure, Phase Diagram, Phase Relations, Experimental, 59)

[2008Cao] Cao, B.B., Kuo, K.H., "Crystal Structure of the Monoclinic η-$Al_{11}Cr_2$", *J. Alloys Compd.*, **458**(1-2), 238-247 (2008), doi:10.1016/j.jallcom.2007.04.022 (Crystal Structure, Experimental, 23)

[2008For] Fornasiero, P., Montini, T., Graziani, M., Zilio, S., Succi, M., "Development of Functionalized Fe-Al-Cr Alloy Fibers as Innovative Catalytic Oxidation Devices", *Catal. Today*, **137**, 475-482 (2008), doi:10.1016/j.cattod.2007.12.097 (Morphology, Experimental, Catalysis, Kinetics, 29)

[2008Gil] Gille, P., Bauer, B., "Single Crystal Growth of $Al_{13}Co_4$ and $Al_{13}Fe_4$ from Al-Rich Solutions by the Czochralski Method", *Cryst. Res. Technol*., **43**(11), 1161-1167 (2008) (Crystal Structure, Morphology, Phase Relations, Experimental, Theory, 17)

[2008Gol] Golovin, I.S., Riviere, A., "Mechanical Spectroscopy of the Fe - 25 Al - Cr Alloys in Medium Temperature Range", *Solid State Phen.*, **137**, 99-108 (2008), doi:10.4028/www.scientific.net/SSP.137.99 (Crystal Structure, Experimental, Phase Relations, 14)

[2008Gru] Grushko, B., Przepiorzynski, B., Pavlyuchkov, D., "On the Constitution of the High-Al Region of the Al-Cr Alloy System", *J. Alloys Compd.*, **454**, 214-220 (2008), doi:10.1016/j.jallcom.2007.01.001 (Crystal Structure, Experimental, Morphology, Phase Diagram, Phase Relations, 13)

[2008Jac] Jacobs, M.H.G., Schmid-Fetzer, R., Markus, T., Motalov, V., Borchardt, G., Spit, K.-H., "Thermodynamics and Diffusion in Ternary Fe-Al-Cr Alloys. Part I: Thermodynamic Modeling", *Intermetallics*, **16**(8), 995-1005 (2008), doi:10.1016/j.intermet.2008.04.020 (Morphology, Phase Diagram, Phase Relations, Thermodynamics, Calculation, Experimental, *, 34)

[2008Lu] Lu, W.M., Pan, T.J., Niu, Y., "Accelerated Corrosion of Fe-*x*Cr-10Al Alloys Containing 0-20 at.% Cr Induced by Sulfur and Chlorine in a Reducing Atmosphere at 600°C", *Oxid. Met.*, **69**(1), 63-76 (2008), doi:10.1007/s11085-007-9083-9 (Crystal Structure, Morphology, Phase Relations, Experimental, Interface Phenomena, Kinetics, 26)

[2008Pav1] Pavlova, T.S., Golovin, I.S., Gunderov, D.V., Siemers, C., "Effect of Severe Plastic Deformation on the Structure and Low-Temperature Internal Friction of Fe_3Al and $(Fe, Cr)_3Al$", *Phys. Met. Metallogr.*, **105**(1), 36-44 (2008), doi:10.1134/S0031918X08010043, translated from *Fiz. Met. Metalloved.*, **105**(1), 41-49 (2008) (Morphology, Phase Relations, Experimental, Magnetic Properties, Mechanical Properties, 9)

[2008Pav2] Pavlyuchkov, D.V., Przepiorzynski, B., Grushko, B., Velikanova, T.Ya., "Complex Orthorhombic Phase in the Al-Cr-Fe System", *Powder Metall. Met. Ceram.*, **47**(11-12), 698-701 (2008), doi:10.1007/s11106-009-9081-3, translated from *Poroshk. Metallurgiya*, **47**(11-12), 94-98 (2008) (Crystal Structure, Phase Diagram, Phase Relations, Experimental, *, 8)

[2008Pav3] Pavlyuchkov, D.V., Przepiorzynski, B., Grushko, B., Velikanova, T.Ya., "Hexagonal Phase in Al-Cr-Fe System" (in Russian), *Metallofizika Nov. Tekhnol.*, **30**(10), 1423-1428 (2008) (Crystal Structure, Phase Diagram, Phase Relations, Experimental, *, 9)

[2008Pin] Pint, B.A., Dwyer, M.J., Deacon, R.M., "Internal Oxidation-Nitridation of Ferritic Fe(Al) Alloys in Air", *Oxid. Met.*, **69**(3), 211-231 (2008), doi:10.1007/s11085-008-9094-1 (Morphology, Experimental, Interface Phenomena, Kinetics, 32)

[2008Shr] Shreder, E., Streltsov, S.V., Svyazhin, A., Makhnev, A., Marchenkov, V.V., Lukoyanov, A., Weber, H.W., "Evolution of the Electronic Structure and Physical Properties of Fe_2MeAl (Me = Ti, V, Cr) Heusler Alloys", *J. Phys.: Condens. Matter*, **20**(4), 045212 (2008), doi:10.1088/0953-8984/20/04/045212 (Crystal Structure, Calculation, Experimental, Electronic Structure, Electrical Properties, Magnetic Properties, Optical Properties, 33)

[2009Bau] Bauer, B., Pedersen, B., Gille, P., "$Al_4(Cr, Fe)$: Single Crystal Growth by the Czochralski Method and Structural Investigation with Neutrons at FRM II", *Z. Kristallogr. Crystal Mater.*, **224**(1-2), 109-111 (2009), doi:10.1524/zkri.2009.1076 (Crystal Structure, Experimental, 9)

[2009Che] Chen, H., Weitzer, F., Krendelsberger, N., Du, Y., Schuster, J.C., "Reaction Scheme and Liquidus Surface of the Ternary System Aluminum-Chromium-Titanium", *Metall. Mater. Trans. A*, **40**(12), 2980-2986 (2009), doi:10.1007/s11661-009-0014-z (Crystal Structure, Experimental, Phase Diagram, Phase Relations, 24)

[2009Dea] Deacon, R.M., DuPont, J.N., Kiely, C.J., Marder, A.R., Tortorelli, P.F., "Evaluation of the Corrosion Resistance of Fe-Al-Cr Alloys in Simulated Low NO_x Environments. Part 1: Corrosion Exposures and Scanning Electron Microscopy", *Oxid. Met.*, **72**(1), 67-86 (2009), doi:10.1007/s11085-009-9148-z (Morphology, Experimental, Interface Phenomena, Kinetics, 37)

[2009Gol] Golovin, I.S., Riviere, A., "Anelasticity in Fe-Al-Cr Alloys at Elevated Temperatures", *Mater. Sci. Eng. A*, **521-522**, 67-72 (2009), doi:10.1016/j.msea.2008.09.103 (Crystal Structure, Morphology, Phase Relations, Experimental, Magnetic Properties, Mechanical Properties, 15)

[2009Pav] Pavlyuchkov, D., Balanetskyy, S., Kowalski, W., Surowiec, M., Grushko, B., "Stable Decagonal Quasicrystals in the Al-Fe-Cr and Al-Fe-Mn Alloy Systems", *J. Alloys Compd.*, **477** (1-2), L41-L44 (2009), doi:10.1016/j.jallcom.2008.11.005 (Crystal Structure, Phase Diagram, Experimental, *, 13)

[2010Air] Airiskallio, E., Nurmi, E., Heinonen, M.H., Vaeyrynen, I.J., Kokko, K., Ropo, M., Punkkinen, M.P.J., Pitkaenen, H., Alatalo, M., Kollar, J., Johansson, B., Vitos, L., "High Temperature Oxidation of Fe-Al and Fe-Cr-Al Alloys: The Role of Cr as a Chemically Active Element", *Corros. Sci.*, **52** (10), 3394-3404 (2010), doi:10.1016/j.corsci.2010.06.019 (Morphology, Calculation, Experimental, Theory, Electronic Structure, Interface Phenomena, Kinetics, 84)

[2010Bau] Bauer, B., "Single Crystal Growth and Characterization of Al-rich Complex Metallic Phases in Al-Cr-Fe and Adjacent Systems" (in German), *PhD Thesis, Ludwig-Maximilians-Universitaet Muenchen, Muenchen*, 1-137 (2010) (Crystal Structure, Phase Diagram, Experimental, Review, 98)

[2010Bra] Brady, M.P., Tortorelli, P.F., More, K.L., Walker, L.R., "Sulfidation-Oxidation Behavior of FeCrAl and TiCrAl and the Third-Element Effect", *Oxid. Met.*, **74**(1), 1-9 (2010), doi:10.1007/s11085-010-9194-6 (Morphology, Experimental, Interface Phenomena, Kinetics, 40)

[2010Chu] Chumak, I., Richter, K.W., Ehrenberg, H., "Redetermination of Iron Dialuminide, $FeAl_2$", *Acta Crystallogr., Sect. C*, **C66**, i87-i88 (2010), doi:10.1107/S0108270110033202 (Experimental, Crystal Structure, 10)

[2010Gal] Galano, M., Audebert, F., Escorial, A.G., Stone, I.C., Cantor, B., "Nanoquasicrystalline Al-Fe-Cr-Based Alloys with High Strength at Elevated Temperature", *J. Alloys Compd.*, **495**(2), 372-376 (2010), doi:10.1016/j.jallcom.2009.10.208 (Crystal Structure, Morphology, Phase Relations, Experimental, Mechanical Properties, Nano, 16)

[2010Kob] Kobayashi, S., Takasugi, T., "Mapping of 475°C Embrittlement in Ferritic Fe-Cr-Al Alloys", *Scr. Mater.*, **63**(11), 1104-1107 (2010), doi:10.1016/j.scriptamat.2010.08.015 (Morphology, Phase Relations, Experimental, Mechanical Properties, 13)

[2010Kra] Krainikov, A.V., "Effect of the Structure and Chemical Inhomogeneity of Rapidly Solidified Powders on the Properties of Aluminum Alloys", *Powder Metall. Met. Ceram.*, **49**(7-8), 397-409 (2010), doi:10.1007/s11106-010-9250-4, translated from *Poroshkovaya Metallurgiya*, **49**(7-8), 34-50 (2010) (Morphology, Phase Relations, Experimental, Review, Kinetics, Mechanical Properties, Physical Properties, Transport Phenomena, 40)

[2010Pav] Pavlyuchkov, D., Bauer, B., Kowalski, W., Surowiec, M., Grushko, B., "On the Constitution of $Al_4(Cr,Fe)$", *Intermetallics*, **18**(1), 22-26 (2010), doi:10.1016/j.intermet.2009.06.002 (Crystal Structure, Phase Diagram, Phase Relations, Experimental, *, 21)

[2010Pop] Popcevic, P., Smontara, A., Ivkov, J., Wencka, M., Komelj, M., Jeglic, P., Vrtnik, S., Bobnar, M., Jaglicic, Z., Bauer, B., Gille, P., Borrmann, H., Burkhardt, U., Grin, Yu., Dolinsek, J., "Anisotropic Physical Properties of the $Al_{13}Fe_4$ Complex Intermetallic and its Ternary Derivative $Al_{13}(Fe,Ni)_4$", *Phys. Rev. B: Condens. Matter.*, **81**(18), 184203 (2010), doi:10.1103/PhysRevB.81.184203 (Crystal Structure, Experimental, Magnetic Properties, Physical Properties, Transport Phenomena, 42)

[2010Sch] Schneibel, J.H., Ruehe, H., Heilmaier, M., Saage, H., Goncharenko, M., Loboda, P., "Low Cycle Fatigue of Fe_3Al-Based Iron Aluminide with and without Cr", *Intermetallics*, **18**(7), 1369-1374 (2010), doi:10.1016/j.intermet.2010.03.013 (Crystal Structure, Morphology, Experimental, Mechanical Properties, 17)

[2010Ste] Stein, F., Vogel, S.C., Eumann, M., Palm, M., "Determination of the Crystal Structure of the ε Phase in the Fe-Al System by High-Temperature Neutron Diffraction", *Intermetallics*, **18**, 150–156 (2010), doi:10.1016/j.intermet.2009.07.006 (Crystal Structure, Morphology, Experimental, 40)

[2010Xio] Xiong, W., Selleby, M., Chen, Q., Odqvist, J., Du, Y., "Phase Equilibria and Thermodynamic Properties in the Fe-Cr System", *Crit. Rev. Solid State Mater. Sci.*, **35**(2), 125-152 (2010), doi:10.1080/10408431003788472 (Calculation, Phase Diagram, Thermodynamics, 227)

[2010Zha] Zhao, F.-Z., Zeng, P.-H., Ji, S.-F., Yang, X., Li, C.-Y., "Catalytic Combustion of Toluene over Cu_xCo_{1-x}/Al_2O_3/FeCrAl Monolithic Catalysts", *Acta Phys. Chim. Sin.*, **26**(12), 3285-3290 (2010), doi:10.3866/PKU.WHXB20101137 (Crystal Structure, Morphology, Calculation, Experimental, Catalysis, Electronic Structure, Kinetics, 26)

[2011Bau] Bauer, B., Gille, P., "Crystal Growth of Al-Rich Complex Metallic Phases in the System Al-Cr-Fe Using the Czochralski Method", *Z. Anorg. Allg. Chem.*, **637**(13), 2052-2058 (2011), doi:10.1002/zaac.201100290 (Crystal Structure, Morphology, Phase Relations, Experimental, *, 18)

[2011Hei] Heinonen, M.H., Kokko, K., Punkkinen, M.P.J., Nurmi, E., Kollar, J., Vitos, L., "Initial Oxidation of Fe-Al and Fe-Cr-Al Alloys: Cr as an Alumina Booster", *Oxid. Met.*, **76**(3-4), 331-346 (2011), doi:10.1007/s11085-011-9258-2 (Morphology, Calculation, Experimental, Theory, Electronic Structure, Interface Phenomena, Kinetics, 41)

[2011Kho1] Khoruzha, V.G., Kornienko, K.E., Pavlyuchkov, D.V., Grushko, B., Velikanova, T.Ya., "The Al-Cr-Fe Phase Diagram. I. Phase Equilibria at Subsolidus Temperatures over Composition Range 58-100 at.% Al", *Powder Metall. Met. Ceram.*, **50**(1-2), 83-97 (2011), doi:10.1007/s11106-011-9306-0, translated from *Poroshk. Metallurgiya*, **50**(1-2), 106-123 (2011) (Crystal Structure, Morphology, Phase Diagram, Phase Relations, Experimental, Review, #, 25)

[2011Kho2] Khoruzha, V.G., Kornienko, K.E., Pavlyuchkov, D.V., Grushko, B., Velikanova, T.Ya., "The Al-Cr-Fe Phase Diagram. II. Liquidus Surface and Phase Equilibria for Crystallization of 58-100 at.% Al Alloys", *Powder Metall. Met. Ceram.*, **50**(3-4), 217-229 (2011), doi:10.1007/s11106-011-9321-1, translated from *Poroshk. Metallurgiya*, **50**(3-4), 117-132 (2011) (Crystal Structure, Morphology, Phase Diagram, Phase Relations, Experimental, Review, #, 9)

[2011Kim] Kim, S.-Y., Choi, S.-H., Yun, J.-Y., Kim, B.-K., Kong, Y.-M., Lee, K.-A., "High-Temperature Oxidation Behaviors of Fe-Cr-Al Bulk and Powder-Sintered Materials", *Met. Mater. Int.*, **17**(6), 983-992 (2011), doi:10.1007/s12540-011-6017-5 (Crystal Structure, Morphology, Experimental, Interface Phenomena, Kinetics, 14)

[2011La] La, P., Wang, H., Bai, Y., Yang, Y., Wei, Y., Lu, X., Zhao, Y., Cheng, C., "Microstructures and Mechanical Properties of Bulk Nanocrystalline Fe_3Al Materials with 5, 10 and 15 wt.% Cr Prepared by Aluminothermic Reaction", *Mater. Sci. Eng. A*, **528**(21), 6489-6496 (2011), doi:10.1016/j.msea.2011.05.011 (Crystal Structure, Morphology, Phase Relations, Experimental, Mechanical Properties, Nano, 35)

[2011Tom] Tomaru, M., Yakou, T., "Effect of Cr Contents on Corrosion Resistance of FeAl in HCl Solution" (in Japanese), *Tetsu to Hagane*, **97**(3), 117-122 (2011), doi:10.2355/tetsutohagane.97.117 (Crystal Structure, Morphology, Experimental, Electrochemistry, Interface Phenomena, Kinetics, 7)

[2011Xio] Xiong, W., Hedström, P., Selleby, M., Odqvist, J., Thuvander, M., Chen, Q., "An Improved Thermodynamic Modeling of the Fe-Cr System down to Zero Kelvin Coupled with Key Experiments", *Calphad*, **35**(3), 355-366 (2011), doi:10.1016/j.calphad.2011.05.002 (Calculation, Crystal Structure, Electronic Structure, Experimental, Morphology, Phase Diagram, Phase Relations, Thermodynamics, 55)

[2012Lam] Lambri, O.A., Perez-Landazabal, J.I., Recarte, V., Cuello, G.J., Golovin, I.S., "Order Controlled Dislocations and Grain Boundary Mobility in Fe-Al-Cr Alloys", *J. Alloys Compd.*, **537**, 117-122 (2012), doi:10.1016/j.jallcom.2012.04.119 (Crystal Structure, Morphology, Phase Relations, Experimental, Interface Phenomena, Magnetic Properties, 39)

[2012Rag] Raghavan, V., "Al-Cr-Fe (Aluminum-Chromium-Iron)", *J. Phase Equilib. Diffus.*, **33**(1), 55-58 (2012), doi:10.1007/s11669-012-9981-7 (Phase Diagram, Phase Relations, Review, 12)

[2012Sah] Saha, R., Srinivas, V., Venimadhav, A., "Observation of Magnetic Cluster Phase above Curie Temperature in Fe_2CrAl Heusler Alloy", *J. Magn. Magn. Mater.*, **324**(7), 1296-1304 (2012), doi:10.1016/j.jmmm.2011.11.014 (Crystal Structure, Experimental, Magnetic Properties, 40)

[2012Ume] Umetsu, R.Y., Morimoto, N., Nagasako, M., Kainuma, R., Kanomata, T., "Annealing Temperature Dependence of Crystal Structures and Magnetic Properties of Fe_2CrAl and Fe_2CrGa Heusler Alloys", *J. Alloys Compd.*, **528**, 34-39 (2012), doi:10.1016/j.jallcom.2012.02.163 (Crystal Structure, Phase Relations, Experimental, Magnetic Properties, 28)

[2012Yil] Yildirim, M., Akdeniz, M.V., Mekhrabov, A.O., "Effect of Ternary Alloying Elements Addition on the Order-Disorder Transformation Temperatures of *B*2-Type Ordered Fe-Al-X Intermetallics", *Metall. Mater. Trans. A*, **43**(6), 1809-1816 (2012), doi:10.1007/s11661-011-1059-3 (Crystal Structure, Morphology, Phase Relations, Calculation, Experimental, 35)

[2013Bau] Bauer, B., Pedersen, B., Frey, F., "Chapter 22. $Al_4(Cr,Fe)$: A Structure Survey" in "*Aperiodic Crystals*", Schmid, S., Withers, R.L., Livshitz, R. (Eds.), Springer, Dordrecht, 163-170 (2013), doi:10.1007/978-94-007-631-6_22 (Crystal Structure, Review, 10)

[2013Hu] Hu, B., Zhang, W., Peng, Y., Du, Y., Liu, S., Zhang, Y., "Thermodynamic Reassessment of the Al-Cr-Si System with the Refined Description of the Al-Cr System", *Thermochim. Acta*, **561**, 77-90 (2013), doi:10.1016/j.tca.2013.03.033 (Calculation, Crystal Structure, Experimental, Phase Diagram, Phase Relations, Thermodynamics, 66)

[2013Khv] Khvan, A., Watson, A., "Al-Cr Binary Phase Diagram Evaluation", in *MSI Eureka*, Effenberg, G. (Ed.), MSI, Materials Science International Services GmbH, Stuttgart (2013), Document ID: 20.12106.1.1 (Crystal Structure, Phase Diagram, Phase Relations, Assessment, 73)

[2013Mar] Markus, T., Motalov, V.B., Kath, D., Singheiser, L., "Thermodynamic Properties of Al-Cr-Fe Alloys: Experimental Investigation by Knudsen Effusion Mass Spectrometry", *ESC Trans.*, **46**(1), 291-301 (2013), doi:10.1149/04601.0291ecst (Thermodynamics, Experimental, 12)

[2013Nei] Neikov, O.D., Sirko, A.I., Zakharova, N.P., Efimov, N.A., Vasil´eva, G.I., Sharovskii, A.O., Samelyuk, A.V., Goncharuk, V.A., Ivashchenko, R.K., "Effect of Starting Powder Properties on the Structure and Mechanical Characteristics of Al-8Cr-1.5Fe Alloy for High-Temperature Applications", *Powder Metall. Met. Ceram.*, **52**(3-4), 144-153 (2013), doi:10.1007/s11106-013-9507-9, translated from *Poroshkovaya Metallurgiya*, **52**(3-4), 36-47 (2013) (Crystal Structure, Morphology, Experimental, Mechanical Properties, 15)

[2014Gas] Gaspari, R., Erni, R., Arroyo, Y., Parlinska-Wojtan, M., Dshemuchadse, J., Pignedoli, C.A., Passerone, D., Schmutz, P., Beni, A., "Real Space Crystallography of a Complex Metallic Alloy: High-angle Annular Dark-field Scanning Transmission Electron Microscopy of o-$Al_4(Cr, Fe)$",

J. Appl. Crystallogr., **47**(3), 1026-1031 (2014), doi:10.3929/ethz-a-010160251 (Crystal Structure, Experimental, 53)

[2014Pav] Pavlyuchkov, D., Przepiorzynski, B., Kowalski, W., Velikanova, T.Ya., Grushko, B., "Al-Cr-Fe Phase Diagram. Isothermal Sections in the Region above 50 at.% Al", *Calphad*, **45**, 194-203 (2014), doi:10.1016/j.calphad.2013.12.007 (Crystal Structure, Morphology, Phase Diagram, Phase Relations, Experimental, #, 25)

[2014Ste] Stein, F., He, C., Wossack, I., "The Liquidus Surface of the Cr-Al-Nb System and Re-Investigation of the Cr-Nb and Al-Cr Phase Diagrams", *J. Alloys Compd.*, **598**, 253-265 (2014), doi:10.1016/j.jallcom.2014.02.045 (Crystal Structure, Experimental, Morphology, Phase Diagram, Phase Relations, 48)

[2014Wu] Wu, H., Zhang, M., Xu, B., Ling, G., "Preparation and Characterization of $Al_{11}Cr_4$ Phase by Diffusion of Al/Cr Composite Film", *J. Alloys Compd.*, **610**, 492-497 (2014), doi:10.1016/j.jallcom.2014.05.022 (Crystal Structure, Experimental, Kinetics, Phase Diagram, Phase Relations, Transport Phenomena, 33)

[2015Kur] Kurtuldu, G., Jessner, P., Rappaz, M., "Peritectic Reaction on the Al-rich Side of Al-Cr System", *J. Alloys Compd.*, **621**, 283-286 (2015), doi:10.1016/j.jallcom.2014.09.174 (Crystal Structure, Morphology, Phase Relations, Experimental, Theory, 28)

[2015Sus] Susner, M.A., Parker, D.S., Sefat, A.S., "Importance of Doping and Frustration in Itinerant Fe-doped Cr_2Al", *J. Magn. Magn. Mater.*, **392**, 68-73 (2015), doi:10.1016/j.jmmm.2015.05.024 (Crystal Structure, Calculation, Experimental, Electronic Structure, Electrical Properties, 27)

[2015Wit] Witusiewicz, V.T., Bondar, A.A., Hecht, U., Velikanova, T.Ya., "Thermodynamic Re-Modelling of the Ternary Al-Cr-Ti System with Refined Al-Cr Description", *J. Alloys Compd.*, **644**, 939-958 (2015), doi:10.1016/j.jallcom.2015.04.231 (Crystal Structure, Morphology, Phase Diagram, Phase Relations, Thermodynamics, Assessment, Calculation, Experimental, *, 92)

[2015Zho] Zhou, Zh., Li, Zh., Xie, Y., Wang, X., Liu, Y., Long, Zh., Yin, F., "Experimental Study of the Phase Relationships in the Al-Rich Corner of the Al-Si-Fe-Cr Quaternary System at 700°C", *Int. J. Mater. Res. (Z. Metallkd.)*, **106**(5), 470-480 (2015), doi:10.3139/146.111202 (Crystal Structure, Morphology, Phase Diagram, Phase Relations, Experimental, #, 32)

[2016Dah] Dahmane, F., Mogulkoc, Y., Doumi, B., Tadjer, A., Khenata, R., Bin Omran, S., Rai, D.P., Murtaza, G., Varshney, Dinesh, "Structural, Electronic and Magnetic Properties of Fe_2-Based Full Heusler Alloys: A First Principle Study", *J. Magn. Magn. Mater.*, **407**, 167-174 (2016), doi:10.1016/j.jmmm.2016.01.074 (Crystal Structure, Calculation, Electronic Structure, Magnetic Properties, 47)

[2016Li1] Li, X., "Al-rich Fe-Al Based Alloys: Phase Equilibria, Microstructures, Coarsening Kinetics and Mechanical Behavior", *Ph. Dr. Thesis,* Ruhr Univ. Bochum, 1-90 (2016) (Crystal Structure, Morphology, Phase Diagram, Phase Relations, Experimental, Review, Interphase Phenomena, Mechanical Properties, Transport Phenomena, 127)

[2016Li2] Li, X., Scherf, A., Heilmaier, M., Stein, F., "The Al-Rich Part of the Fe-Al Phase Diagram", *J. Phase Equilib. Diffus.*, **37**, 162-173 (2016), doi:10.1007/s11669-015-0446-7 (Crystal Structure, Phase Diagram, Phase Relations, Experimental, 38)

[2016Sve] Svec, M., Kejzlar, P., "The Influence of Ternary Alloying Element in Iron Aluminides on Coefficient of Thermal Expansion", *Kovove Mater.*, **54**(2), 83-89 (2016), doi:10.4149/km-2016-2-83 (Crystal Structure, Morphology, Phase Relations, Experimental, Mechanical Properties, 18)

[2017Cao] Cao, B.B., "On the Structure of the Hexagonal μ-Al_4Cr and its Relation to the Monoclinic η-$Al_{11}Cr_2$", *J. Alloys Compd.*, **698**, 605-610 (2017), doi:10.1016/j.jallcom.2016.12.270 (Crystal Structure, Experimental, 25)

[2017Cui] Cui, S., Jung, I.-H., Kim, J., Xin, J., "A Coupled Experimental and Thermodynamic Study of the Al-Cr and Al-Cr-Mg Systems", *J. Alloys Compd.*, **698**, 1038-1057 (2017), doi:10.1016/j.jallcom.2016.12.298 (Crystal Structure, Morphology, Thermodynamics, Phase Diagram, Assessment, Calculation, Experimental, Interphase Phenomena, Transport Phenomena, 73)

[2017Kra] Kratochvil, P., Danis, S., Minarik, P., Pesicka, J., Kral, R., "Strengthening of Fe_3Al Aluminides by One or Two Solute Elements", *Metall. Mater. Trans. A*, **48**(9), 4135-4139 (2017), doi:10.1007/s11661-017-4211-x (Crystal Structure, Morphology, Experimental, Mechanical Properties, 22)

[2017Wan] Wang, S., Li, Z., Qin, Z., Wang, S., Lu, X., Li, C., "Thermodynamic Modeling of Al-Fe-Cr Ternary System", *TMS 2017 146th Ann. Meeting Exhib. Suppl. Proceed.*, 443-454 (2017),

doi:10.1007/978-3-319-51493-2_42 (Phase Diagram, Phase Relations, Thermodynamics, Assessment, Calculation, 31)

[2019Cha] Chang, K., Meng, F., Ge, F., Zhao, G., Du, Sh., Huang, F., "Theory-Guided Bottom-up Design of the FeCrAl Alloys as Accident Tolerant Fuel Cladding Materials", *J. Nucl. Mater.*, **516**, 63-72 (2019), doi:10.1016/j.jnucmat.2019.01.002 (Crystal Structure, Phase Diagram, Thermodynamics, Calculation, Experimental, Review, Magnetic Properties, Mechanical Properties, *, 67)

[2019Eze] Ezemenaka, D., Phiri, A., Khvan, A., Cheverikin, V., Fartushna, I., Dinsdale, A., "An Experimental Investigation of Phase Transformations in the Al-Rich Corner of the Al-Cr-Fe System", *J. Alloys Compd.*, **808**, 151692 (2019), doi:10.1016/j.jallcom.2019.151692 (Crystal Structure, Morphology, Phase Diagram, Phase Relations, Experimental, #, 50)

[2019Ran] Rank, M., Franke, P., Hoffmann, J., Seifert, H.J., "Experimental Investigation of Phase Equilibria in the Al-Cr-Fe System", *Calphad*, **66**, 101638 (2019), doi:10.1016/j.calphad.2019.101638 (Crystal Structure, Phase Diagram, Experimental, Interphase Phenomena, Transport Phenomena, #, 65)

[2019Wan] Wang, R., Zhang, X., Wang, H., Ni, J., "Phase Diagrams and Elastic Properties of the Fe-Cr-Al Alloys: A First-Principles Based Study", *Calphad*, **64**, 55-65 (2019), doi:10.1016/j.calphad.2018.11.010 (Calculation, Crystal Structure, Electronic Structure, Mechanical Properties, Phase Diagram, Phase Relations, Thermodynamics, 71)

[2020Bou] Boulet, P., de Weerd, M.C., Gaudry, E., Ledieu, J., Fournée, V., "Single Crystal Growth, Crystal Structure and Surface Characterisation of the Binary Phase $Al_{45}Cr_7$", *J. Phys.: Conf. Ser.*, **1458**, 012016 (2020), doi:10.1088/1742-6596/1458/1/012016 (Crystal Structure, Experimental, 10)

[2020Ma] Ma, H., He, Z., Li, H., Zhang, T., Zhang, S., Dong, C., Steurer, W., "Novel Kind of Decagonal Ordering in $Al_{74}Cr_{15}Fe_{11}$", *Nature Comm.*, **11**(1), 1-7 (2020), doi:10.1038/s41467-020-20077-4 (Crystal Structure, Experimental, 29)

[2020Ran] Rank, M., "Thermodynamic-Kinetic Investigations in the Al-Cr-Fe System for ODS Steel Analyses" (in German), *PhD Thesis, Karlsruher Institut fuer Technologie, Karlsruhe, Germany*, 1-244 (2020) (Crystal Structure, Morphology, Phase Diagram, Phase Relations, Assessment, Experimental, Review, Interphase Phenomena, Transport Phenomena, #, 283)

[2021Liu] Liu, Y., Zhang, L., Cui, S., Li, W., "Effects of Transition Metal (Cr, Mn, Mo, Ni, Ti, and V) Doping on the Mechanical, Electronic and Thermal Properties of Fe_3Al", *Vacuum*, **185**, 110030 (2021), doi:10.1016/j.vacuum.2020.110030 (Calculation, Crystal Structure, Electronic Structure, Mechanical Properties, Transport Phenomena, Thermodynamics, 48)

[2021Mil] Milosavljevic, M.D., Burkhardt, U., Moll, P.J., Koenig, M., Borrmann, H., Grin, Y., "Crystal Structures of $AlCr_2$ and $MoSi_2$: Same Structure Type *vs.* Different Bonding Pattern", *Chem. Eur. J.*, **27**(57), 14209-14216 (2021), doi:10.1002/chem.202100817 (Crystal Structure, Experimental, 46)

[2022Ste] Stein, F., "Al-Fe Binary Phase Diagram Evaluation", in *MSI Eureka*, Watson, A. (Ed.), MSI, Materials Science International Services GmbH, Stuttgart (2022), Document ID: 20.10236.2.7 (2022), doi:10.7121/msi-eureka-20.10236.2.7 (Crystal Structure, Phase Diagram, Phase Relations, Assessment, 311)

Table 1: Investigations of the Al-Cr-Fe Phase Relations, Structures and Thermodynamics

Reference	Method/Experimental Technique	Temperature/Composition/Phase Range Studied
[1932Tai1]	Thermal analysis	94-100 at.% Al, liquidus surface
[1932Tai2]	Thermal analysis	94-100 at.% Al, liquidus surface
[1935Gru]	Thermal analysis	$Cr_{29.97}Fe_{59.86}Al_{10.17}$ (at.%)
[1940Kor1]	Thermal analysis	Whole range of compositions, liquidus surface
[1940Kor2]	Thermal analysis	Whole range of compositions, liquidus surface
[1945Kor]	Thermal analysis	Whole range of compositions, liquidus surface, isothermal section at 1150°C
[1946Kor]	Optical microscopy, thermal analysis	800-1300°C, whole range of compositions, liquidus surface, isothermal section at 1150°C
[1951Pra]	Optical microscopy, X-ray diffraction (XRD), thermal analysis, chemical analysis	425°C, 600°C, the Al-rich corner
[1954Chi]	Thermal analysis, optical microscopy	0-50 at.% Al
[1955Tag]	XRD, optical microscopy, thermal analysis	500-1000°C; 20-35 at.% Cr, 0-4 at.% Al

Reference	Method/Experimental Technique	Temperature/Composition/Phase Range Studied
[1958Chu]	XRD, optical microscopy, thermal analysis	600-1000°C, whole range of compositions
[1958Tag]	XRD, optical microscopy, thermal analysis	500-1000°C; 20-35 at.% Cr, 0-4 at.% Al
[1960Zol1], [1960Zol2]	XRD, optical microscopy, thermal analysis	Al-rich corner
[1961Fel]	XRD, electron diffraction	$Cr_{24.8}Fe_{75.02}Al_{0.18}$ (mass%) or $Cr_{26.1}Fe_{73.54}Al_{0.36}$ (at.%)
[1968Bul], [1969Bul1], [1969Bul2]	XRD, dilatometry	≤ 1000°C; 0-25 at.% Cr, 50-100 at.% Fe
[1969Kal]	Neutron diffraction	700-1000°C, $Cr_{2-x}Fe_xAl$ (x = 0 to 0.25)
[1969Sel]	High-temperature XRD	≤ 1000°C; 0-25 at.% Cr, 50-100 at.% Fe
[1970Koz1], [1970Koz2], [1970Koz3]	Optical microscopy, thermal analysis, XRD	0-70 mass% Fe, 0-40 mass% Al
[1971Sto]	Optical microscopy, XRD, scanning electron microscopy (SEM)	$Cr_{12.9}Fe_{85.8}Al_{1.3}$, $Cr_{26.1}Fe_{73}Al_{0.9}$, $Cr_{11.5}Fe_{82.8}Al_{5.7}$, $Cr_{27.8}Fe_{67.3}Al_{4.9}$ (mass%)
[1971Yam]	Differential thermal analysis (DTA), Mössbauer absorption spectroscopy (Fe^{57}, Co^{57}), optical microscopy	36-39 at.% Cr, 64-56 at.% Fe, 0-5 at.% Al
[1972Kaj]	XRD, neutron diffraction	25 at.% Al
[1974Niz]	XRD, neutron diffraction	25 at.% Al
[1975Lit]	XRD, neutron diffraction	25 at.% Al
[1976Vla]	XRD, optical microscopy	490°C, $Cr_{0.6}Fe_{3.5}Al_{95.9}$, $Cr_{0.3}Fe_{3.5}Al_{96.2}$, $Cr_{0.8}Fe_{3.5}Al_{95.7}$ (at.%)
[1977Ost]	Solution calorimetry	1550-1600°C; aluminium solutions in $Fe_{70}Cr_{30}$ (at.%) melt
[1977Tys]	XRD, neutron diffraction	25 at.% Al
[1981Bus]	XRD	800°C, $Cr_{25}Fe_{50}Al_{25}$ (at.%)
[1982Nao]	XRD, optical microscopy, transmission electron microscopy (TEM)	10-50 at.% Cr, 5-40 at.% Al
[1983Bus]	XRD	800°C, $Cr_{25}Fe_{50}Al_{25}$ (at.%)
[1985Okp]	XRD, neutron diffraction, optical microscopy, electron microscopy	830°C, $Cr_{0.5}FeAl_{0.5}$, $Cr_{0.4}FeAl_{0.6}$
[1986Sme]	Optical microscopy, SEM, EDXD	1050°C, $Cr_{25.24}Fe_{71.37}Al_{3.39}$ (mass%)
[1987Wou]	Angular dispersive XRD (ADXD), EDXD, TEM, Mössbauer spectroscopy	$Cr_{0.7}Fe_{0.3}Al_6$
[1988Man]	XRD	850-900°C, > 92 at.% Al
[1988Sch]	ADXD, TEM, EDXD	50 at.% Al
[1989Law1]	XRD, DTA, TEM, electron diffraction	86 at.% Al
[1989Law2]	XRD, DTA	86 at.% Al
[1989Man]	XRD	80 at.% Al
[1989McK]	Optical microscopy, SEM, TEM	$Fe_{72}Al_{28}$ (at.%) with additions 2-6 at.% Cr
[1990Ioa]	XRD, optical microscopy, TEM	$Cr_{2.13}Fe_{0.5}Al_{97.37}$ (at.%)
[1991Pra]	SEM, EDXD, wavelength dispersive X-ray spectrometry (WDS)	50-80 at.% Fe, ≤ 20 at.% Cr
[1991Tre]	XRD, optical microscopy, DTA	≤ 1800°C, Cr-FeAl section
[1992Hil]	Knudsen effusion mass spectroscopy (KEMS)	1040-1283°C, $Cr_{19.96}Fe_{70.72}Al_{9.32}$ (at.%)
[1993Kni]	XRD, SEM, TEM, electron energy loss spectroscopy (EELS)	Fe_3Al with 2 or 5 mass% Cr
[1993Sta]	XRD, DSC, Mössbauer spectroscopy	$Cr_8Fe_6Al_{86}$ (at.%)

Reference	Method/Experimental Technique	Temperature/Composition/Phase Range Studied
[1994Hyd]	Electrical resistivity measurements	$Cr_{1.8}Fe_{72.69}Al_{25.51}$, $Cr_{4.29}Fe_{69.74}Al_{25.97}$ (at.%)
[1994Mor]	XRD, TEM, DSC	$Cr_5Fe_{28}Al_{67}$ (at.%)
[1995Ant]	XRD, high-temperature DTA, differential scanning calorimetry (DSC)	$Cr_1Fe_{73}Al_{26}$, $Cr_2Fe_{72}Al_{26}$, $Cr_4Fe_{70}Al_{26}$ (at.%)
[1995Sta]	XRD, DTA, EDXD	$Cr_8Fe_6Al_{86}$ (at.%)
[1995Sui]	XRD, TEM	$CrFe_2Al_{12}$
[1995Yos]	Electrical resistivity measurements, TEM	$Cr_2Fe_{73}Al_{25}$, $Cr_2Fe_{70}Al_{28}$ (at.%)
[1995Zia]	XRD, SEM, TEM, DSC	Cr_3Al_{97}, $Cr_3Fe_1Al_{96}$, $Cr_3Fe_3Al_{94}$ (at.%)
[1997Nis1], [1997Nis2]	Vickers hardness measurements, electrical resistivity measurements, XRD	$(Fe_{1-x}Cr_x)_3Al$ series
[1997Pal]	XRD, electron microprobe analysis (EPMA)	1000°C, 40-100 at.% Al
[1997Rud]	DSC, EPMA	20-700°C, Fe_3Al–5 at.% Cr
[1997Sat]	XRD, neutron diffraction, Mössbauer studies	10-300 K, $Cr_xFe_{3-x}Al$
[1997Sui]	XRD, high-resolution electron microscopy (HREM)	$CrFe_2Al_{12}$
[1998Kim]	Neutron diffractometry, XRD, TEM	25-1100°C, $Cr_5Fe_{67}Al_{28}$ (at.%)
[1998Lia]	Electron diffraction, HREM	$CrFe_2Al_{12}$
[1998Sun]	Neutron diffractometry, XRD, SEM, TEM	500°C, Fe_3Al + 5 at.% Cr
[1999Sui]	Electron diffraction, TEM	$CrFe_2Al_{12}$
[1999Wit]	TEM, EDXD, atomic force microscopy (AFM), lateral force microscopy (LFM)	0-18 at.% Cr, 7-25 at.% Al
[2000Bla]	EPMA, Mössbauer spectroscopy	1200°C, ≤ 1 at.% Al
[2000Dem]	DTA, TEM, SEM, EMPA	$Cr_{11}Fe_8Al_{81}$
[2000Mo]	TEM, HREM, XRD	$CrFe_2Al_{12}$
[2000Spi]	XRD, TEM	9.3-18 at.% Cr, 7.6-25.5 at.% Al
[2001Alo]	XRD, Mössbauer spectroscopy	830°C, $Cr_xFe_{0.7-x}Al_{0.3}$ ($x \leq 0.35$)
[2001Dem]	DTA, TEM, SEM, EPMA	$Cr_{11}Fe_8Al_{81}$
[2002Ban]	Calculation based on the Bragg-Williams theory of order-disorder transformation	Atomic ordering in (Cr,Fe)Al
[2003Zou]	High-resolution TEM, electron diffraction	$CrFe_2Al_{12}$
[2004Dem]	TEM, EDXD, EPMA	25-584°C, thin films $Cr_{23.3}Fe_{9.1}Al_{67.6}$, $Cr_{22}Fe_8Al_{70}$, $Cr_{19.5}Fe_8Al_{72.5}$, $Cr_{15.8}Fe_{8.7}Al_{75.5}$, $Cr_{14.5}Fe_8Al_{77.5}$ (at.%)
[2004Den]	XRD (on the single crystal), EPMA	$CrFe_2Al_{12}$
[2004Wu]	X-ray Laue back reflection technique	400°C, $Cr_3Fe_{57}Al_{40}$ (at.%)
[2004Zha]	XRD	$Cr_{25}Fe_{50}Al_{25}$ (at.%)
[2005Bel]	XRD, SEM, backscattered electron (BSE) imaging, EDXD	$Cr_{16.5}Fe_6Al_{77.5}$ (at.%)
[2005Reg1]	SEM	500°C, 14.5 and 19 at.% Al, 1, 2 and 5 at.% Cr
[2005Reg2]	SEM	500°C, 14.5 and 19 at.% Al, 1, 2 and 5 at.% Cr
[2005Zha]	XRD, SEM, EDXD	1000°C, $Cr_5Fe_{85}Al_{10}$ and $Cr_{10}Fe_{80}Al_{10}$ (at.%)
[2006Bih]	XRD, SEM, optical microscopy, EDXD, BSE imaging	$Cr_{19.5}Fe_8Al_{72.5}$, $Cr_{21.5}Fe_6Al_{72.5}$, $Cr_{23.7}Fe_{9.1}Al_{67.6}$ (at.%)
[2006Dem]	TEM, electron diffraction	65-81 at.% Al
[2006Gol1], [2006Gol2]	Inductively coupled plasma optical emission spectroscopy (ICPOES), TEM, SEM, optical microscopy, XRD, DSC	Fe_3Al + (2.5-25) at.% Cr
[2006Kar]	Melt spinning, high-temperature XRD	$Cr_2Fe_4Al_{94}$, $Cr_{3.4}Fe_8Al_{88.6}$ (at.%)
[2006Sha]	TEM, SEM, optical microscopy	600-1000°C, $Cr_3Fe_{69}Al_{28}$ (at.%)

Reference	Method/Experimental Technique	Temperature/Composition/Phase Range Studied
[2007Chi]	Chemical analysis, optical microscopy	$Cr_5Fe_{67}Al_{28}$, $Cr_2Fe_{70}Al_{28}$ (at.%)
[2007Cho]	SEM, EDXD, optical microscopy	$Cr_6Fe_{69}Al_{25}$ (at.%)
[2007Pad]	XRD, Mössbauer spectroscopy	400°C, $Cr_{22.5}Fe_{52.5}Al_{25}$, $Cr_{25}Fe_{50}Al_{25}$, $Cr_{27.5}Fe_{47.5}Al_{25}$ (at.%)
[2007Pan]	Auger electron spectroscopy (AES), XRD	300°C, 400°C, 500°C, Cr/Al/Fe thin films
[2008For]	SEM	Fibers $Cr_{25}Fe_{70}Al_5$ (at.%)
[2008Jac]	KEMS, EDXD, SEM	877-1277°C, $Cr_{15.1}Fe_{45.1}Al_{39.8}$, $Cr_{30.2}Fe_{49.9}Al_{19.9}$ (at.%)
[2008Lu]	XRD, EPMA, SEM, EDXD	600°C, 5-20 at.% Cr, 10 at.% Al
[2008Pav1]	TEM, DSC	$Cr_5Fe_{69}Al_{26}$ (at.%)
[2008Pav2]	EDXD-SEM, electron diffraction	1000°C, 70-81 at.% Al
[2008Pav3]	SEM, EPMA, TEM, DTA	800°C, 80-90 at.% Al, 5-15 at.% Cr
[2008Pin]	SEM, EPMA	900-1000°C, 10-19 at.% Al, 1-20 at.% Cr
[2008Shr]	XRD	$Cr_{25}Fe_{50}Al_{25}$ (at.%)
[2009Bau]	Czochralski method, neutron diffraction	$Cr_{19}Fe_3Al_{78}$ (at.%)
[2009Dea]	Combustion-infrared absorbance, inert gas fusion-thermal conductivity, inductively-coupled plasma analysis, Netzsch STA 409 high-temperature thermogravimetric analysis (TGA), SEM, EDXD	$Cr_5Fe_{85}Al_{10}$, $Cr_5Fe_{82.5}Al_{12.5}$ (mass%)
[2009Gol]	XRD, TEM, DSC	25-28 at.% Al, 3-25 at.% Cr
[2009Pav]	XRD, SEM, EDXD, TEM, DTA	700-1000°C, ~$Cr_{16}Fe_{12}Al_{72}$ (at.%)
[2010Bau], [2011Bau]	Bridgman method, Czochralski method, optical microscopy, neutron diffraction measurement, EPMA, single crystal XRD, DTA, X-ray topography	75-81 at.% Al, 1-11 at.% Cr
[2010Bra]	SEM, EPMA, high angle annular dark field (HAADF) scanning transmission electron microscopy (STEM)	$Cr_{20}Fe_{70}Al_{10}$ (at.%)
[2010Gal]	XRD, TEM, DSC	$Cr_{2.8}Fe_{4.2}Al_{93.0}$ (at.%)
[2010Kob]	Optical microscopy, SEM, TEM	475°C, ≤ 20 at.% Al, 10-30 at.% Cr
[2010Kra]	SEM, TEM, secondary ion mass spectrometry (SIMS), AES	Water-atomized powders, 5-8 at.% Cr, 1.5-5 at.% Fe
[2010Pav]	XRD, SEM, EDXD, TEM, DTA	700-980°C, 78.0-82.3 at.% Al, ≤ 4.9 at.% Fe
[2010Sch]	XRD, SEM, BSE imaging, energy dispersive spectroscopy (EDS)	$Cr_{4.0}Fe_{69.6}Al_{26.4}$ (at.%)
[2011Kho1]	Optical microscopy, XRD, DTA, SEM, EPMA	600-1165°C, 58-100 at.% Al
[2011Kho2]	Optical microscopy, XRD, DTA, SEM, TEM, EPMA	58-100 at.% Al
[2011Kim]	Optical microscopy, XRD, SEM, field emission-scanning electron microscopy (FE-SEM), EPMA	$Cr_{22}Fe_{72.2}Al_{5.8}$ (mass%) or $Cr_{21.9}Fe_{66.95}Al_{11.15}$ (at.%)
[2011La]	Optical microscopy, XRD, EPMA, TEM	Fe_3Al + 5 (10, 15) mass% Cr
[2011Tom]	Optical microscopy, XRD, SEM	44.8-48.0 at.% Al, 1-11.7 at.% Cr
[2012Lam]	ICPOES, optical microscopy, DSC, mechanical spectroscopy (MS), DTA	$Cr_8Fe_{67}Al_{25}$, $Cr_{25}Fe_{50}Al_{25}$ (at.%)
[2012Sah]	EDXD, SEM, XRD	1000°C, $CrFe_2Al$
[2012Ume]	Optical microscopy, EPMA, DSC, XRD, electron diffraction, TEM	600°C, 400°C, $Cr_{25}Fe_{50}Al_{25}$ (at.%)
[2012Yil]	EDXD, SEM-EPMA, XRD, DSC	400°C, $Cr_1Fe_{50}Al_{49}$ (at.%)

Reference	Method/Experimental Technique	Temperature/Composition/Phase Range Studied
[2013Bau]	Czochralski method, XRD, neutron diffraction	$Al_{79.1}Cr_{17.8}Fe_{3.1}$ (at.%)
[2013Mar]	KEMS, wavelength dispersive X-ray (WDX) analysis	961-1335°C, 11-31 at.% Al, 13-35 at.% Cr
[2013Nei]	Melt atomization, pulsed hot pressing (PHP), hot extrusion (HE), XRD, SEM	20, 190, and 300°C, $Cr_5Fe_{82.5}Al_{12.5}$ (mass%) or $Cr_{4.7}Fe_{72.55}Al_{22.75}$ (at.%)
[2014Gas]	XRD, EPMA, X-ray topography, TEM, HAADF STEM	$Cr_{17.8}Fe_{3.1}Al_{79.1}$ (at.%) single crystal
[2014Pav]	XRD, SEM, EDXD, TEM, DTA	700-1160°C, 50-100 at.% Al
[2015Sus]	XRD	1050°C, 33.3 at.% Al, ≤ 33.3 at.% Cr
[2015Zho]	XRD, SEM-EDXD, BSE imaging	700°C, 70-100 at.% Al
[2016Li1]	XRD, SEM, EPMA, DTA	As-cast, 1000°C, $Cr_2Fe_{37}Al_{61}$ (at.%)
[2016Sve]	XRD, SEM, EDXD, EBSD technique	As-cast, 460-1200°C, $Cr_2Fe_{72}Al_{26}$ (at.%)
[2017Kra]	XRD, TEM	26 at.% Al, 0 to 8 at.% Cr
[2019Cha]	XRD, EDXD	Magnetron-sputtered films, 60-75 at.% Fe
[2019Eze]	XRD, SEM, DTA, EPMA	81-99.6 at.% Al
[2019Ran], [2020Ran]	XRD, SEM-EDXD, EPMA, ICPOES, carrier gas hot extraction (CGHE), DSC, DTA, dilatometry, diffusion couples (DC) technique	10-70 at.% Al
[2019Wan]	Kohn-Sham equations of the density-functional theory, cluster variation method, cluster expansion method	FeAl, Fe_3Al, 327-2727°C
[2020Ma]	TEM, HAADF STEM, selected-area electron diffraction, energy dispersive X-ray spectrometry	1000°C, $Cr_{15}Fe_{11}Al_{74}$ (at.%)
[2020Ran]	Calphad-type assessment	Calculated isothermal sections between 700 and 1160°C, isopleth at 47.5 at.% Cr, liquidus surface

Table 2: Crystallographic Data of Solid Phases

Phase/ Temperature Range (°C)	Pearson Symbol/ Space Group/ Prototype	Lattice Parameters (pm)	Comments/References
(Al) < 660.452	*cF*4 $Fm\bar{3}m$ Cu	*a* = 404.96	pure Al at 25°C [Mas2] solubility of Cr: < 0.39 at.% [2015Wit] (Al-Cr) solubility of Fe: 0.023 at.% [2019Ran] (Al-Fe) dissolves up to 0.08 at.% Fe at 0.3 at.% Cr (Al-Cr-Fe) [2019Eze]
(Cr, αδFe) < 1863	cI2 $Im\bar{3}m$		Strukturbericht designation: *A2*
Cr < 1863	W	*a* = 288.48	pure Cr at 25°C [Mas2]
αFe < 912		*a* = 286.65	at 25°C [Mas2]
δFe 1538-1394		*a* = 293.15	[Mas2] solubility of Al in (αδFe): 45.0 at.% [1993Kat, 2007Ste] (Al-Fe) solubility of Al in (Cr): up to 53 at.% [2014Ste] (Al-Cr)
(γFe) 1394-846	*cF*4 $Fm\bar{3}m$ Cu	*a* = 364.67	at 915°C [V-C2, Mas2] solubility of Al: 1.35 at.% [1993Kat] (Al–Fe) solubility of Cr: < 11.9 at.% [2010Xio] (Cr-Fe)

Phase/ Temperature Range (°C)	Pearson Symbol/ Space Group/ Prototype	Lattice Parameters (pm)	Comments/References
$CrAl_7$	*mC*104		sometimes named Cr_2Al_{13}, Cr_7Al_{45}, θ-$CrAl_7$ or θ
< 794	*C*2/*m*		from 86.6 to 86.9 at.% Al [2013Khv]
	V_7Al_{45}	*a* = 2065.0±0.2	single crystal [2020Bou] (denoted as Cr_7Al_{45})
		b = 759.78±0.08	
		c = 1096.74±0.11	
		β=(107.308±0.002)°	
		a = 2060.28	for $Cr_{11.3}Fe_{2.4}Al_{86.3}$ (at.%) [2019Eze]
		b = 758.50	
		c = 1093.85	
		β = 107.33°	
			solubility of Fe: < 2.5 at.% [2019Eze] (Al-Cr-Fe)
Cr_2Al_{11}	*mC*616		sometimes named $CrAl_5$, η-Cr_2Al_{11} or η
(913<*T*<985)-(~500-~	*C*2/*c*		from 83.5 to 84 at.% Al [2013Khv]
600)	Cr_2Al_{11}	*a* = 1773.48±0.10	single crystal [2008Cao]
		b = 3045.55±0.17	
		c = 1773.44±0.10	
		β = (91.052±0.012)°	
		a = 1771.5±1.2	for $Cr_{16.8}Fe_{2.9}Al_{80.3}$ (at.%) at 910°C [2010Pav]
		b = 3069±3	
		c = 1773.8±2.5	
		β = (90.39±0.05)°	solubility of Fe: up to ~3 at.% at around 80 at.% Al [2010Pav] (Al-Cr-Fe)
$CrAl_4$	*hP*574		sometimes named μ-$CrAl_4$ or μ
< 1040	$P6_3/mmc$		from 78.7 to 81.3 at.% Al [2013Khv]
	$MnAl_4$	*a* = 2019.11±0.15	single crystal [2017Cao]
		c = 2485.40±0.19	
		a = 2013.79±0.04	single crystal $Cr_{20.6}Fe_{0.7}Al_{78.7}$ (at.%) [2010Bau]
		c = 2482.92±0.09	Solubility of Fe: < 1.7 at.% [2011Kho1] (Al-Cr-Fe)
Cr_4Al_{11}	*aP*15		sometimes named ν
< 829	$P\bar{1}$	*a* = 508.9±0.5	[2006Gru]
	Mn_4Al_{11}	*b* = 903.3±0.8	
		c = 504.4±0.2	
		α=(91.84±0.08)°	
		β=(100.77±0.07)°	
		γ=(107.59±0.09)°	
αCr_5Al_8 (r)	*hR*78		Strukturbericht designation: $D8_{10}$
< 1138	$R\bar{3}m$		sometimes named Cr_5Al_8(l), γ_2-Cr_5Al_8 or γ_2
	Cr_5Al_8	*a* =1272.8	[V-C2]
		c = 794.2	
		a =1271.5±0.1 to 1281.3±0.1	58.0 to 67.9 at.% Al [1989Ell]
		c = 792.8±0.1 to 795.1±0.1	
		a = 1253.7	for 31.2 at.% Fe at 1000°C [1997Pal]
		c = 779.1	
			solubility of Fe: up to ~35 at.% [2014Pav] (Al-Cr-Fe)

Phase/ Temperature Range (°C)	Pearson Symbol/ Space Group/ Prototype	Lattice Parameters (pm)	Comments/References
Cr_2Al	*tI*6		Strukturbericht designation: $C11_b$
< 910	*I*4/*mmm*		~28.6 to ~35.5 at.% Al [2013Khv]
	$MoSi_2$	a = 300.86 ± 0.02	[2021Mil]
		c = 865.31 ± 0.11	Solubility of Fe: up to 22 at.% Fe [2019Ran, 2020Ran] (Al-Cr-Fe)
σ, CrFe	*tP*30		~50.2 to ~57.3 at.% Fe [2010Xio]
820-(~500-~510)	$P4_2/mnm$	a = 879.95±0.04	single crystals [1954Ber]
	CrFe	c = 454.42±0.02	
			solubility of Al: up to 3 at.% [1958Chu] (Al-Cr-Fe)
Fe_3Al	*cF*16		sometimes named α_1 phase
< 545	$Fm\bar{3}m$		Strukturbericht designation: $D0_3$
	BiF_3		~24 to ~34 at.% Al at 400°C [1993Kat]
		a = 579.30	at 23.1 at.% Al, water-quenched from 250°C [1958Tay]
		a = 578.86	at 35.0 at.% Al, water-quenched from 250°C [1958Tay]
FeAl	*cP2*		sometimes named α_2 phase
< 1318	$Pm\bar{3}m$		Strukturbericht designation: *B*2
	CsCl		23.5 to ~53 at.% Al [2007Ste]
		a = 289.53 to 290.90	at 36.2 to 50.0 at.% Al, water-quenched from 250°C [1958Tay]
$FeAl_2$	*aP*18		sometimes named ζ phase
< 1146	$P\bar{1}$		64.7 to 66.7 at.% Al [2022Ste]
	$FeAl_2$	a = 487.45	at 66.4 at.% Al [2010Chu]
		b = 645.45	
		c = 873.61	
		α = 87.930°	
		β = 74.396°	
		γ = 83.062°	
		a = 486.3	at 4.5 at.% Cr at 1000°C [1997Pal]
		b = 645.4	
		c = 880.1	
		α = 91.92°	
		β = 72.95°	solubility of Cr: up to 4.5 at.% [1997Pal]
		γ = 96.87°	(Al-Cr-Fe)
Fe_2Al_5	*oC*24		sometimes named η phase
1159 - ~331	*Cmcm*		68.4 to 72.5 at.% Al [2022Ste]
	Fe_2Al_5		
		a = 765.59 ± 0.08	at 71.5 at.% Al [1994Bur]
		b = 641.54 ± 0.06	
		c = 421.84 ± 0.04	
		a = 769.4	at 6.2 at.% Cr at 1000°C [1997Pal]
		b = 644.3	
		c = 422.7	solubility of Cr: up to 6.2 at.% [1997Pal] (Al-Cr-Fe)

Phase/ Temperature Range (°C)	Pearson Symbol/ Space Group/ Prototype	Lattice Parameters (pm)	Comments/References
Fe_4Al_{13}	*mC*102		referred to as $FeAl_3$ in old literature before ~1995
< 1150	*C2/m*		sometimes named θ phase
	Fe_4Al_{13}		74.5 to 76.9 at.% Al [2022Ste]
		a = 1548.8 ± 0.1	single crystal grown by Czochralski
		b = 808.66 ± 0.05	technique [2008Gil, 2010Pop]
		c = 1247.69 ± 0.08	
		β =(107.669±0.004)°	
		a = 1554.3	at 6.4 at.% Cr at 1000°C [1997Pal]
		b = 802.9	
		c = 1245.0	solubility of Cr: up to 7 at.% [2019Ran, 2020Ran]
		β = 107.47°	(Al-Cr-Fe)
$FeAl_6$	*oC28*		metastable
	$Cmc2_1$	*a* = 744.0	single crystal [1965Wal]
	$FeAl_6$	*b* = 646.4	
		c = 877.9	
$(Cr,Fe)_5Al_8$	*cI*52		Strukturbericht designation: $D8_2$
< 1185	$I\bar{4}3m$		Continuous solid solution at 1160°C [2014Pav]
βCr_5Al_8 (h)	Cu_5Zn_8		sometimes named Cr_5Al_8(h), γ_1-Cr_5Al_8 or γ_1
1321-1060			(Al-Cr)
			59.2 to 68.4 at.% Al [2013Khv, 2015Wit]
		a = 909.0±0.1	at 67.3 at.% Al [1992Bra]
		a = 910.4±0.1 to 904.7±0.1	58.0 to 70.0 at.% Al [1989Ell]
Fe_5Al_8			sometimes named ε phase (Al-Fe)
1231-1095			56.0 to 64.5 at.% Al [2016Li2]
		a = 897.57 ± 0.02	at 1120°C, 59.4 at.% Al [2010Ste]
*ε-$(Cr,Fe)Al_4$	*oC*584		sometimes named as ε-Al_4Cr or ε
< 1055	*Cmcm*	*a* = 1252.1±0.1	single crystal [1997Li] (metastable in Al-Cr).
		b = 3470.5±0.2	
		c = 2022.3±0.1	
		a = 1249.841±0.03	for $Cr_{19.3}Fe_{1.8}Al_{78.9}$ (at.%), single crystal
		b = 3473.73±0.09	[2010Bau]
		c = 2021.29±0.05	
			This phase is metastable in Al-Cr. It is stabilized in Al-Cr-Fe at around 2-3 at.% Fe and 78-77 at.% Al [2010Bau, 2011Bau, 2011Kho1]
*o-$(Cr,Fe)Al_4$	*oP**	*a* = 1248.0±0.1	Compound possesses a highly modulated
<~ 1026	*Pmm*2	*b* = 2502.9±0.1	structure [2013Bau]
		c = 3058.1±0.1	Homogeneity range extends between 3 and 6 at.% Fe at around 78 at.% Al [2010Bau, 2011Bau]
*O_1	*o**		Stoichiometry is unknown.
< 1087			sometimes named as O_1 or $C_{3,I}$-Al-Cr-Fe
		a ≈ 3270	[2008Pav2]
		b ≈ 1240	
		c ≈ 2340	Homogeneity range extends between ca. $Cr_{15.0}Fe_{11.0}Al_{74.0}$ to $Cr_{19.7}Fe_{4.3}Al_{76.0}$ and $Cr_{15.0}Fe_{6.9}Al_{78.1}$ to $Cr_{18.3}Fe_{8.9}Al_{72.8}$ (at.%) [2011Kho1, 2011Kho2, 2014Pav]

Phase/ Temperature Range (°C)	Pearson Symbol/ Space Group/ Prototype	Lattice Parameters (pm)	Comments/References
*H < 998	*hR*1512 $R\bar{3}$	 a = 1772.28 ± 0.03 c = 8068.1 ± 0.2	Stoichiometry is unknown. Also named ν, H-(Al-Fe-Cr) or H-Al_4(Cr,Fe) for $Cr_{13.35}Fe_{6.63}Al_{80.02}$ (at.%), single crystal [2010Bau, 2011Bau] Large homogeneity extends between approximately $Cr_{12.0}Fe_{8.0}Al_{80.0}$ to $Cr_{19.7}Fe_{4.3}Al_{76.0}$ and $Cr_{11.0}Fe_{6.3}Al_{82.7}$ to $Cr_{13.5}Fe_{7.0}Al_{79.4}$ (at.%) [2011Kho1, 2019Eze]
*D < 1096	- $P10_5/mmc$ -	 n ≈ 1230 along the 10-fold symmetry axis	Stoichiometry is unknown. $Cr_{15}Fe_{11}Al_{74}$ (at.%) single crystal [2020Ma] Homogeneity range may extend from 70 to 72 at.% Al and from 14 to 18 at.% Cr [2011Kho1]
i (m)	simple icosahedral-type	 a_{6D}= 654.2 ± 0.2	metastable phase emerging at high cooling rates Proposed composition is $Cr_{12\pm1}Fe_{12\pm1}Al_{75\pm0.5}$ (at.%) [1995Zia] [1995Sta]

Table 3: Invariant Equilibria

Reaction	*T* (°C)	Type	Phase	Composition (at.%)		
				Al	Cr	Fe
L + (Cr, Fe)$_5Al_8$ ⇌ αCr_5Al_8	1185	p_3, max	L	~69.5	~17.7	~12.8
L ⇌ αCr_5Al_8 + Fe_2Al_5	1136	e_2, max	L	~67.2	~10.2	~22.6
L ⇌ (Cr, Fe)$_5Al_8$ + αCr_5Al_8 + Fe_2Al_5	1125	E_1	L	66	10	24
			(Cr, Fe)$_5Al_8$	63.1	13.0	23.9
			αCr_5Al_8	63.4	13.7	22.8
			Fe_2Al_5	70.2	4.3	25.5
L ⇌ αCr_5Al_8 + Fe_4Al_{13}	1115	e_3, max	L	~70.4	~10.7	~18.9
L ⇌ Fe_4Al_{13} + αCr_5Al_8 + Fe_2Al_5	1105	E_2	L	69.2	10.0	20.8
			Fe_4Al_{13}	74.0	4.5	21.5
			αCr_5Al_8	64.8	18.4	16.8
			Fe_2Al_5	71.2	5.3	23.5
L + αCr_5Al_8 ⇌ D	1096	p_5, max	L	~72.1	~13.6	~14.3
L ⇌ D + Fe_4Al_{13}	1093	e_4, max	L	~73.2	~11.4	~15.4
L + αCr_5Al_8 ⇌ O_1	1087	p_6, max	L	~76.2	~15.7	~8.1
L ⇌ D + Fe_4Al_{13} + αCr_5Al_8	1085	E_3	L	71	11	18
			D	69.8	16.4	13.8
			Fe_4Al_{13}	74.0	5.2	20.8
			αCr_5Al_8	66.0	21.9	12.1
L + αCr_5Al_8 ⇌ O_1 + D	1085	U_1	L	74.3	14.5	11.2
			αCr_5Al_8	67.0	23.8	9.2
			O_1	~72.8	~18.3	~8.9
			D	71.4	18.0	10.6
L + D ⇌ O_1 + Fe_4Al_{13}	~1075	U_2	L	74.8	13.0	12.2
			D	72.4	15.3	12.3
			O_1	74.0	15.0	11.0
			Fe_4Al_{13}	75.5	6.0	18.5
L + αCr_5Al_8 ⇌ ε-(Cr,Fe)Al_4	1055	p_7, max	L	~82.6	~15.0	~2.4

Reaction	*T* (°C)	Type	Phase	Composition (at.%)		
				Al	Cr	Fe
L + αCr_5Al_8 ⇌ ε-(Cr,Fe)Al_4 + O_1	1045	U_3	L	82.4	14.3	3.3
			αCr_5Al_8	~70	~27	~3
			ε-(Cr,Fe)Al_4	~77	~20	~3
			O_1	~76	~20	~4
L + αCr_5Al_8 ⇌ ε-(Cr,Fe)Al_4 + $CrAl_4$	1035	U_4	L	83.0	15.0	2.0
			αCr_5Al_8	~70	~28	~2
			ε-(Cr,Fe)Al_4	~77	~21	~2
			$CrAl_4$	~78	~20	~2
L + ε-(Cr,Fe)Al_4 + O_1 ⇌ o-(Cr,Fe)Al_4	~1026	P_1	L	~84	~13	~3
L + O_1 + Fe_4Al_{13} ⇌ H	998	P_2	L	84.0	9.0	7.0
			O_1	77.1	14.7	8.2
			Fe_4Al_{13}	76.7	4.8	18.4
			H	80.0	12.0	8.0
L+ ε-(Cr,Fe)Al_4 ⇌ $CrAl_4$ + o-(Cr,Fe)Al_4	~985	U_5	L	~85	~13	~2
L + O_1 ⇌ o-(Cr,Fe)Al_4 + H	~980	U_6	L	~85	~9	~6
L + $CrAl_4$ + o-(Cr,Fe)Al_4 ⇌ Cr_2Al_{11}	913<*T*<985	P_3	-	-	-	-
L + o-(Cr,Fe)Al_4 ⇌ Cr_2Al_{11} + H	900<*T*<980	U_7	-	-	-	-
L + Cr_2Al_{11} ⇌ $CrAl_7$ + H	750	U_8	L	96.8	2.3	0.9
			Cr_2Al_{11}	~83.0	~15.5	~1.5
			$CrAl_7$	~86.0	~13.0	~1.0
			H	~82.3	~14.2	~3.5
L + H ⇌ $CrAl_7$ + Fe_4Al_{13}	660	U_9	L	97.6	0.6	1.8
			H	82.7	11.0	6.3
			$CrAl_7$	86.0	11.5	2.5
			Fe_4Al_{13}	~77	~4	~19
L + $CrAl_7$ ⇌ Fe_4Al_{13} + (Al)	657	U_{10}	L	98.0	0.3	1.7
			$CrAl_7$	86.6	11.0	2.4
			Fe_4Al_{13}	~77	~1	~22
			(Al)	99.7	0.2	0.1

* Compositions of liquid phase for the maxima in the monovariant lines are as-read from the original figure by [2011Kho2]

Table 4: Thermodynamic Properties of the (Cr, αδFe) Phase

Phase	Temperature (°C)	Property per mole of atoms (J, mol, K)	Comments
(Cr, αδFe)	1227	$a_{Al} = (3.3 \pm 1.4)\cdot 10^{-3}$ $a_{Cr} = 0.28 \pm 0.4$ $a_{Fe} = 0.50 \pm 0.07$ $^{ex}\mu_{Al} = -42.0 \pm 7.0$ $^{ex}\mu_{Cr} = 4.3 \pm 1.9$ $^{ex}\mu_{Fe} = -4.4 \pm 2.0$	$Cr_{19.8}Fe_{71.2}Al_9$ (at.%), Knudsen effusion mass spectrometry [1992Hil]
(Cr, αδFe)	1177		[2013Mar], Knudsen effusion mass spectrometry
		$a_{Al} = 0.11$ $a_{Cr} = 0.19$ $a_{Fe} = 0.33$ $\Delta G_f = -18.4$	$Cr_{13}Fe_{56}Al_{31}$ (at.%)
		$a_{Al} = 0.07$ $a_{Cr} = 0.23$ $a_{Fe} = 0.35$ $\Delta G_f = -19.1$	$Cr_{17}Fe_{54.5}Al_{28.5}$ (at.%)

Phase	Temperature (°C)	Property per mole of atoms (J, mol, K)	Comments
(Cr, αδFe) (continued)	1177 (continued)	$a_{Al} = 0.048$ $a_{Cr} = 0.26$ $a_{Fe} = 0.38$ $\Delta G_f = -19.0$	$Cr_{19}Fe_{55}Al_{26}$ (at.%)
		$a_{Al} = 0.16$ $a_{Cr} = 0.23$ $a_{Fe} = 0.19$ $\Delta G_f = -20.2$	$Cr_{21}Fe_{44}Al_{35}$ (at.%)
		$a_{Al} = 0.031$ $a_{Cr} = 0.28$ $a_{Fe} = 0.41$ $\Delta G_f = -18.2$	$Cr_{24.4}Fe_{55}Al_{20.5}$ (at.%)
		$a_{Al} = 0.028$ $a_{Cr} = 0.34$ $a_{Fe} = 0.35$ $\Delta G_f = -19.2$	$Cr_{31}Fe_{48}Al_{21}$ (at.%)
		$a_{Al} = 0.009$ $a_{Cr} = 0.43$ $a_{Fe} = 0.53$ $\Delta G_f = -14.0$	$Cr_{35}Fe_{54}Al_{11}$ (at.%)
(Cr, αδFe)	1027	$\Delta H_{mix} = -22.74 \pm 2.0$ $\Delta H_{mix} = -11.05 \pm 1.1$	[2008Jac], Knudsen effusion mass spectrometry $Cr_{15.1}Fe_{45.1}Al_{39.8}$ (at.%) $Cr_{30.2}Fe_{49.9}Al_{19.9}$ (at.%)

Table 5: Investigations of the Al-Cr-Fe Materials Properties

Reference	Method/Experimental Technique	Type of Property
[1940Kor2]	Electrical measurements	Electrical resistivity
[1946Kor]	Brinell indentation, electrical measurements, dialtometry	Hardness, electrical resistivity, thermal expansion RT to 1000°C
[1955Tag], [1958Tag]	Rockwell indentation	Hardness
[1968Bul]	Brinell hardness test, electrical measurements	Hardness, electrical resistivity RT to 950°C
[1969Kal]	Magnetic measurements, neutron diffraction	Magnetic susceptibility RT to 500°C, magnetic moment, Néel temperature
[1971Sto]	TGA in O_2 atmosphere	Oxidation behaviour at 1000°C and 1200°C
[1974Niz], [1975Lit]	Magnetic measurements, neutron diffraction	Magnetic susceptibility -170°C to 500°C, magnetic moment
[1981Bus]	VSM	Curie temperature, magnetization at RT
[1982Nao]	Vickers indentation, tensile tests, bending tests, electrical measurements	Microhardness, yield stress, UTS, elongation, and electrical resistivity at RT; temperature coefficient of resistivity RT to 500°C
[1983Bus]	VSM, Kerr rotation measurements	Curie temperature, saturation moment at -269°C, magnetization at RT, Kerr rotation
[1985Okp]	VSM	Magnetization and magnetic susceptibility -196°C to RT
[1986Sme]	Oxidation tests in air	Oxidation behaviour at 1050°C
[1989McK]	Tensile tests	(0.2%) yield stress at RT and 600°C
[1991Pra]	Knoop indentation on melt-spun ribbons	Microhardness
[1991Sik1]	Tensile tests	0.2% yield stress, UTS, elongation, creep behaviour 450 to 704°C

Reference	Method/Experimental Technique	Type of Property
[1993Kni]	Tensile tests	Yield stress and elongation 700 to 850°C
[1994Hyd]	Electrical measurements	Electrical resistivity RT to 1200°C
[1995Sta]	VSM	Magnetic susceptibility -273 to -73°C
[1996Jim]	Compression tests	Creep behaviour 750°C to 1000°C
[1997Sat]	Magnetic balance, neutron diffraction	Magnetization at -196°C and RT, magnetic moments at -263°C, -196°C and RT
[1998Su]	Tensile tests	0.2% yield stress, UTS and elongation at RT
[1998Sun]	Tensile tests	UTS and elongation at RT
[2000Spi]	Compression tests	Compressive yield stress, work-hardening behavior
[2002Zho]	Torsion measurements	Internal friction RT-620°C
[2004Dem]	Optical measurements and wetting of thin films	Reflectivity, absorption and contact-angle
[2004Hua]	Tensile tests	0.2% yield stress and elongation at RT & 600°C, creep behaviour at 600°C
[2004Wu]	VSM	Magnetization -196°C to RT
[2004Zha]	SQUID, electrical measurements	Magnetic susceptibility, magnetization, and electrical resistivity -273°C to RT, DOS
[2005Bel]	SQUID, electrical measurements, NMR spin-lattice relaxation, SXES	Magnetic susceptibility and electrical resistivity -273°C to RT, relaxation rates -196°C to RT, DOS
[2005Reg1], [2005Reg2]	TGA	Oxidation, sulfidation and oxidation/sulfidation behaviour at 500°C
[2005Zha]	TGA in O_2 atmosphere	Oxidation behaviour and mass gain at 1000°C
[2006Bih]	SQUID, electrical measurements, heat flow	Magnetization, electrical resistivity -269°C to RT, thermal conductivity -265°C to 42°C
[2006Gol1], [2006Gol2]	Mechanical spectroscopy, DSC, VSM, Vickers indentation	Curie temperature, magnetization RT to 650°C, internal friction RT to 600°C, microhardness
[2006Sha]	Tensile tests	Yield stress 600°C to 1000°C
[2007Chi]	TIG weldability study, Vickers indentation, four-point bending	Microhardness, time-to-failure in humid air and WD40 oil
[2007Cho]	Electrochemical corrosion tests	E_{corr}, E_{trans}, E_{pp}, I_a , I_p in 0.1M H_2SO_4 and 0.1 M H_2SO_4 + 0.001M KSCN; pitting corrosion in 0.1 M HCl
[2007Pad]	Magneto balance, SQUID	Curie temperature, magnetization -273°C to 70°C, magnetic saturation & magnetic moment at -269°C
[2007Pan]	Nanoindentation, electrical measurements	Nanohardness, electrical conductivity
[2008For]	Catalytic activity measurements	Hydrocarbon and CO conversion ability
[2008Lu]	Corrosion tests in H_2-CO_2 and H_2-HCl-H_2S-CO_2	Corrosion behavior at 600°C
[2008Pav1]	Magnetometer, mechanical spectroscopy	Curie temperature, magnetization RT to 650°C, internal friction -180°C to 650°C
[2008Pin]	Cyclic oxidation tests in air	Oxidation behaviour and mass gain 700°C to 1000°C
[2009Dea]	Sulfidation-oxidation tests	Corrosion behaviour at 500°C and 700°C, mass change
[2009Gol]	Mechanical spectroscopy, VSM	Internal friction 400°C to 650°C
[2010Air]	Oxidation tests in O_2	Oxidation behavior at 1000°C
[2010Bra]	Sulfidation-oxidation tests in H_2S-H_2-H_2O-Ar	Corrosion behaviour at 600°C
[2010Gal]	Tensile tests	UTS RT to 355°C

Reference	Method/Experimental Technique	Type of Property
[2010Kob]	Vickers indentation	Microhardness at 475°C
[2010Kra]	Tensile tests	Tensile strength
[2010Sch]	Tensile tests, fatigue tests	0.2% yield stress, UTS, Young's modulus, LCF at RT & 300°C
[2011Hei]	Oxidation, XPS, DFT-EMTO	Initial stages of oxidation
[2011Kim]	Oxidation tests in air	Oxidation behavior 900-1100°C
[2011La]	Vickers indentation, compression tests	Hardness, compressive 0.2% yield stress at RT
[2011Tom]	Electrochemical corrosion tests in 0.1 mol/L HCl	Anodic polarization curves, mass change
[2012Lam]	Mechanical spectroscopy, DSC	Internal friction, Curie temperature
[2012Ume]	SQUID, VSM	Magnetization, thermomagnetization -273°C to 100°C, magnetic moment, Curie temperature
[2013Nei]	Vickers indentation, tensile tests	Microhardness; yield stress, UTS, and elongation RT to 300°C
[2015Sus]	Physical property measurements, SQUID	Magnetic susceptibility -273°C to 100°C, magnetic ordering, DOS
[2016Li1]	Vickers indentation, four-point bending tests, compression tests	Martens microhardness, brittle-to-ductile transition temperature (BDTT), compressive 0.2% yield stress at 600°C to 1000°C
[2016Sve]	Dilatometry	Thermal expansion
[2017Kra]	Compression tests	Compressive 0.2% yield stress at 800°C
[2019Cha]	Nanoindentation	Hardness, Young's modulus

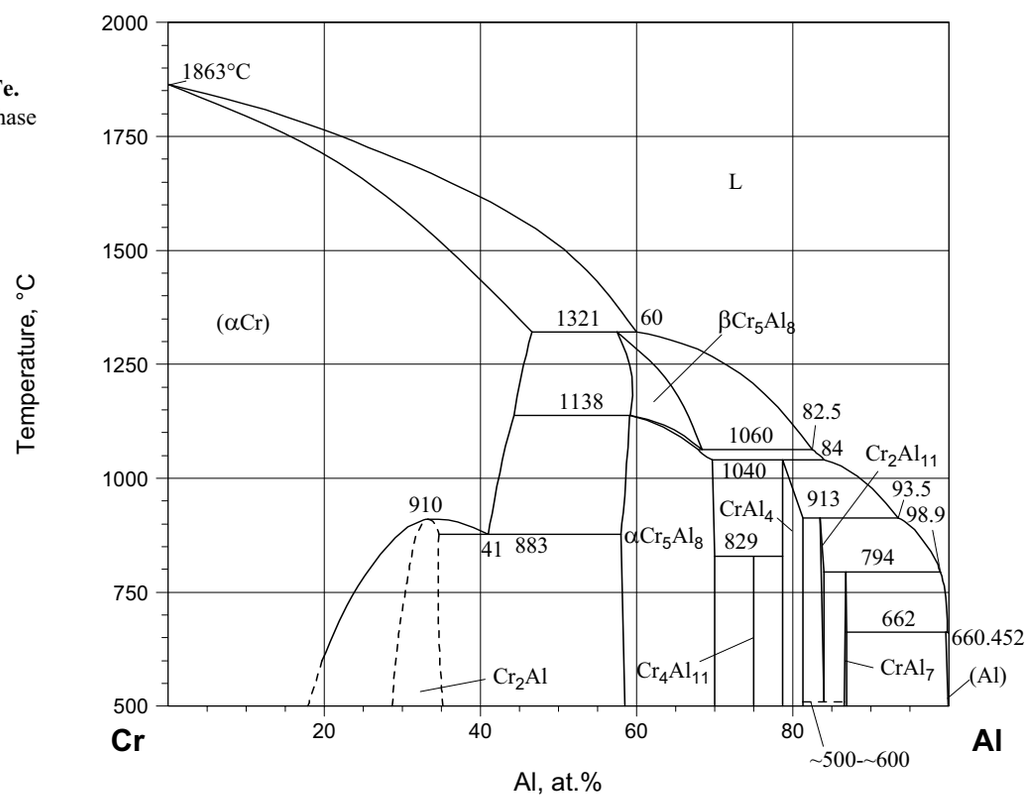

Fig. 1: Al-Cr-Fe. Assessed Al-Cr phase diagram

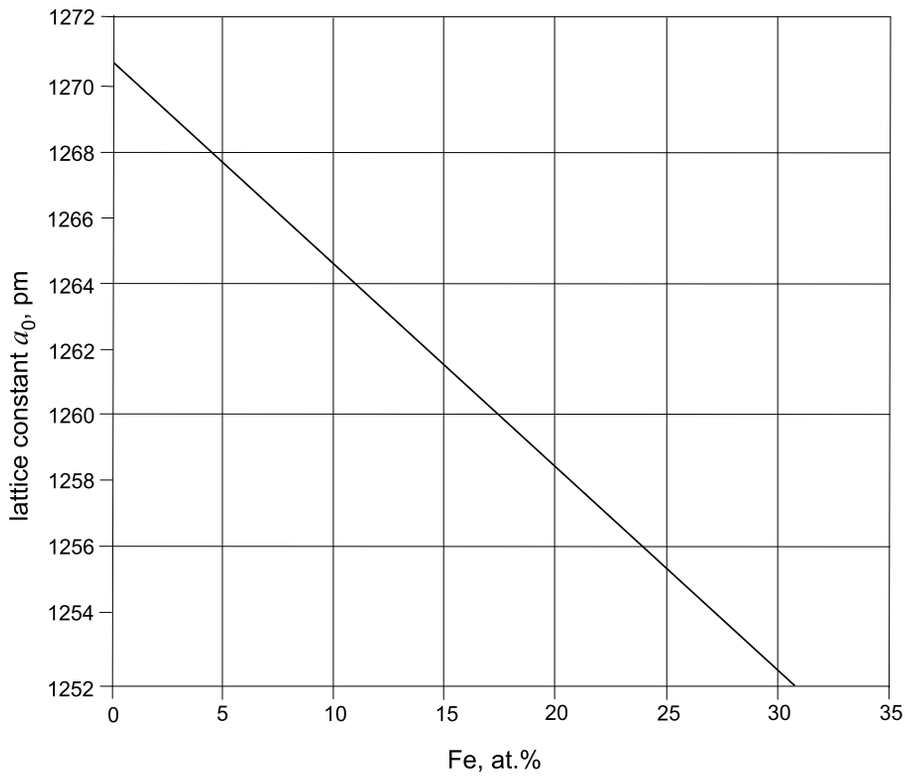

Fig. 2a: Al-Cr-Fe. Lattice constant a_0 of the Cr_5Al_8(r) phase in dependence of Fe content (Al content is 55 to 58 at.%)

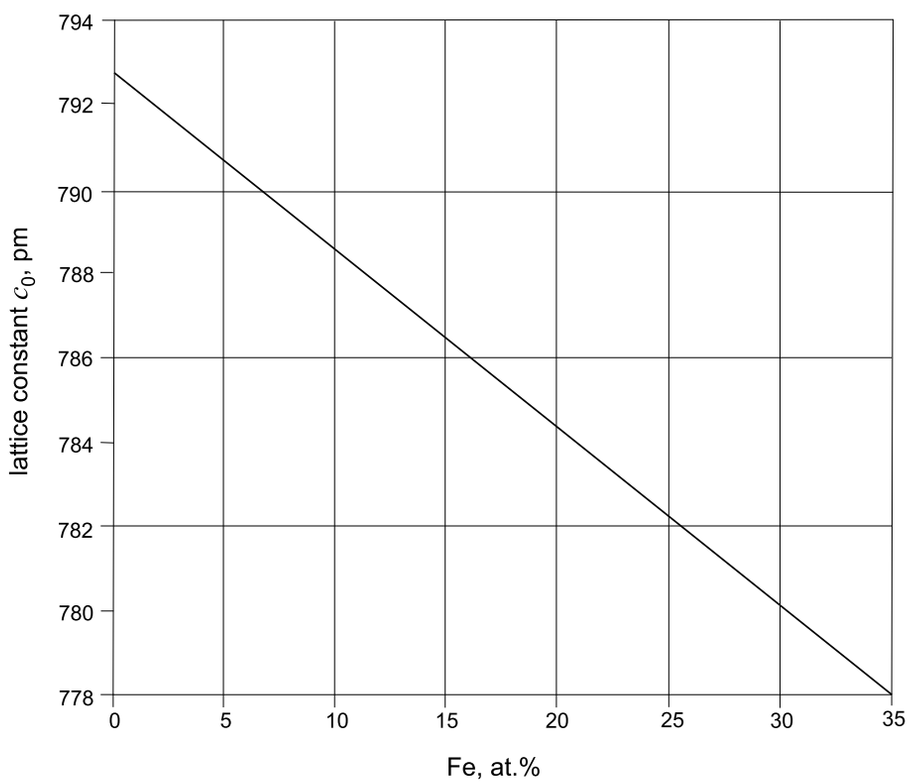

Fig. 2b: Al-Cr-Fe. Lattice constant c_0 of the Cr_5Al_8(r) phase in dependence of Fe content (Al content is 55 to 58 at.%)

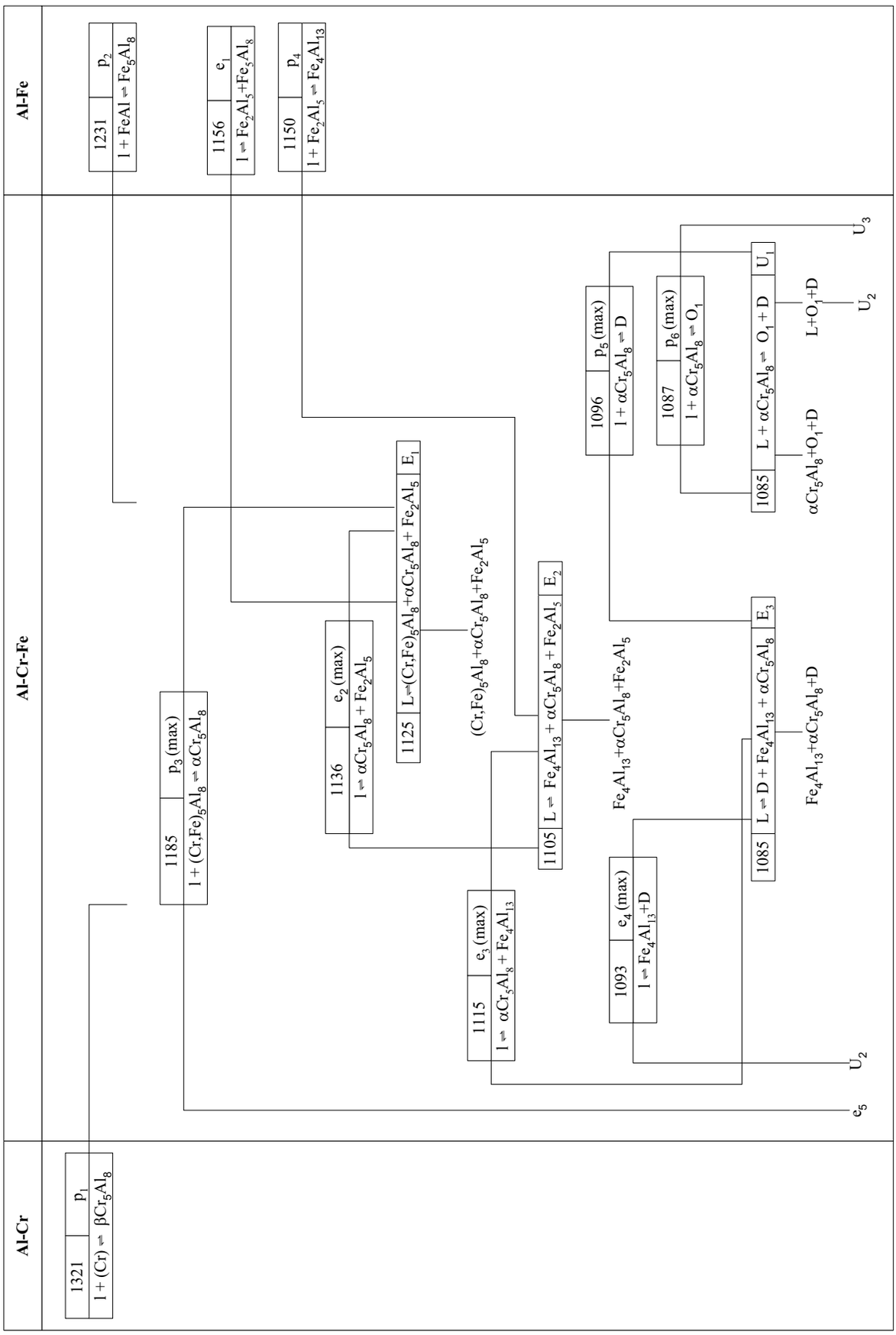

Fig. 3a: Al-Cr-Fe. Reaction scheme

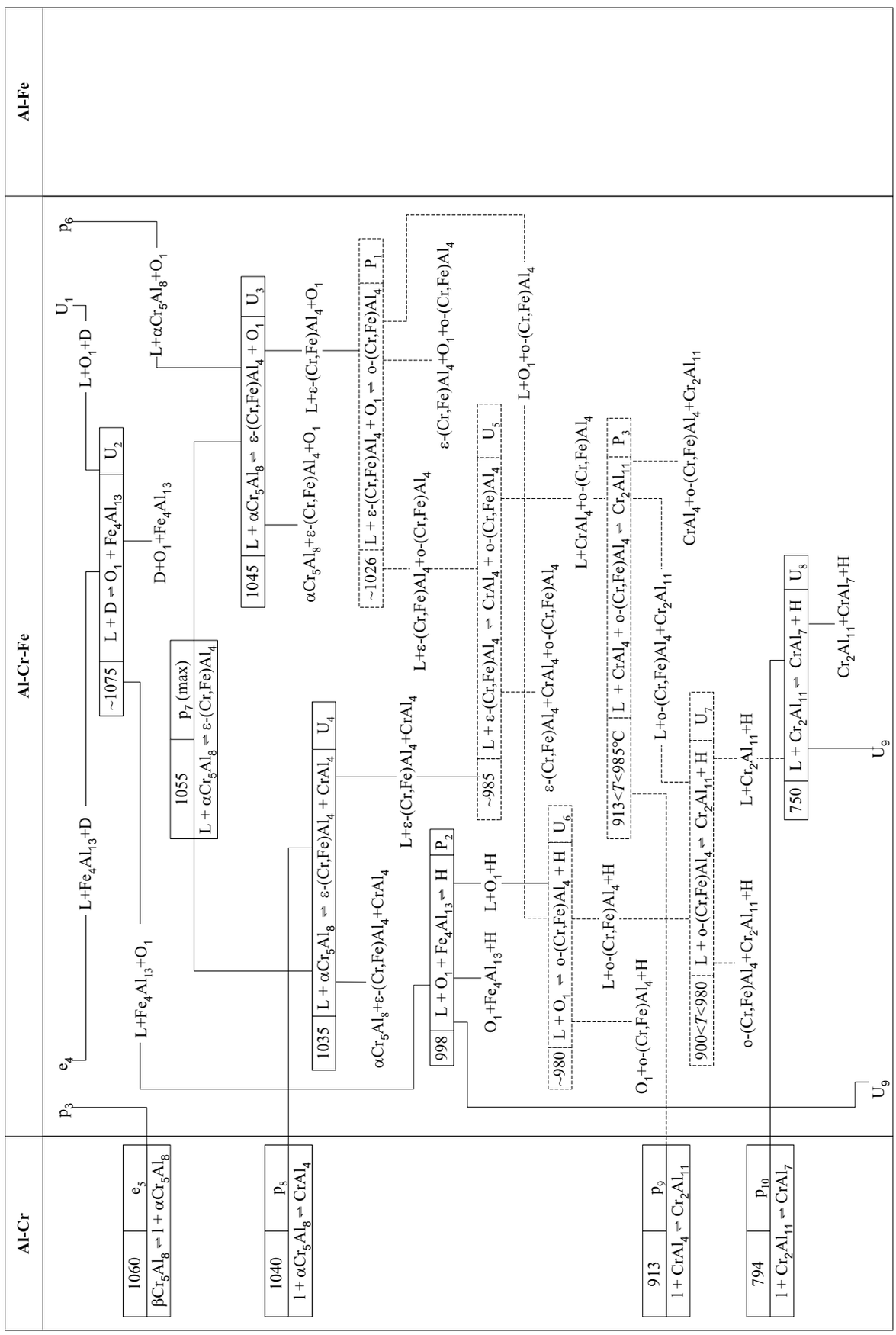

Fig. 3b: Al-Cr-Fe. Reaction scheme

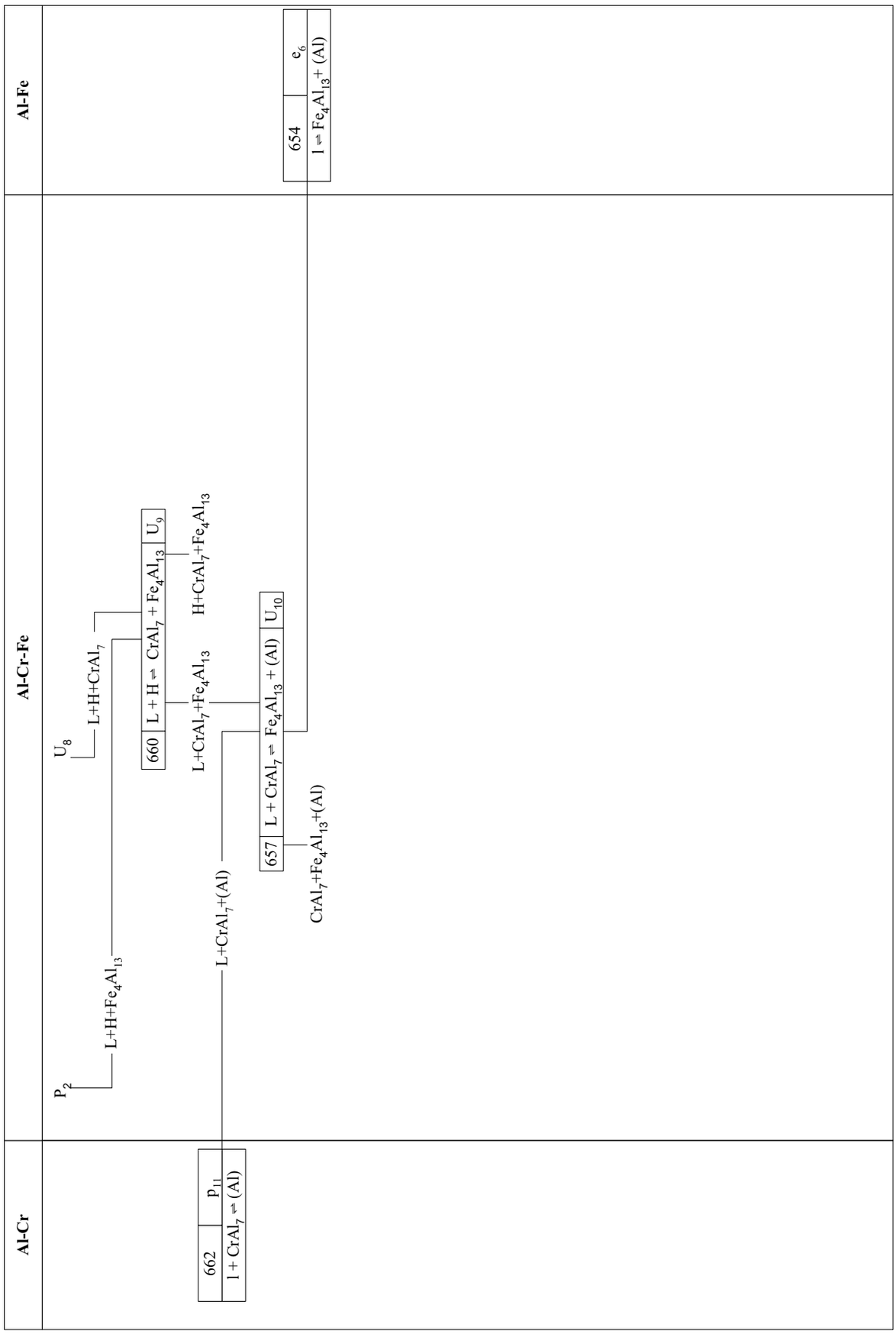

Fig. 3c: Al-Cr-Fe. Reaction scheme

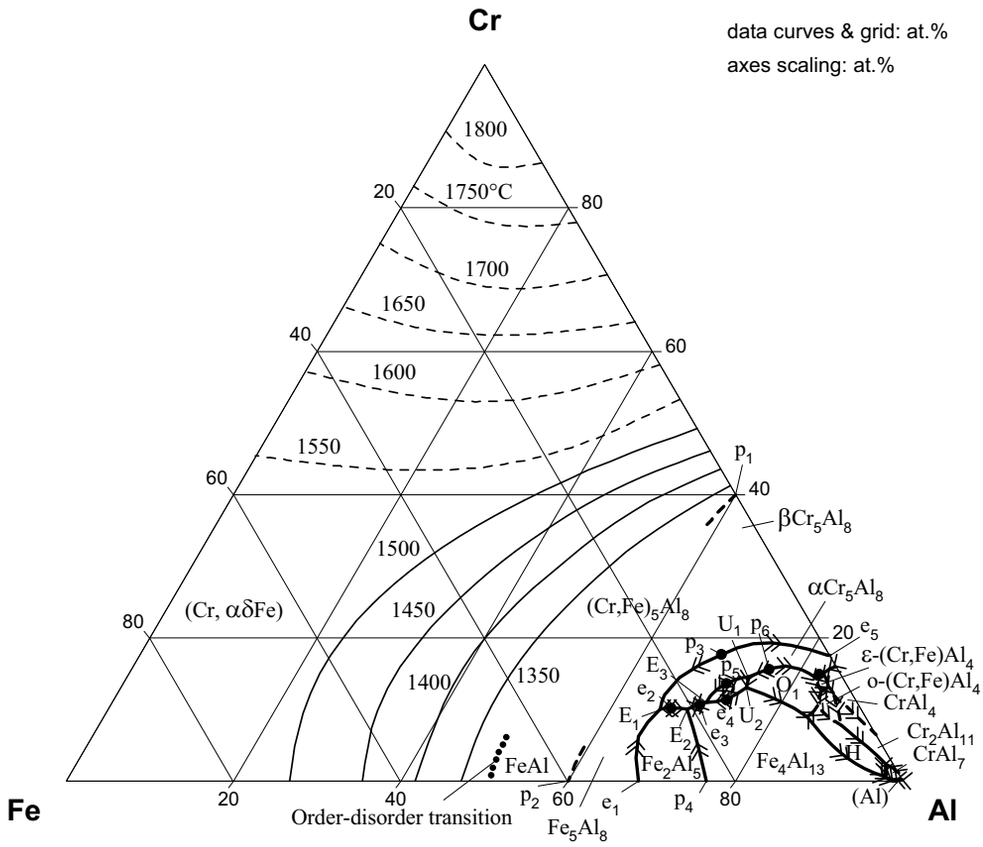

Fig. 4a: Al-Cr-Fe.
Liquidus surface projection

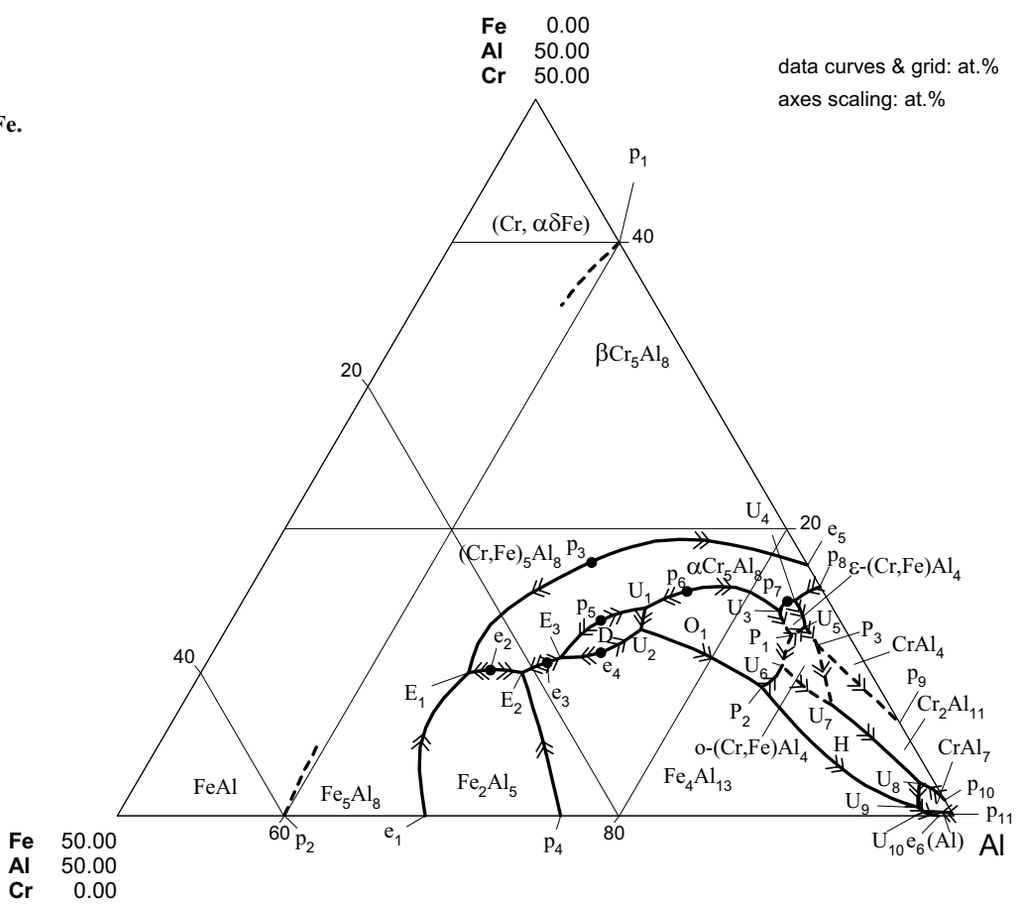

Fig. 4b: Al-Cr-Fe.
Liquidus surface projection at 50-100 at.% Al

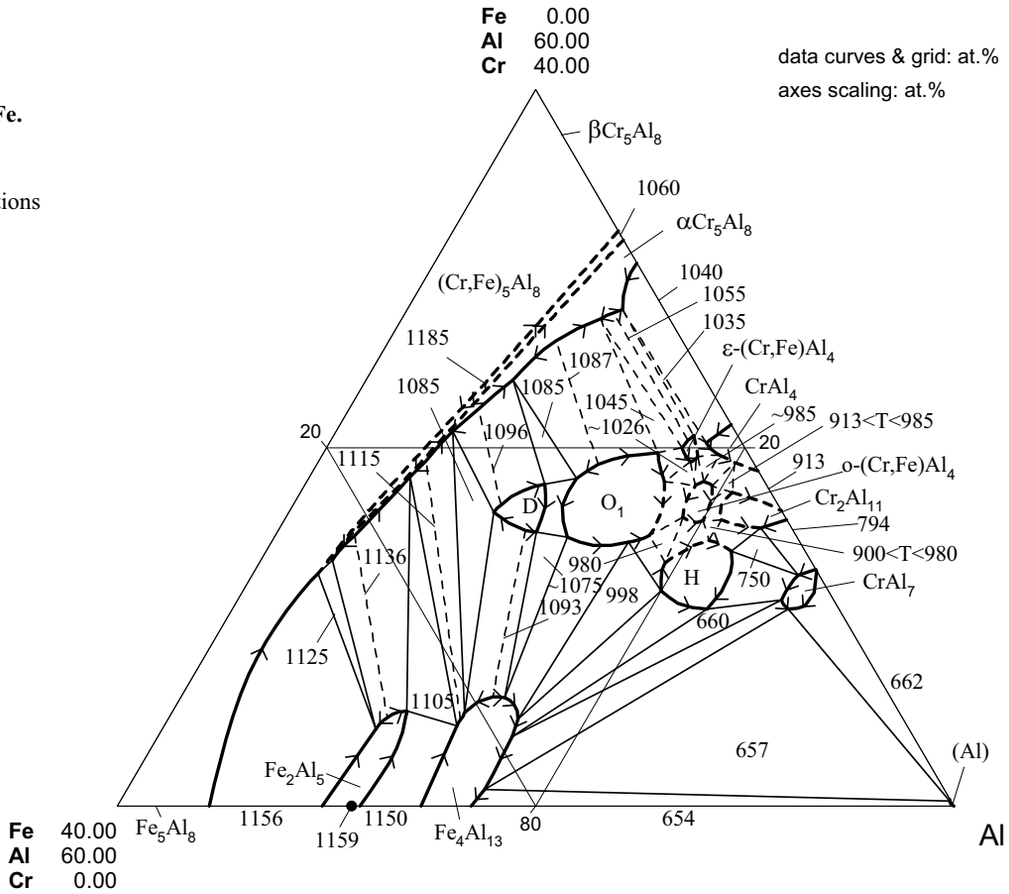

Fig. 5: Al-Cr-Fe. Solidus surface projections in the range of compositions 60-100 at.% Al

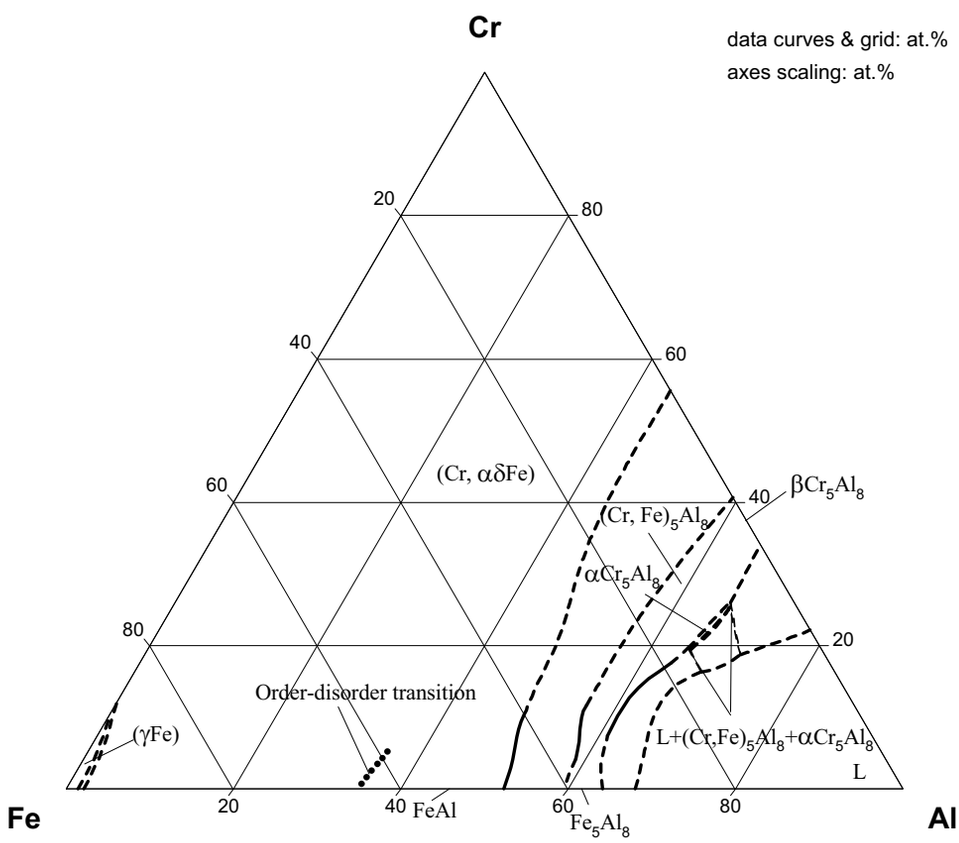

Fig. 6: Al-Cr-Fe. Isothermal section at 1160°C

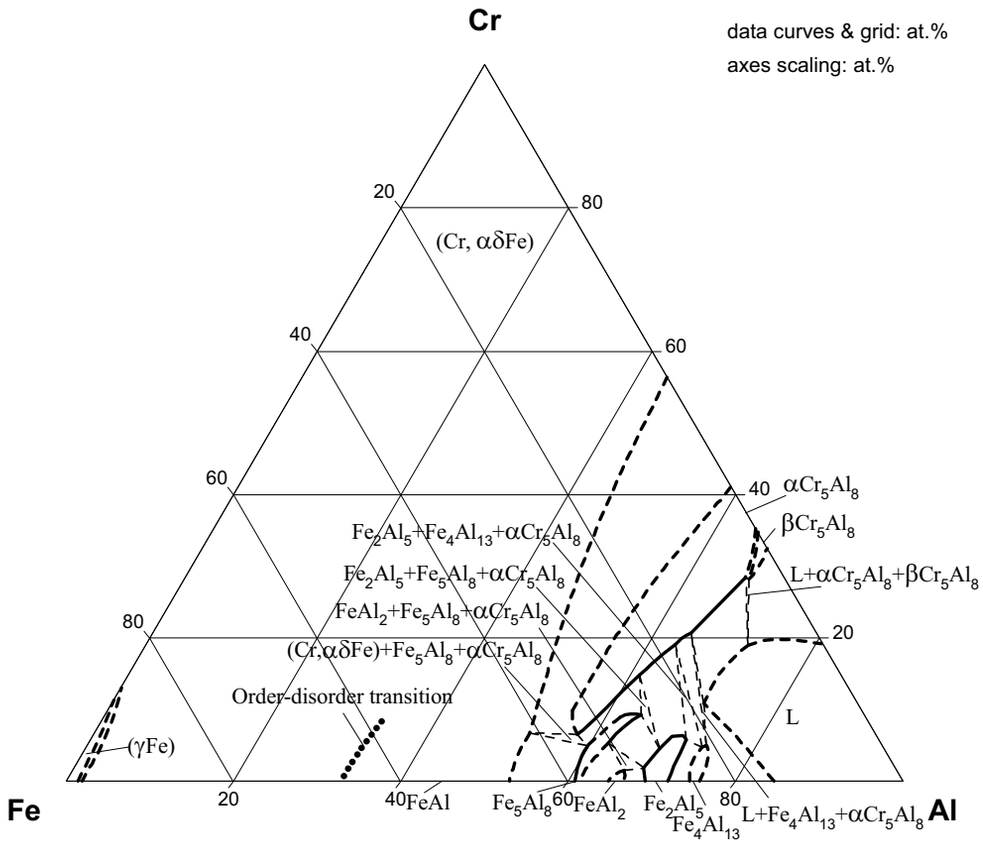

Fig. 7: Al-Cr-Fe.
Isothermal section at 1100°C

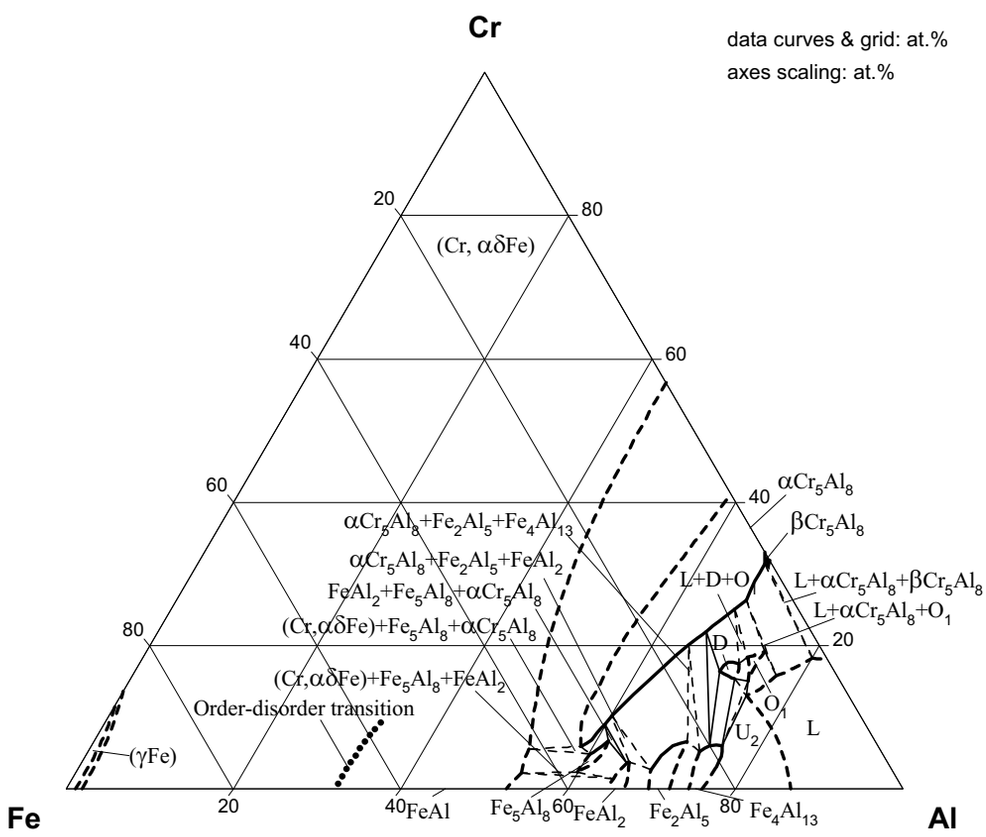

Fig. 8: Al-Cr-Fe.
Isothermal section at 1075°C

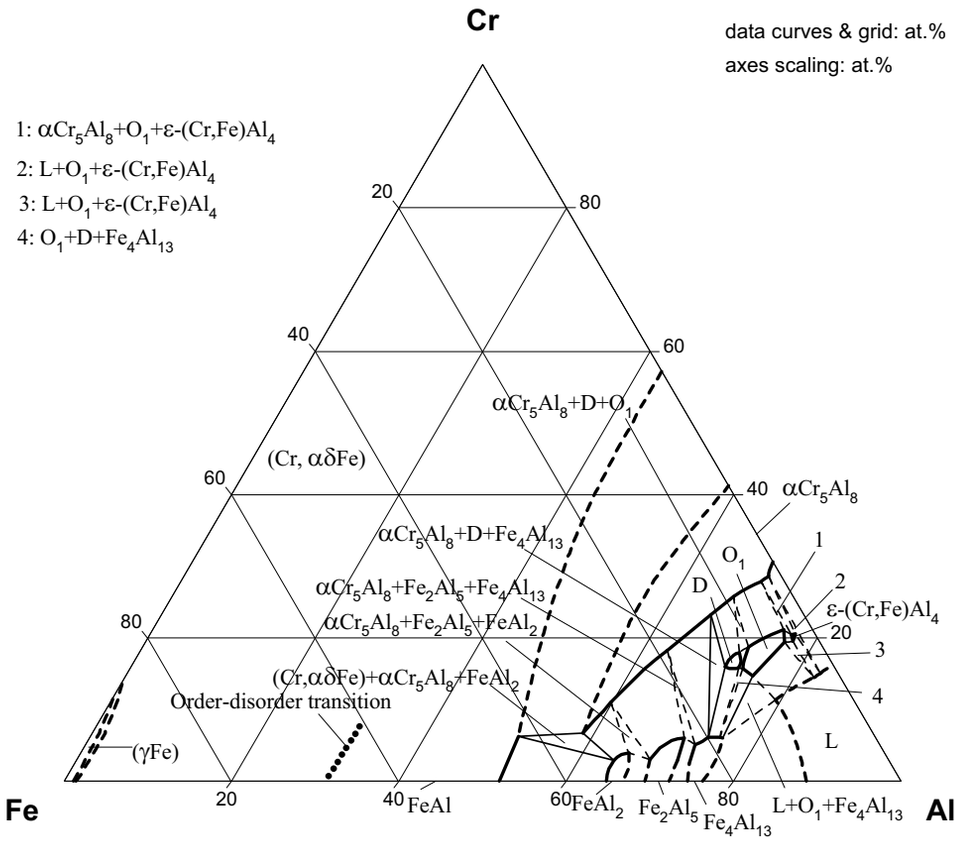

Fig. 9: Al-Cr-Fe. Isothermal section at 1042°C

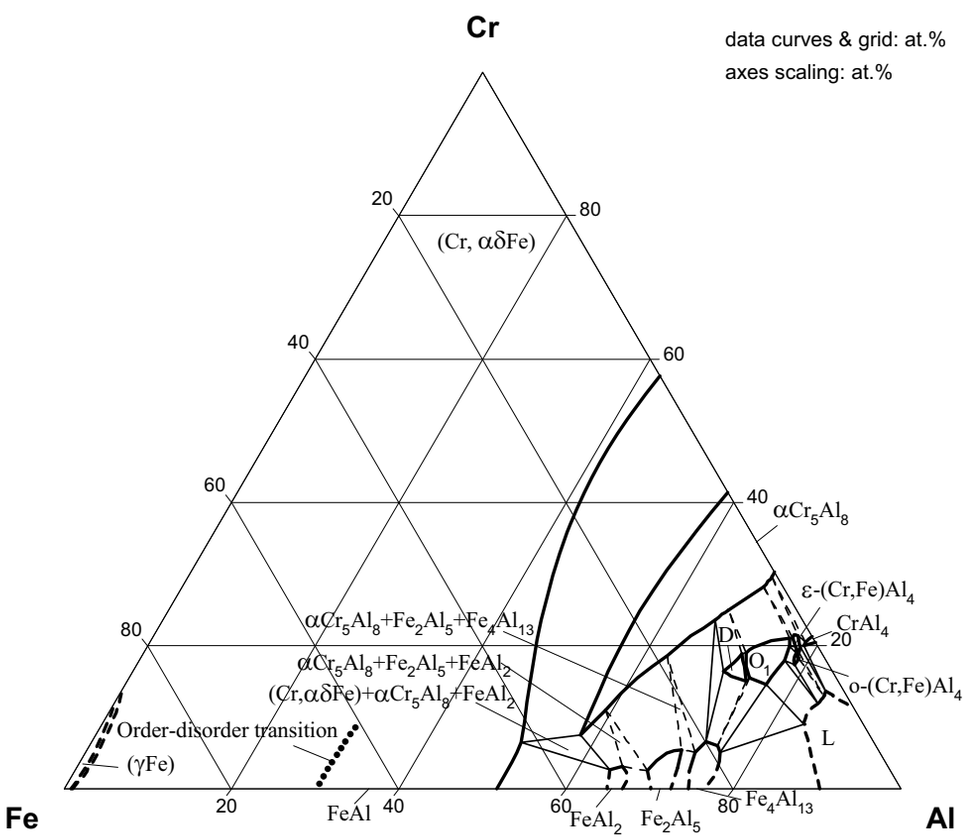

Fig. 10a: Al-Cr-Fe. Isothermal section at 1000°C

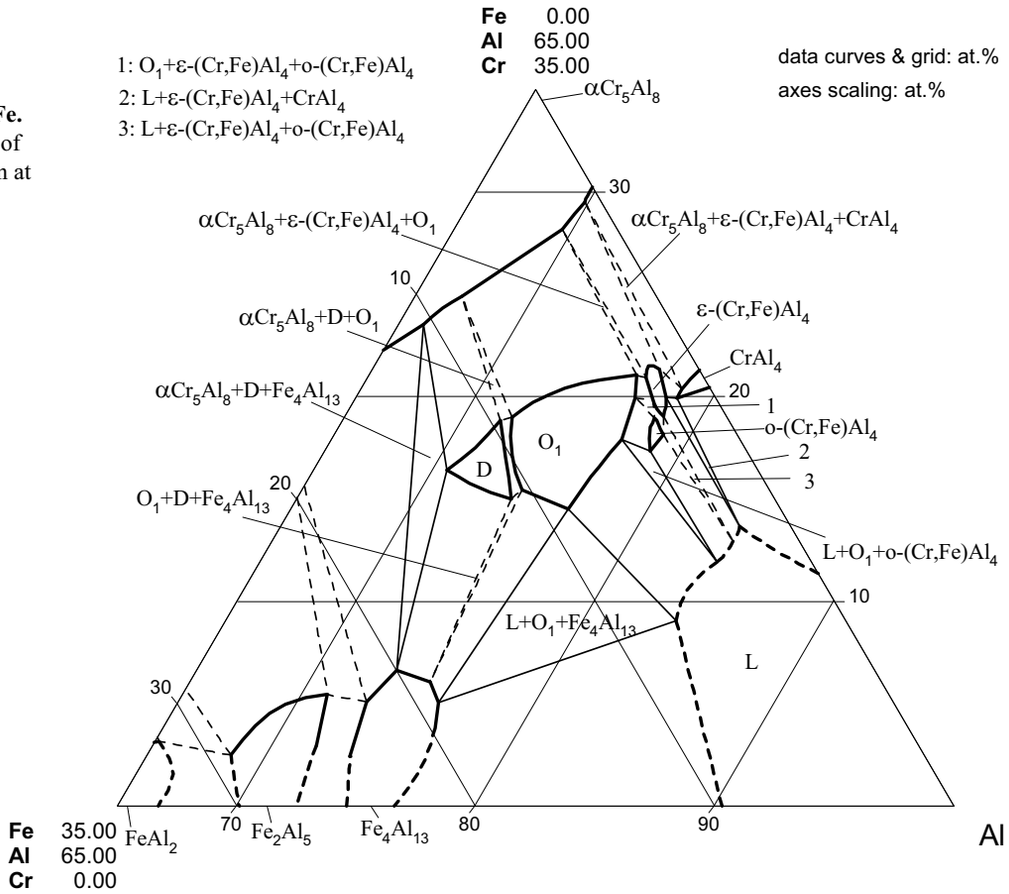

Fig. 10b: Al-Cr-Fe. Enlarged portion of isothermal section at 1000°C

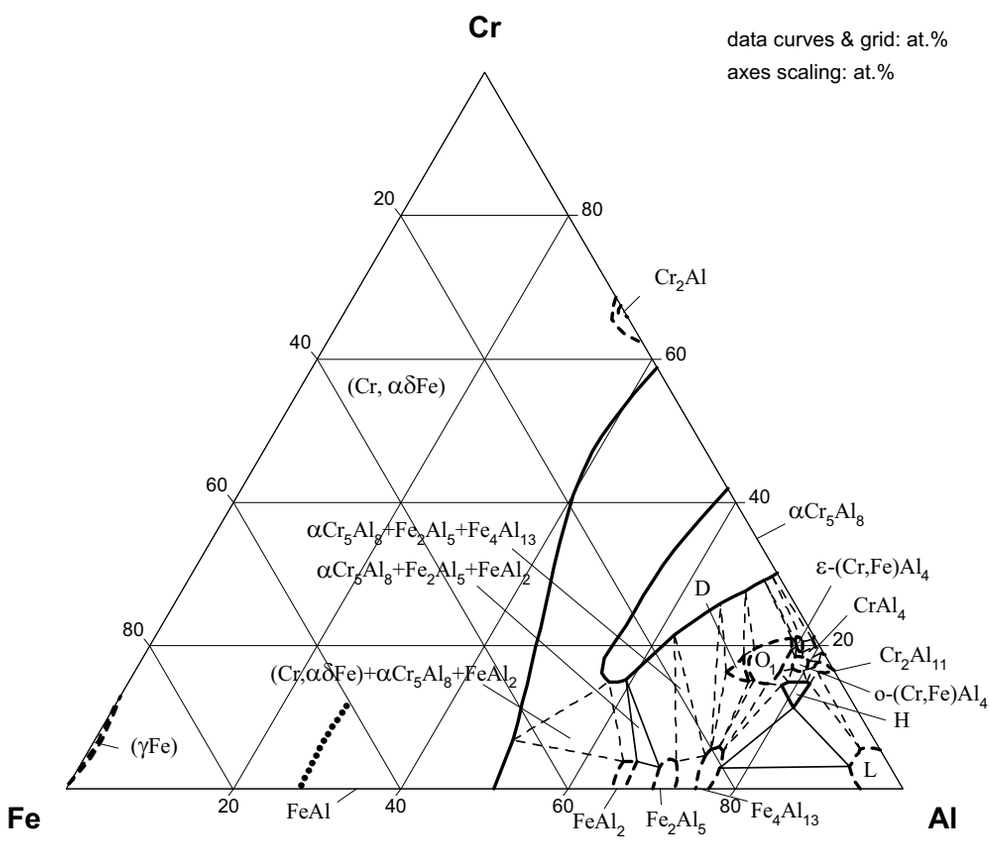

Fig. 11a: Al-Cr-Fe. Isothermal section at 900°C

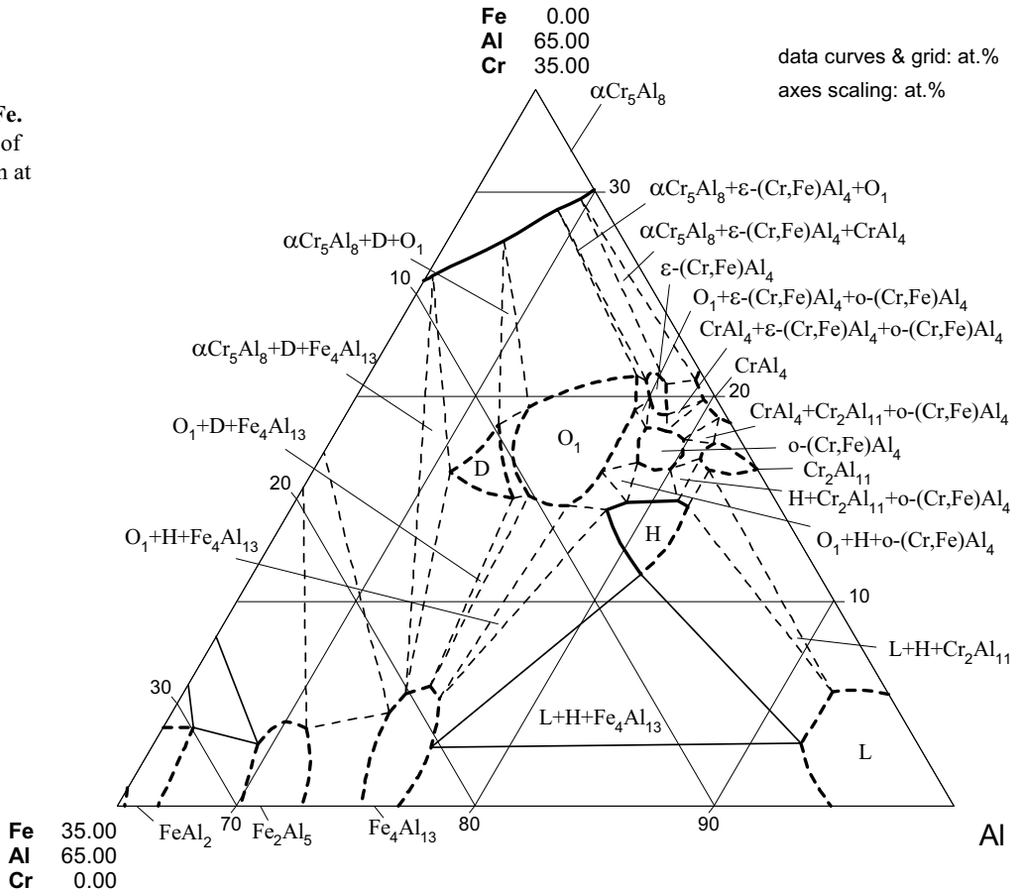

Fig. 11b: Al-Cr-Fe. Enlarged portion of isothermal section at 900°C

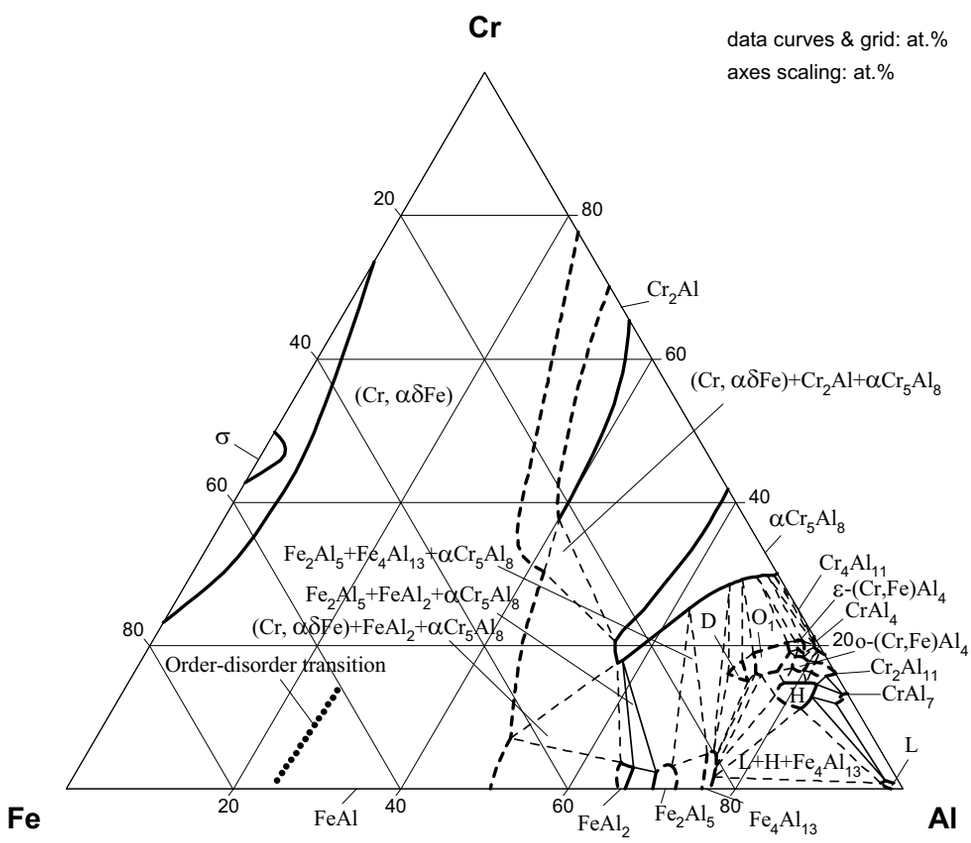

Fig. 12a: Al-Cr-Fe. Isothermal section at 700°C

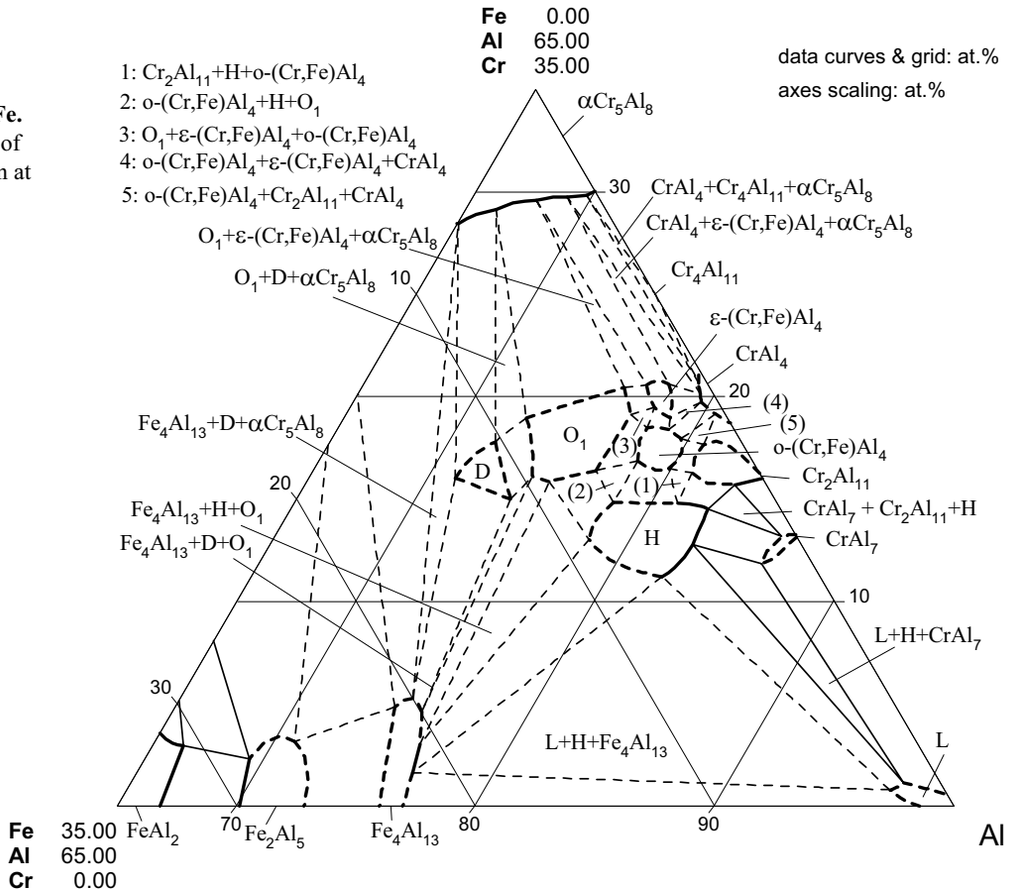

Fig. 12b: Al-Cr-Fe. Enlarged portion of isothermal section at 700°C

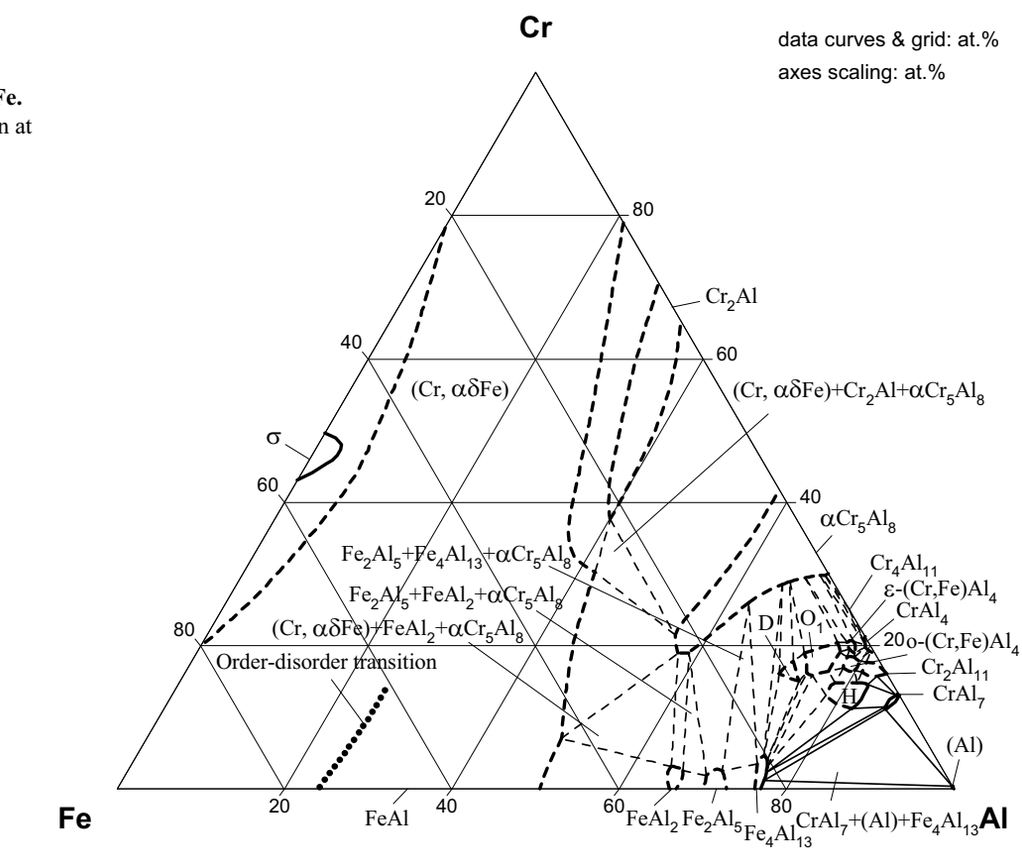

Fig. 13a: Al-Cr-Fe. Isothermal section at 650°C

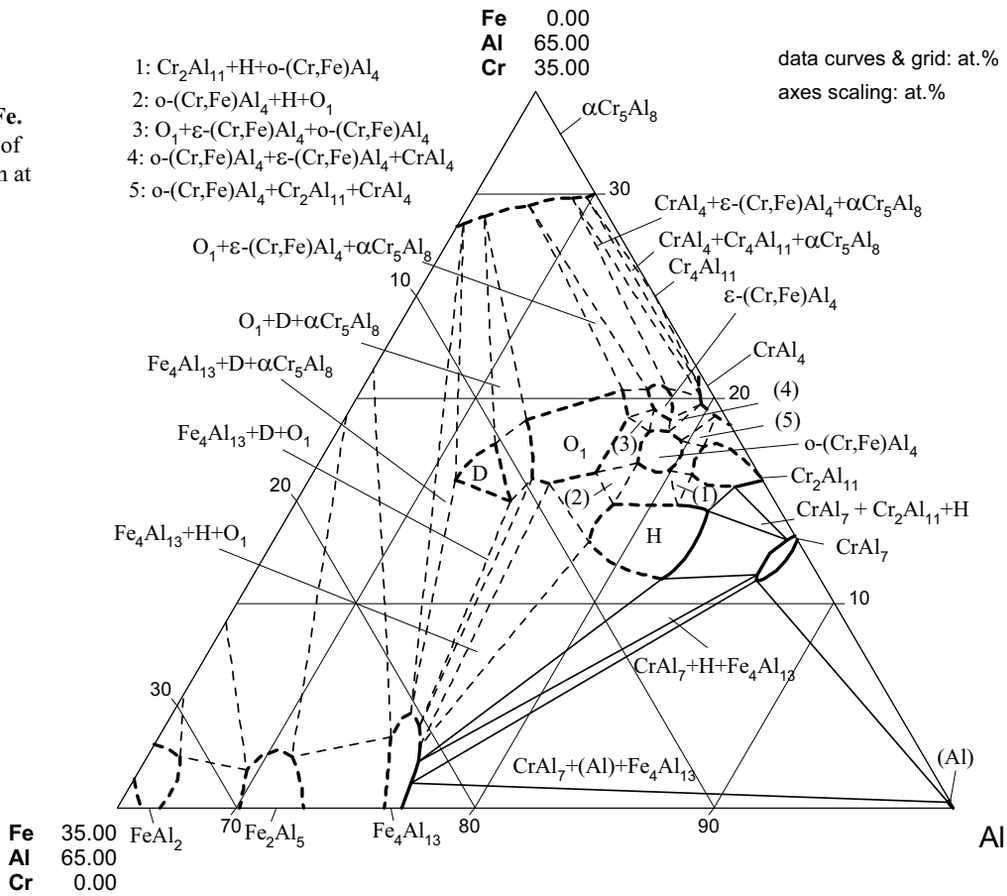

Fig. 13b:Al-Cr-Fe. Enlarged portion of isothermal section at 650°C

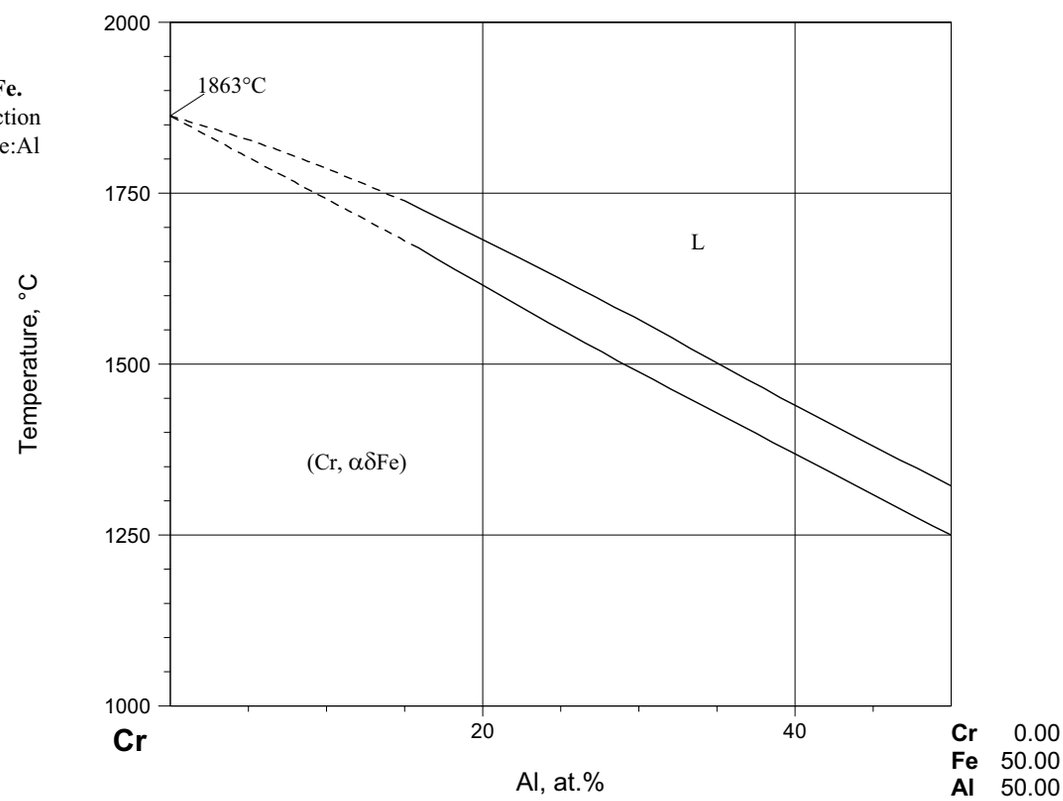

Fig. 14: Al-Cr-Fe. Partial vertical section at molar ratio of Fe:Al as 1:1